Analysis of Land Surface Dynamics in Ukraine Observed by Satellite Sensors

Dissertation
zur
Erlangung des Doktorgrades (Dr. rer. nat.)
der
Mathematisch-Naturwissenschaftlichen Fakultät
der
Rheinischen Friedrich-Wilhelms-Universität Bonn

vorgelegt von

Gohar Ghazaryan

aus Kapan, Armenien

Bonn 2019

Angefertigt mit Genehmigung der Mathematisch-Naturwissenschaftlichen Fakultät der Rheinischen Friedrich-Wilhelms-Universität Bonn

Referent: PD Dr. Jürgen Schellberg

Korreferent: Prof. Dr. Klaus Greve

Tag der Promotion: 08.10.2019

Erscheinungsjahr: 2020

Abstract

Land surface changes, induced by anthropogenic or climatic drivers, can dramatically impact ecosystem functioning. The growing amount of data from remote sensing and complementary data sources greatly supports the quantification of land surface changes. This research aimed to use several remotely sensed datasets to explore inter-annual and seasonal variability of land surface in Ukraine at multiple spatial scales. The country was chosen as a study area, as it has experienced immense institutional and environmental changes during recent decades.

For the analysis at country scale, the main aim was to understand land surface dynamics and to assess processes underlying the changes. For this, Global Inventory Modeling and Mapping Studies (GIMMS) Normalized Difference Vegetation Index (NDVI) time series were used. Abrupt and gradual changes were delineated, and we addressed the relationships of land surface changes and climatic variables. Among the factors analyzed, air temperature explained the largest portion of NDVI variability. High air temperature/NDVI correlation coefficients were observed over the entire country. Soil moisture content had a significant influence in eastern regions and precipitation was most influential in the central regions of the country.

For the analysis at local scale the focus was put on crop identification and crop condition monitoring. As croplands are often faced with high inter-annual and seasonal variability, the monitoring of cropland extent and condition is essential to improve food security. For crop mapping, the combined use of time series observations derived from Landsat-8 and Sentinel-1 was tested. The phenology was modeled by fitting harmonic function and we generated training samples based on the fit. Three classification algorithms (support vector machines, random forest, decision fusion) were tested for crop mapping. Overall classification accuracies exceeded 80% for random forest and decision fusion when using Landsat and Sentinel based seasonal composites.

For drought impact monitoring in croplands, time series from optical (Landsat, MODIS, Sentinel-2) and Synthetic Aperture Radar (SAR) data was used. Indicators were derived based on optical (NDVI, Normalized Difference Moisture Index (NDMI), Land Surface Temperature (LST), Tasselled Cap Indices) and Sentinel-1 (backscattering intensity and relative surface moisture) data.

Logistic regression was used to evaluate the drought-induced variability of remotely sensed parameters estimated for specific phases of crop growth. The parameters with the highest prediction rate were further used to estimate thresholds for drought/non-drought classification. The results revealed that remotely sensed variables do not respond uniformly to drought conditions. Growing season maximum NDMI and NDVI (70-75%) and SAR backscatter (60%) reflect the impact of agricultural drought. LST was also a useful indicator of crop condition, especially for maize and sunflower, with prediction rates of 86% and 71% respectively.

Furthermore, to contribute to not only remotely sensed data analysis but also their dissemination, a web application was developed that enables the provision of customizable geospatial tools and products. The user is able to define either spatial or temporal parameters (or both), change the used algorithms (e.g. change detection, anomaly detection) or visualization parameters based on the preferred data sources and get access to previously discussed outputs, such as vegetation index time series, LST, backscattering intensity, land cover and crop condition parameters.

The research for this thesis combined different trend analysis techniques, integrated multiple datasets, and advanced statistical modeling at different scales. This allowed analyses to go beyond descriptive information like overall vegetation status and dynamics, land degradation or crop stress; but to derive valuable spatially explicit information towards a better understanding of change drivers. This information forms the essential basis for advanced models and leads the way to better decision making for sustainable land management.

Zusammenfassung

Anthropogen- oder klimabedingte Veränderungen der Landoberfläche können einen gravierenden Einfluss auf Ökosysteme und ihre Funktionen haben. Durch die zunehmende Anzahl an frei verfügbaren Sensordaten sowie komplementären Datenquellen wird die Quantifizierung von Landoberflächenveränderungen stetig verbessert. Ziel dieser Forschungsarbeit war es jährliche und saisonale Schwankungen der Landoberfläche und Vegetation der Ukraine mithilfe verschiedener Fernerkundungsdatensätze auf unterschiedlichen räumlichen Skalen zu untersuchen. Das Land wurde als Untersuchungregion gewählt, da es in den vergangenen Jahrzehnten immense institutionelle und ökologische Veränderungen erfahren hat.

Das Ziel der landesweiten Analyse war, die Landoberflächendynamiken und ihre treibenden Prozesse zu verstehen. Hierfür wurden GIMMS- (Global Inventory Modeling and Mapping Studies) NDVI-(Normalized Difference Vegetation Index) Zeitreihen verwendet. Abrupte und graduelle Veränderungen, sowie die Beziehungen zwischen Landoberflächenveränderungen und Klimavariablen wurden beschrieben und untersucht. Bei den hierfür analysierten Faktoren war die Lufttemperatur für den Großteil der NDVI-Variabilität ausschlaggebend. Über der gesamten Landesfläche konnten hohe Lufttemperaturen bzw. NDVI-Korrelationskoeffizienten beobachtet werden, während in den östlichen Regionen insbesondere der Feuchtigkeitsgehalt des Bodens sowie in den zentralen Regionen des Landes der Niederschlag signifikanten Einfluss hatte.

Für die Analyse auf lokaler Ebene wurde der Fokus auf der Klassifikation und dem Zustandsmonitoring von Nutzpflanzengelegt. Da die Anbauflächen oftmals hohen jährlichen und saisonalen Schwankungen unterliegen, ist das Nutzpflanzen-Monitoring für die Ernährungssicherung von großer Bedeutung. Für die Nutzpflanzenklassifikation wurden Zeitreihenaufnahmen, kombiniert aus Landsat-8- und Sentinel-1-, getestet. Die Phänologie wurde mit „fitting harmonic funtion“ modeliert. Darauf basierend wurden Trainingsbeispiele entwickelt. Es wurden drei Klassifizierungsalgorithmen (Support Vector Machines, Random Forest, Decision Fusion) getestet. Die Klassifizierungsgenauigkeit für Random Forest und Decision Fusion betrug bei Landsat- und Sentinel-basierten saisonalen Kompositen über 80%.

Für das Dürre-Monitoring der Nutzpflanzen wurden Zeitreihen von optischen (Landsat, MODIS, Sentinel-2) und Radar-Daten (Synthetic Aperture Radar (SAR)) verwendet. Die Indikatoren wurden von optischen Daten (NDVI, Normalized Difference Moisture Index (NDMI), Oberflächentemperatur (OFT), Tasselled Cap Indices) und Sentinel-1-Daten (Rückstreuintensität und relative Oberflächenfeuchtigkeit) abgeleitet. Zur Ermittlung der Dürre-induzierten Variabilität der Fernerkundungsparameter wurde das Verfahren der logistischen Regression angewandt, um spezielle Wachstumsphasen bestimmen zu können. Die Parameter mit der höchsten Vorhersagegenauigkeit wurden zur Einschätzung der Schwellenwerte für Dürre bzw. Nicht-Dürre-Klassifizierung weiter verwendet. Die Ergebnisse zeigten, dass Variablen, die aus Fernerkundungsdaten abgeleitet werden, nicht einheitlich auf Dürrebedingungen reagieren. Die Maximalwerte während der Wachstumperiode von NDMI, NDVI (70-75%) und SAR-Rückstreuung (60%) spiegeln die Auswirkungen der landwirtschaftlichen Dürre wider. OFT erwies sich als nützlicher Indikator für den Zustand der Pflanzen, insbesondere für Mais und Sonnenblumen. Hier betrugen die Vorhersageraten 86% bzw. 71%.

Weiterhin wurde eine Webanwendung entwickelt, die nicht nur der Analyse von Fernerkundungsdaten, sondern auch der Verbreitung der Ergebnisse dient. Diese stellt flexible raumbezogene Werkzeuge und Produkte zur Verfügung. Benutzer können räumliche oder zeitliche Parameter (oder beides) definieren, die verwendeten Algorithmen (z.B. Veränderungsdetektion, Anomalie-Erkennung) anpassen, oder Visualisierungsparameter, basierend auf den favorisierten Datenquellen, ändern und dadurch Zugriff auf zuvor beschriebenen Produkte, bspw. Vegetationsindexzeitreihen, OFT, Rückstreuintensität, Landbedeckung und Erntezustandsparameter, erhalten.

Die Forschung für diese Arbeit kombinierte verschiedene Techniken der Trend-Analyse, integrierte mehrere Datensätze und verbesserte statistische Modellierung auf verschiedenen Skalen. Dies erlaubt Analysen, die über deskriptive Informationen wie Vegetationsstatus und -dynamiken, Landdegradation oder Trockenstress hinausgehen und sondern vielmehr wichtige räumliche Informationen zu liefern, die zu einem besseren Verständnis von Ursachen des Landnutzungswandels führen. Informationen, welche die notwendige Basis für hoch entwickelte Modelle bilden und den Weg für verbesserte Entscheidungsbildungen hin zu einem nachhaltigen Landmanagement bereiten.

Acknowledgment

I could not have finished this journey without the help and encouragement of my supervisor PD Dr. Jürgen Schellberg. I am grateful for the support throughout the thesis preparation with his constructive remarks, support, and guidance. The critical questions and discussions helped me to become an independent researcher that I am today.

I would like to express my gratitude to the late Prof. Dr. Gunter Menz, as this journey started with him, and he encouraged me to develop my own ideas. Also, I would like to thank PD Dr. Olena Dubovyk for her support starting from day one, for her feedback and challenging tasks. My thanks go to Prof. Dr. Klaus Greve, who accepted to be the second reviewer of my thesis and for overall support and kindness during these years. I would like to thank Prof. Dr. Jakob Rhyner for being in my doctoral committee.

Big thanks to my fellow Ph.D. candidates, especially Javier and Fabian for interesting discussions, I learned a lot from you! My sincere thanks go to all the colleagues at Center for Remote Sensing of Land Surfaces, Remote Sensing Research Group, and Center for Development Research for an amazing working atmosphere. I thank Dr. Valerie Graw, Carsten Oldenburg, Jonas Schreier and Layla Hashweh for the support. Special thanks to Ellen Götz, who supported with all the questions and helped with settling and focusing on research.

I would like to thank for the great support that I had during my fieldwork in Ukraine. I would like to particularly thank Tatyana Adamneko, Tetyana Kuchma and Prof. Nataliia Kussul for their help during and after my stay in Ukraine.

Special thanks to Noa Kallioinen and Dr. Konrad Hentze for proofreading and advice on how to improve the thesis.

Finally, I can not thank enough my sisters (Anush, Carmen, Hrachuhi, Narine, and Gayane) for their motivation, encouragement, and help during the challenging times. Last but not least I want to thank Ayoub, for his love and endless patience.

This would not have been possible without all of you.

Thank you!

Contents

List of Figures

List of Tables

List of Acronyms

AVHRR	Advanced Very High Resolution Radiometer
API	Application Programming Interface
ASCAT	Advanced Scatterometer
DOY	Day Of Year
EO	Earth Observation
EVI	Enhanced Vegetation Index
ESA	European Space Agency
ET	EvapoTranspiration
FMASK	Function of Mask
GEE	Google Earth Engine
GIMMS	Global Inventory Monitoring and Modeling System
HTML	Hypertext Markup Language
L8	Landsat 8
LST	Land Surface Temperature
MODIS	Moderate Resolution Imaging Spectrometer
NDVI	Normalized Difference Vegetation Index
RF	Random Forest
RS	Remote Sensing
S2	Sentinel-2
SWIR	Shortwave Infrared
SDG	Sustainable Development Goals
SR	Surface Reflectance
SVM	Support Vector Machine
SAR	Synthetic Aperture Radar
TIR	Thermal Infrared
TOA	Top Of Atmosphere

USGS United States Geological Survey

VCI Vegetation Condition Index

VNIR Visible and Near Infrared

Chapter 1

Introduction

Land surface changes are one of the critical drivers of global change. They can dramatically impact ecosystems, climate and social development (Seddon, Macias-Fauria, Long, Benz, & Willis, 2016). Rapid urbanization, deforestation, socioeconomic transformations, climate variability, and natural hazards change the Earth's surface. These changes, in turn, contribute to the intensification of agriculture and the cultivation of non-arable land, which can accelerate the degradation of natural ecosystems (Kuenzer, Dech, & Wagner, 2015; Landmann & Dubovyk, 2014). Changes in land surface, especially those of anthropogenic origin, have broad impacts on critical environmental processes. Mapping and monitoring of such changes and quantifying their impact in a continuous and timely manner is necessary to address several important issues such as the global carbon budget, ecosystem dynamics, sustainable land management and to support decision-making processes. Furthermore, ongoing changes in climate can further amplify the pressure on the already limited resources (Kogan, 2018). The increasing food and water demand coupled with the finite land and water resources will further affect agriculture. The changing patterns of water availability and an increasing number of extreme weather events can alter agricultural production and sustainable land management (Godfray et al., 2010). With large area acquisition and repairability, satellite imagery is one of the primary sources of information regarding land surface changes (Ban, 2016). Different sensors provide large volumes of multitemporal and multiscale data that can be used for land surface change analysis at global, regional and local scales. As a result of these analyses, various indicators as well as environmental and agricultural statistics can be derived. Particularly, the information on land use and land cover change, crop type and deforestation can be derived from Remote Sensing (RS) data. Further, the statistics and metrics derived from remote sensing data can be used to support the United Nations 2030 Agenda for Sustainable Development (Holloway & Mengersen, 2018). Remote sensing aids the monitoring and reporting of Sustainable Develop-

ment Goals (SDGs), thereby giving an opportunity to develop data-driven indicators and spatially explicit statistical outputs (Paganini et al., 2018). Remote sensing based time series analysis is a powerful tool to reveal land surface dynamics and to analyze the magnitude of these changes within a defined monitoring time span (Kuenzer et al., 2015) and can be used for assessing their environmental impact and/or attributing to driving processes (Rogier de Jong, Schaepman, Furrer, de Bruin, & Verburg, 2013).

1.1 Transformations in Ukraine as a Background for Land Surface Changes

While land surface changes are a global phenomenon, with hotspots of changes spread across the world, this dissertation focuses on Ukraine, a country that has experienced institutional and environmental changes during recent decades and is a prime example of an area with diverse agro-climatic conditions with both long and short term changes (Baumann et al., 2011; Schierhorn et al., 2013). The collapse of the Soviet Union induced major socio-economic and institutional dislocations in Ukraine starting from the early 1990s. The integration of concepts of open-market economy induced policy changes that had direct and indirect effects on the agricultural sector. Such policy transformations included the abolition of state subsidies used for calibration of output and input prices, which, in turn, resulted in abruptly declining conditions for trade and negatively affected agricultural profitability (Rozelle & Swinnen, 2004). Furthermore, after post-socialist land reforms, collective and state farming was substituted by individualized land use (Lerman, 2004; Lerman, Sedik, Pugachov, & Goncharuk, 2007). The effects of this socio-economic disturbance were comparable to the impact of the nuclear disaster in Chernobyl in 1986. It is reported, that land abandonment rates were similar in Ukraine and neighboring Belarus after the nuclear disaster (28% and 36% of previously farmed land), but the rates of land abandonment after the collapse of the Soviet Union in Ukraine were two times higher compared to changes in Belarus (Hostert et al., 2011). As a result, the institutional changes had an impact on distribution and extent of land cover types, land use intensity, enforcement of water pollution regulations, the economic productivity in the industrial and agricultural sectors, and changes in regional biogeochemical cycles. Considering the fact that for decades Ukraine was seen as a "breadbasket of Europe," (Smaliychuk et al., 2016),these changes in the agricultural sector can have a significant impact on local crop production and more substantial socio-economic impacts. Ukraine accounts for 2.1% of the global arable land and about 25% of fertile black soil, which makes the country unique regarding its agricultural

potential. Nowadays, Ukraine is the world's largest sunflower oil exporter, second largest grain exporter, fourth largest corn and barley exporter, and sixth largest wheat and soybean producer (FAO, 2018). Following the economic recovery and cultivation of previously abandoned croplands, changes in the agricultural sector continued. Generally, the restructuring processes evolved in two directions: the expansion of managed farmland and the decrease of smallholder farms (Stefanski et al., 2014). These transformations also manifested themselves as significant changes in land surface phenology which have been previously observed and reported (Kovalskyy & Henebry, 2009). Besides the ongoing socio-economic transformations, changes in climate conditions have been reported. Specifically, recent studies reported fluctuations in crop production related to extreme weather conditions. For example, in the past 30–50 years, droughts have become more frequent and intense, covering up to half of the area of Ukraine every 10–12 years, and up to 20% every 2–3 years (Adamenko & Prokopenko, 2011; Kogan, Adamenko, & Guo, 2013; Skakun, Kussul, Shelestov, & Kussul, 2015).This climate fluctuation reduced summer crop production by up to 75%. All these described alterations caused changes in ecosystem that can be reflected on the land surface. To understand the effect of these phenomena, monitoring of land surface changes, particularly vegetation dynamics and crop condition assessment is required. Although there have been studies on land surface change analysis in Ukraine, little attention has been paid to the understanding of the main drivers of land surface changes and the appropriate data and algorithm selection. Thus, the focus of this thesis was on enhancing our understanding of the spatiotemporal changes and trends in land surface. To address differences in the dynamics at different spatial scales, we ran the analyses from country to the local level with the use of multi-source remotely sensed time series. Considering the large area of the country, diverse ecosystems, agroclimatic conditions, and different factors, the integration of different data sources, with diverse spatial, as well as temporal and spectral characteristics is essential.

1.2 Analysis of Land Cover Dynamics With Remotely Sensed Data

Remotely sensed imagery has been used over the past decades in order to detect and classify changes on the Earth's surface (Kuenzer et al., 2015; Schmullius, Thiel, Pathe, & Santoro, 2015). Remote sensing can be defined as *"the acquisition of information about the Earth's surface without being in physical contact with it"* (Wegmann, Leutner, & Dech, 2016). Satellite imagery is applicable for land surface change detection as it offers repeatable observations at a different spatial scale which in turn can be used for understanding changes caused by both natural and anthropogenic processes

(Verbesselt, Hyndman, Newnham, & Culvenor, 2010).

1.2.1 Optical Remotes Sensing

Data from optical remote sensing has been available for over four decades and has been widely used for land surface monitoring (Joshi et al., 2016). The long time series were particularly useful for this (e.g., the Landsat Thematic Mapper (TM) has been available since 1983, Satellite Pour l'Observation de la Terre (SPOT) since the mid-1980s and data from Moderate Resolution Imaging Spectroradiometer (MODIS) has been available since 1999) (Roy et al., 2014; Vogelmann, Xian, Homer, & Tolk, 2012). With the launch of new sensors, the availability of optical data has dramatically increased (Hostert, Griffiths, van der Linden, & Pflugmacher, 2015) and together with Sentinel-2 observations, a massive amount of data can be acquired. Nevertheless, the primary constraint on optical remote sensing is cloud cover, which limits the sensors from collecting usable data and subsequently decreasing the number of valid observations (Alparone et al., 2015).

1.2.2 Thermal Remote Sensing

Thermal remote sensing uses radiation emitted from objects in the portion of the spectrum between approximately 3 and 14 µm wavelength. According to Planck's law, this is the typical spectral emission range corresponding to the temperature of objects located on the Earth's surface. Natural surfaces as well as man-made objects emit thermal radiation if their temperature is above absolute zero (0 K or −273 °C).

The data obtained from thermal remote sensing are complementary to optical and microwave remote sensing data and therefore can be used synergistically (Alparone et al., 2015). Although there were low-resolution thermal remote sensing data available since the 1960s (NOAA TIROS II), Landsat provides the longest thermal data record which has been widely used for a vast number of applications. With the launch of Landsat-4 TM in 1984, data with a spatial resolution of 60 to 120 m were available in the thermal infrared (TIR) spectrum from 10.5 to 12.5 µm (Cristóbal et al., 2018). Other data, with shorter data records are also available (e.g. Terra ASTER) (Joshi et al., 2016).

1.2.3 Microwave Remote Sensing

Microwave remote sensing uses electromagnetic radiation with wavelengths of centimeters to meters. Land surface characteristics determine the amount of energy that backscatters towards the radar antenna receiving the signal. As active microwave sensors have long wavelengths, SAR images

provide information on surface roughness, orientation and volumetric moisture content. The intensity depends on the signal properties such as wavelength, incidence angle, polarization and scan direction, in addition to the above-mentioned properties of the surface (Inglada, Vincent, Arias, & Marais-Sicre, 2016). Although the information content in radar images is a function of several surface characteristics, the application of microwave data for vegetation monitoring is historically less than optical and NIR data. This is due to several reasons such as complexity of preprocessing (i.e. speckle filtering), availability of long term and dense time series and data distribution policy constraints. Several studies showed the use of observations from global C-band data such as ERS-2 in ASAR (Advanced Synthetic Aperture Radar) and ENVISAT (Environmental Satellite) (Nguyen et al., 2015; Pathe, Wagner, Sabel, Doubkova, & Basara, 2009; Schlaffer, Chini, Dettmering, & Wagner, 2016). Other datasets, such as RADARSAT were used, but were limited to small-scale local studies (Moran et al., 2012). Nevertheless, the availability of long term C-band data allowed the development of automated routines for land cover mapping. This, in turn, can further aid the development of new algorithms based on freely available Sentinel-1 dense time series data.

1.3 Vegetation Dynamics Using Remotely Sensed Time Series Data

As satellite data are acquired at a frequent time, the data can be mapped in a three-dimensional array in space-time (Maus et al., 2016). Remotely sensed time series variables can be categorized in the following groups: geophysical variables, index variables, thematic variables, topographic variables, and texture variables (Hostert et al., 2015). Geophysical variables have a specific physical unit (i.e. surface reflectance, land surface temperature (LST)). In contrast, index variables are dimensionless, such as the Normalized Difference Vegetation Index (NDVI), the Enhanced Vegetation Index (EVI) and other indices or feature space components, such as Tasseled Cap components. NDVI is one of the most commonly used indices, which uses the reflectance in the red and near-infrared (NIR) portions of the electromagnetic spectrum. These time series are particularly valuable as they provide repeatable observations at various scales at which environmental and anthropogenic changes occur (Rogier de Jong, Verbesselt, Schaepman, & de Bruin, 2012). Thematic variables are usually estimated prior to time series analysis based on classification or regression and are often binary data. Topographic variables include data such as height, slope, and surface roughness. However, the most commonly used series are based on synthetic aperture radar (SAR) data in order to generate surface deformation information based on phase. The final group of variables are texture variables such as object size, shape, fragmentation which are not widely used in time series

analysis. Nonetheless, the improvements of algorithms based on spatial and temporal segmentation will lead to the use of these variables (Hostert et al., 2015). Remote sensing time series can be decomposed into three components: a long-term directional trend, seasonal component, and short-term fluctuations (Figure 1.1). These components can be used to analyze land surface dynamics (Kuenzer et al., 2015).

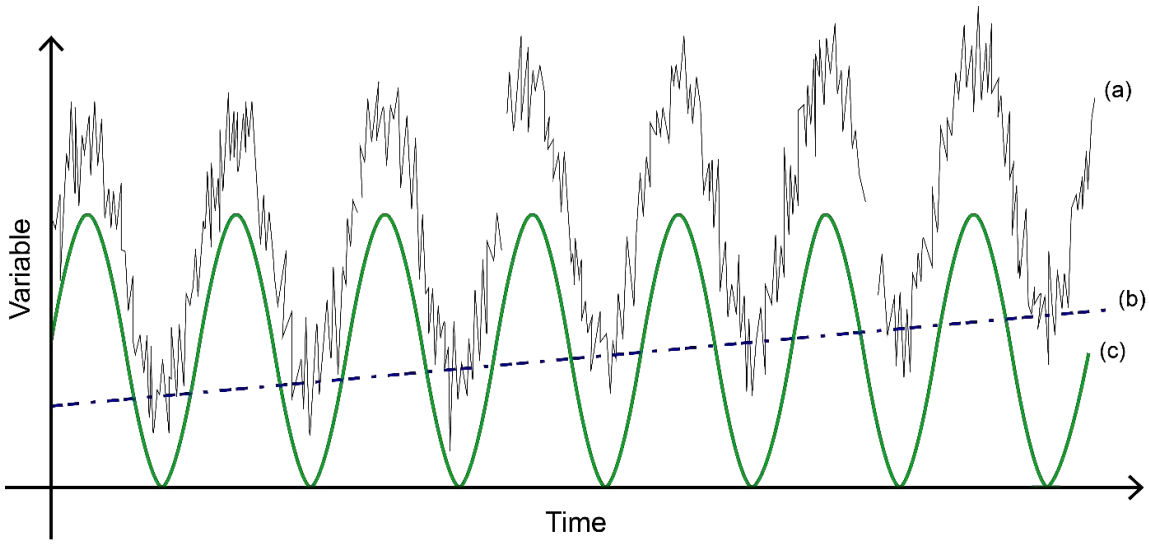

Figure 1.1: Time series components a) raw data, b) trend and c) seasonal component (Adapted from Kuenzer et al. (2015)).

The selection of an algorithm for time series analysis highly depends on land surface processes that should be understood. Generally, any phenology-driven, highly dynamic or gradual and long-term change processes can be analyzed using time series. Nevertheless, data needs for these different processes are not the same: Highly dynamic processes require time series with a sufficient observation frequency as dense time series are needed for capturing even subtle changes. Meanwhile, long-term gradual change can be estimated only when long time series are available. In summary, time series analysis can be based on one or several remotely-sensed derived variables, from which temporal metrics can be extracted, such as maxima or minima of a vegetation index, the slope of a linear trend, function fitted to model seasonal trajectory over several years, or a breakpoint indicating the abrupt change (Fensholt, Rasmussen, Nielsen, & Mbow, 2009; Hostert et al., 2015; Jamali, Jönsson, Eklundh, Ardö, & Seaquist, 2015; S. Wang, Azzari, & Lobell, 2019).

1.4 Crop Monitoring

Monitoring crop type, condition and sown area are critical to support food security. Remotely sensed time-series observations could provide essential and timely information especially in areas

where ground data is not available, is scattered or data is not collected homogeneously (Araya, Ostendorf, Lyle, & Lewis, 2017; Atzberger, 2013; Bégué et al., 2018). Derivation of information on plant phenology and productivity has been shown to be useful for quantitatively analyzing seasonal characteristics of vegetation (Parplies, Dubovyk, Tewes, Mund, & Schellberg, 2016). Crop phenology, the timing of seasonal activity, is describing the continuous development of plants during the cultivation cycle. It is usually expressed with a numerical scale depicting stages of growth from sowing to harvest (Rogier de Jong et al., 2012). The phenological dynamics of ecosystems, in general reflect the response to inter- and intra-annual dynamics of the climate and hydrologic regimes (Xiaoyang Zhang et al., 2003). Furthermore, the mapping of phenometrics is important as the phenology can be associated with biomass production and crop yield (Meroni, Verstraete, Rembold, Urbano, & Kayitakire, 2014). Besides, these metrics can be used for distinguishing different land cover types and for land use change studies. Remotely sensed derived phenology, commonly referred to as Land Surface Phenology (LSP), is defined as the analysis of spatiotemporal dynamics of the vegetation observed by satellite sensors (de Beurs & Henebry, 2010). It was shown by several studies that LSP is related to plant phenology due to absorption and reflectance of electromagnetic radiation but it is also affected by several factors such as cloud cover, atmospheric scattering, and anthropogenic drivers such as land use change and different management practices that impact the land surface dynamics (Kovalskyy & Henebry, 2009; Verbesselt, Hyndman, Zeileis, & Culvenor, 2010). Several studies have been conducted in order to derive the characteristics of LSP (Bégué et al., 2018). For the majority of cases, optical data from sensors such as AVHRR, MODIS and Landsat have been used for LSP detection. Most of these studies have extracted critical points in the seasonal growth -phenometrics (Parplies et al., 2016) such as start, end of the growing season, the timing of the peak (Figure 1.2) for different biomes, including croplands. Several freely distributed software such as Timesat (Jönsson & Eklundh, 2004) and libraries such as GreenBrown (Forkel et al., 2015) can be used to derive these metrics. In general, microwave data has been used less for agricultural applications, due to the limited number of available datasets and the constraints of data pre-processing. With the launch of Sentinel-1 and freely distributed data with high spatial and temporal resolution new opportunities arise for investigation of multitemporal changes in crop growth and condition (Moran et al., 2012; Schroeder, McDonald, Azarderakhsh, & Zimmermann, 2016).

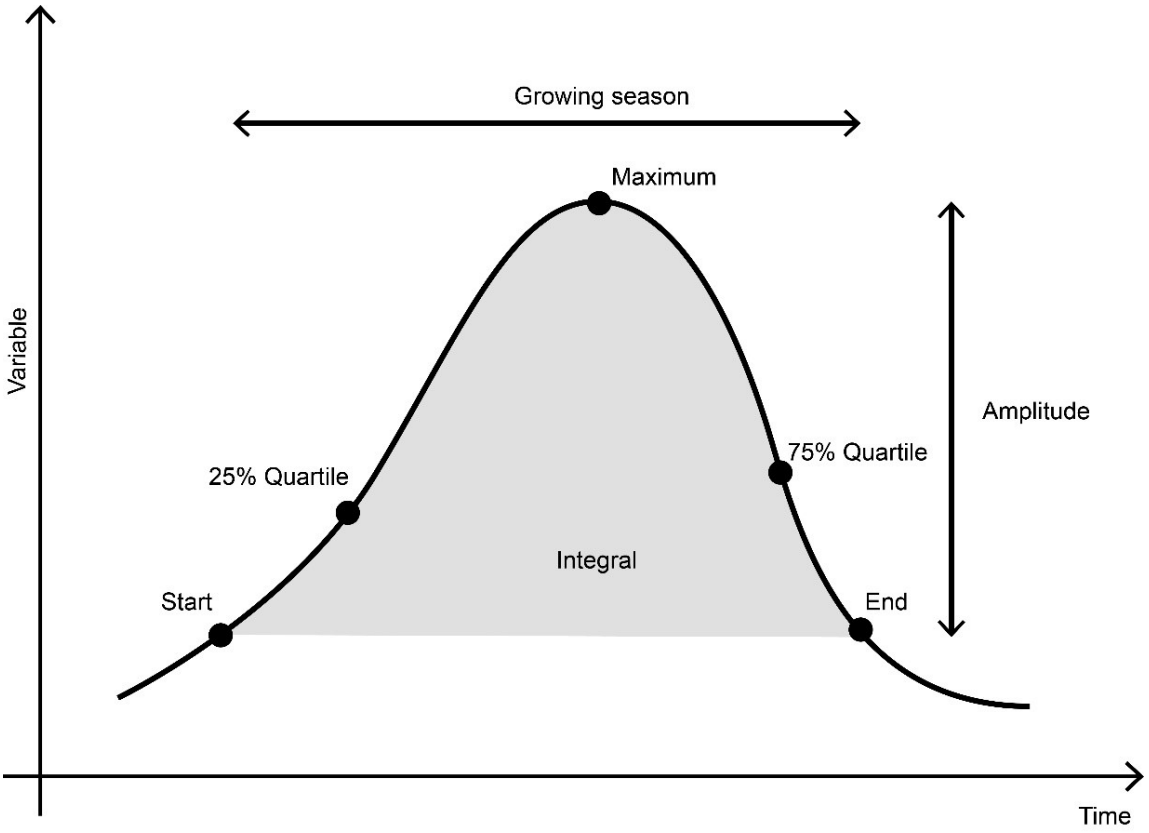

Figure 1.2: Phenometrics that can be extracted from remotely sensed time series (Adapted from Fabian Löw et al. (2017), Parplies et al. (2016)).

1.5 Drought Monitoring

One of the extreme events having an impact on crop production is drought, which can have a drastic impact on food and water security (Sadegh et al., 2017). Based on timing and impact, four types of drought are distinguished: meteorological, agricultural, hydrological and socio-economic which explicitly reflect precipitation deficit, soil moisture deficit leading to crop damages, lack of surface and ground waters, and diverse socio-economic impacts (Figure 1.3) (AghaKouchak et al., 2015; J. Liu & Zhan, 2016; Skakun et al., 2015). Frequent droughts can cause a colossal impact on crop production, which can then affect food prices and threaten food security. Thus, the monitoring of droughts can aid policy making and agricultural planning in order to address food security issues. Furthermore, as drought impact on agriculture is expected to intensify due to aggravating climate change, accurate and timely monitoring and forecasting of droughts crucial (Kogan, 2019).

Remote sensing has been recognized as an effective tool to provide a reliable data source for agricultural drought monitoring at different scales due to its long-term historical archive, periodic observations, and extensive coverage over vast regions. A number of studies of agricultural drought

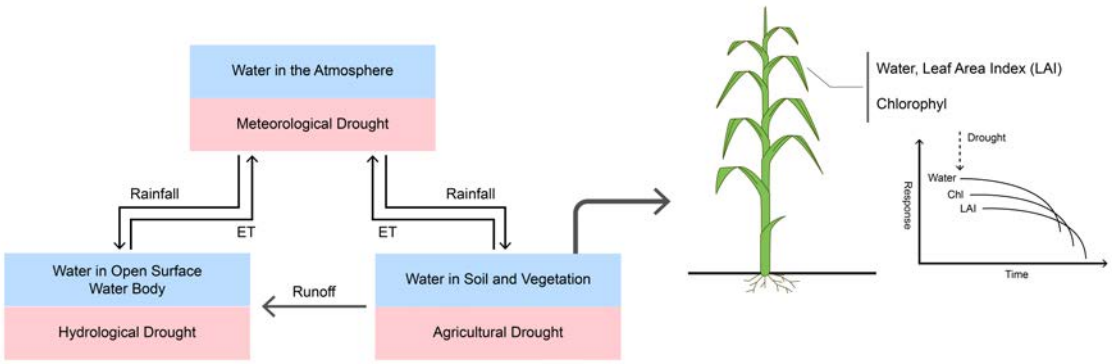

Figure 1.3: Primary remote sensing proxies of crop condition change related to water availability (Adapted from Yuting Zhou et al. (2017)).

monitoring have been carried out using AVHRR and MODIS time series (Anyamba, 2011; Graw et al., 2017; Hazaymeh & Hassan, 2016; Klisch & Atzberger, 2016).Especially, MODIS data have been widely used for regional drought monitoring due to moderate spatial resolution and frequent revisit time (Kogan, 2019). Other datasets, such as Landsat, has been used to assess moisture scarcity and vegetation condition (Ghaleb, Mario, & Sandra, 2015; Urban et al., 2018).

1.6 Remotely Sensed Data Fusion

Most of the land surface monitoring tasks benefit from dense time series observations, as denser and more consistent data can provide timely information on land surface changes (Chastain, Housman, Goldstein, & Finco, 2019; X. Zhu et al., 2018) . The increasing availability of complementary data from different sensors can significantly support the accurate and timely identification of land use and land cover information and quantify subtle and abrupt changes. The integration of multimodal data makes it possible to increase the diversity of data and ensure scalable surface change characterization, even if the data is not available from one of the data sources. As discussed in the previous section, VIR provides multi-band observations influenced by sun illumination and cloud cover. In contrast, SAR delivers texture, geometry, and moisture-sensitive information. Examples of integration of optical and SAR data exist for applications such as land cover and land use classification (Chang & Bai, 2018).Thermal data can further aid the estimation of land surface temperature and assessment of energy balance and water use dynamics (Figure 1.4).

One of the essential methods for data fusion is spatiotemporal data fusion. As most of the data have different spatial and temporal scales, careful data preparation is needed before data integration. Usually it is applied for fusing satellite images from two sensors: data with high

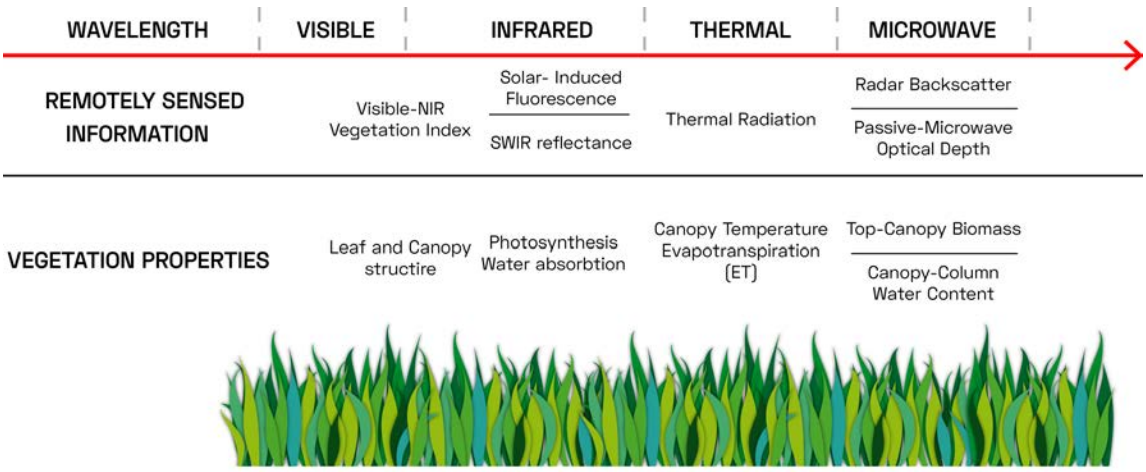

Figure 1.4: Remotely sensed data and corresponding vegetation properties that can be derived.

temporal but coarse spatial resolution (e.g. MODIS), is integrated with imagery which has a higher spatial resolution but lower temporal granularity (e.g. Landsat and Sentinel-2) (F. Gao et al., 2015). The output of spatiotemporal data fusion are synthesized images with higher temporal frequency and spatial resolution. Nevertheless, the algorithm can be used for two sensors with similar spatial and temporal characteristics. This will yield consistent generated datasets, such as harmonizing Landsat and Sentinel-2 images (X. Zhu et al., 2018).

Chapter 2

Thesis Scope

2.1 Thesis Objectives and Research Questions

Currently, several long-term satellite time series are available, such as the Landsat archive, which is the longest open-access data archive (Bhandari, Phinn, & Gill, 2012; Joshi et al., 2016). Along with Landsat, other satellite sensors with complementary data are also available (e.g., Advanced Very High Resolution Radiometer (AVHRR), Advanced Spaceborne Thermal Emission and Reflection Radiameter (ASTER), MODIS). Moreover, the Sentinel satellites of the Copernicus program started offering high-resolution EO data at frequent intervals.

With the increasing availability of data, not only the length of the time series is increasing, but the spatial and spectral properties of new datasets are continuously improving. Particularly, if we look at the volume of the generated data, we can observe that it took several decades for Landsat to reach a PB (petabyte), meanwhile the observations of Sentinel-2 reached a PB of volume in only two years [1]. These increasing data volume also suggests that greater amounts of thematic information is begin collected. The integrated use of these datasets can aid the derivation of detailed information on land surface changes and attribution of these changes to different environmental or anthropogenic drivers.

The overall goal of this dissertation is to increase the understanding of land surface changes in Ukraine at multiple scales through analysis of change patterns with the use of multi-sensor remotely sensed time series (Figure 2.1). In order to develop a methodology that can be utilized for achieving this goal, the following research questions are addressed:

Research Question I: To what extent can the variation of NDVI be explained by environmental conditions?

[1] The size of the datasets was estimated based on publicly available data on Google Earth Engine data catalog.

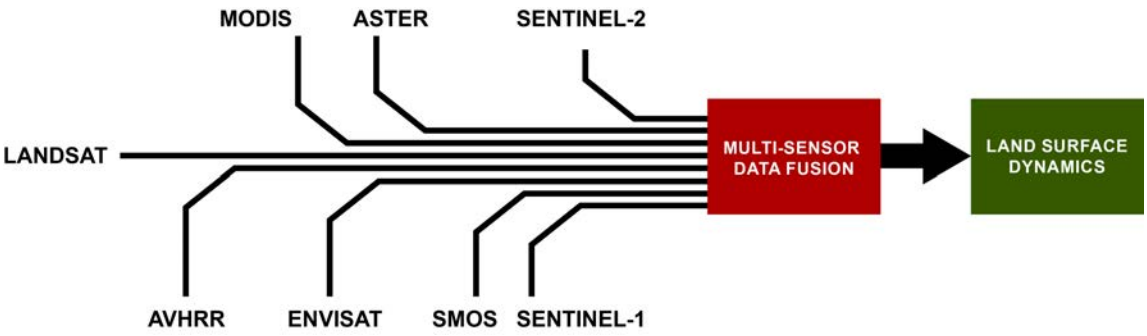

Figure 2.1: Conceptual framework

While several studies derived long term trends in NDVI and attempted explaining the variability in the last decade, the spatially and temporally consistent mapping of the changes and coupling it with environmental factors is still challenging. The objectives related to Research Question 1 are:

- To assess the long-term land surface variability
- To estimate the effects of the essential environmental variables on different land cover types.

The use of coarse scale proxies of vegetation dynamics and environmental conditions can give us spatially explicit information regarding vegetation activity, but for the regional to local analyses, more detailed information is needed. This detailed information is especially crucial for agricultural monitoring, as field scale knowledge can be essential for land management and decision making. In order to derive seasonality metrics which describe different crops, the second research question of the dissertation is:

Research Question II: How can the vegetation seasonality derived from RS contribute to agricultural monitoring? The objectives related to Research Question 2 are:

- To develop a two-step procedure for crop classification and identify crop types based on within-season temporal dynamics
- To identify a favorable selection of input data derived from multiple sources of remote sensing data and from different time intervals of multisource datasets
- To test the suitability of different machine learning algorithms

Remotely sensed derived time series can be used for not only differentiating crop types, but also they can give valuable information about the crop growth and condition during the growing season. Based on this, the third research question was formulated:

Research Question III: How much information can be derived from time series to study crop condition?

The objectives related to Research Question 3 are:

- To investigate features derived from optical sensors and Synthetic Aperture Radar (SAR) imagery for drought-induced crop condition monitoring
- To investigate the spatial variability of drought-impacted fields

With the growing variety and the increasing volumes of available information effective data handling is getting highly important, particularly for tracking vegetation dynamics over several time scales. More emphasis should be given to the adequate characterization of the strengths and limitations of specific remote sensing tools and products, the results of which should be communicated to different user groups.

Research Question IV: How can the multi-source data and analysis methods be used for vegetation monitoring at different scales?

The objectives related to Research Question 4 are:

- To derive optimal data and indicators for vegetation monitoring
- To identify characteristics of vegetation at different spatiotemporal scales
- To integrate product related to vegetation condition and change in an easy to access web application for large-scale information extraction.

2.2 Thesis Structure

Figure 2.2 displays the structure of the research. The first line of research was developed towards the analysis of interannual changes based on AVHRR data. Particularly, the main trends during the extended time period, the breakpoints and the impact of environmental factors were discussed in Chapter 3. The second line of the research focuses on data integration for local level crop classification and condition monitoring. Specifically, we aimed at deriving detailed information about seasonal changes based on Landsat like optical data and Sentinel-1, as highlighted in Chapter 4 and 5. The integration of the results in a web application accessible for users is presented and discussed in Chapter 6.

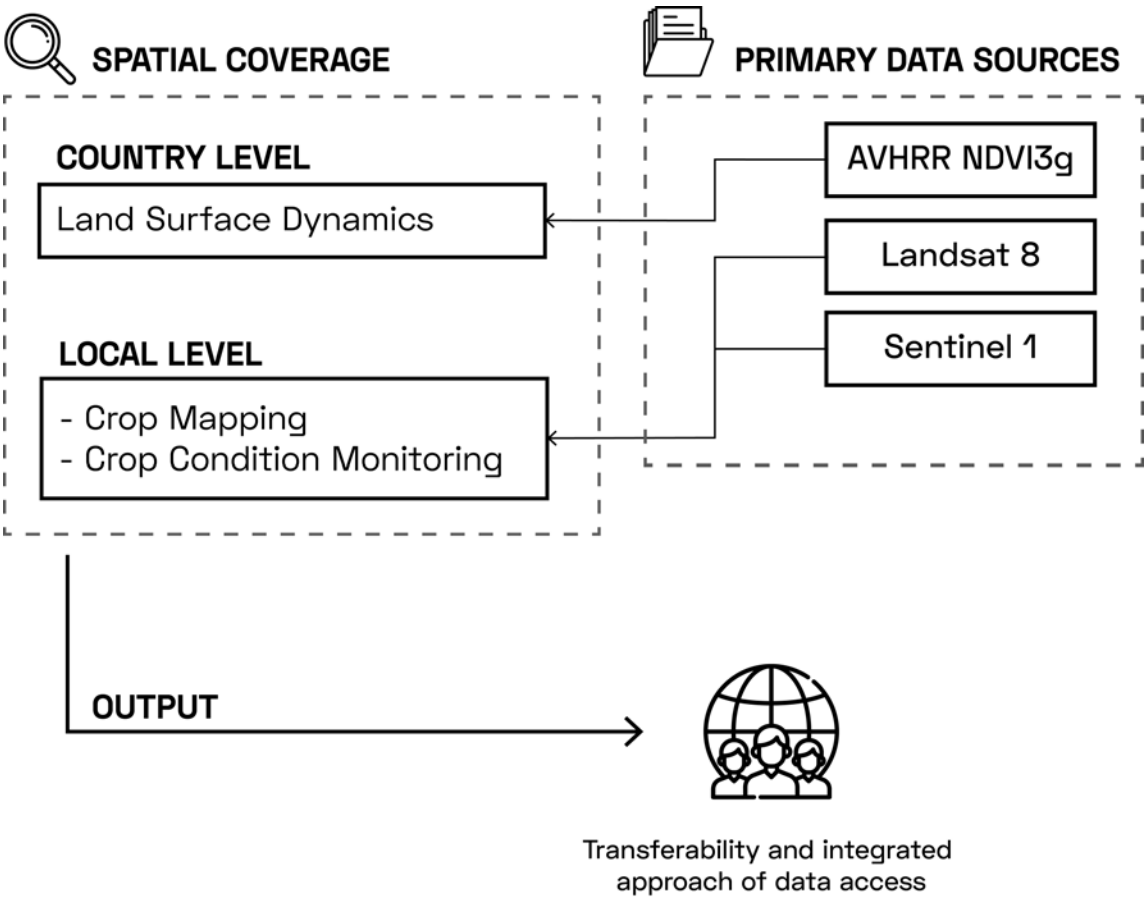

Figure 2.2: Thesis structural components and associated data

Question I	**To what extent can the variation of NDVI be explained by environmental conditions?**	
Hypothesis	The spatiotemporal variation of NDVI are driven by multiple processes and is influenced by precipitation, temperature and soil moisture.	
Verification	**Theoretical and thematic aims** - Understanding of spatial and temporal changes in land surface	**Methodological aims** - Estimation of trends and abrupt changes - Integration of gridded environmental variables
Question II	**How can the vegetation seasonality derived from RS contribute to agricultural monitoring?**	
Hypothesis	Intra-seasonal variability derived from RS time series can improve crop type identification.	
Verification	**Theoretical and thematic aims** Monitoring of cropland extent and spatial distribution	**Methodological aims** - Fusion of optical and SAR - Test of several machine learning algorithms - Optimal input selection
Question III	**How much information can be derived from time series to study crop condition?**	
Hypothesis	Remotely sensed derived time series are sensitive to changes during crop development.	
Verification	**Theoretical and thematic aims** - Estimation of drought impacted vegetation stress and spatial extent	**Methodological aims** - Derivation of parameters for crop condition analysis - Combined use of optical and SAR datas
Question IV	**How can the multi-source data and analysis methods be used for vegetation monitoring at different scales?**	
Hypothesis	It is possible to provide near real-time customizable geospatial data products derived from different sensors.	
Verification	**Theoretical and thematic aims** - Comparison of the RS metrics from different sensors	**Methodological aims** - Development of a web-based platform for information derivation

Table 2.1: The main components of the thesis: Research questions, hypotheses and associated specific aims

2.3 List of Publications

As described above, the thesis is structured into four main research chapters following this introduction. Each of these chapters consists of one stand-alone manuscript published or submitted for publication to a peer-reviewed journal and presented in international conferences. In particular, Research Question I is covered by Chapter III whereas Research Question II is covered by Chapter IV and Research Question III by Chapter V (submitted to journal) and Chapter VI discusses the data accessibility. The dissertation is synthesized in Chapter VI. The publications and manuscripts presented were edited to have a common style in this doctoral thesis. Modifications were applied to the numbering of figures and tables, and citation style. As a result all references were integrated into one reference list.The text, figures, and contents of tables agree with the original publications, with the exception for figure 6.4 which was modified from the original published version.

A reference list of these papers is given below:

Peer Reviewed Journals:

- Ghazaryan, G., Dubovyk, O., Kussul, Schellberg J. (2019). Local Scale Agricultural Drought Monitoring with Satellite-based Multi-sensor Time-series (submitted to journal).

- Ghazaryan, G., Dubovyk, O., Löw, F., Lavreniuk, M., Kolotii, A., Schellberg, J., Kussul, N. (2018). A rule-based approach for crop identification using multi-temporal and multi-sensor phenological metrics. European Journal of Remote Sensing, 51(1), 511-524.

- Ghazaryan, G., Dubovyk, O., Kussul, N., Menz, G. (2016). Towards an Improved Environmental Understanding of Land Surface Dynamics in Ukraine Based on Multi-Source Remote Sensing Time-Series Datasets from 1982 to 2013. Remote Sensing, 8(8), 617.

Conference Proceedings:

- Ghazaryan, G., Dubovyk, O., Graw, V., Schellberg, J. (2018, October). Vegetation monitoring with satellite time series: an integrated approach for user-oriented knowledge extraction. In Remote Sensing for Agriculture, Ecosystems, and Hydrology XX (Vol. 10783, p. 107830W). International Society for Optics and Photonics.

Chapter 3

Towards an Improved Environmental Understanding of Land Surface Dynamics in Ukraine Based on Multi-Source Remote Sensing Time-series Datasets from 1982 to 2013

Abstract: Ukraine has experienced immense environmental and institutional changes during the last three decades. We have conducted this study to analyze important land surface dynamics and to assess processes underlying the changes. This research was conducted in two consecutive steps. To analyze monotonic changes we first applied a Mann–Kendall trend analysis of the Normalized Difference Vegetation Index (NDVI3g) time series. Gradual and abrupt changes were studied by fitting a seasonal trend model and detecting the breakpoints. Secondly, essential environmental factors were used to quantify their possible relationships with land surface changes. These factors included soil moisture as well as gridded air temperature and precipitation data. This was done using partial rank correlation analysis based on annually aggregated time-series. Our results demonstrate that positive NDVI trends characterize approximately one-third of Ukraine's land surface, located in the northern and western areas of the country. Negative trends occurred less frequently, covering less than 2% of the area and are distributed irregularly across the country. Monotonic trends were rarely found; shifting trends were identified with a greater frequency. Trend shifts were seen to occur with an increased frequency following the period of the 2000s. We determined that land surface dynamics and climate variability are functionally interdependent; however, the relative influence of the drivers varies in different locations. Among the factors analyzed, the air temperature variable explains the largest portion of NDVI variability. High air temperature/NDVI correlation coefficients ($r = 0.36 - 0.77$) are observed over the entire country. The soil moisture content is of significant influence in the eastern portion of Ukraine ($r = 0.68$); precipitation ($r = 0.65$) was most influential in the central regions of the country. These results increase our understanding

of ecosystem responses to climatic changes and anthropogenic activities.

3.1 Introduction

Ukraine has experienced immense environmental and institutional changes during the last three decades due to both human-induced and environmental processes such as socio-economic transformation, ongoing urbanization, increased climate variability and frequency of hazardous events (Baumann et al., 2011; Kovalskyy & Henebry, 2009). The drastic social, institutional and economic alterations at the end of 1991 as a result of the Soviet Union collapse induced significant changes in distribution and extent of land cover, land use intensity, economic productivity in the agricultural sector and shifts in the land surface phenology (Kovalskyy & Henebry, 2009; Kuenzer et al., 2015). These socio-economic changes had radical results and one of the consequences was the widespread farmland abandonment especially in the northern and western regions (Alcantara et al., 2013; Baumann et al., 2011; Hostert et al., 2011; Schierhorn et al., 2013; Smaliychuk et al., 2016). Besides the ongoing socio-economic transformations, several studies discussed the changes in climate conditions. In the past 30–50 years, droughts have become more frequent and intense, covering up to half of the area of Ukraine every 10–12 years, and up to 20% every 2–3 years (Adamenko & Prokopenko, 2011). All these described alterations had an impact on the ecosystem that can be reflected on the land surface. To understand the effect of these phenomena, long-term monitoring of land surface changes is required. There is a limited number of studies on long-term land surface change analysis for all of Ukraine, as previous studies focused on specific applications of land cover change (e.g., forest loss, farmland abandonment) in particular areas of the country (Carpathian ecoregion, the river basin of the Dnieper river) (Baumann et al., 2011; Kovalskyy & Henebry, 2009; Kuemmerle et al., 2009). Moreover, little attention has been paid to the understanding of the main drivers of these changes as most of the studies focused on the factors influencing land abandonment (Baumann et al., 2011; Meyfroidt, Schierhorn, Prishchepov, Müller, & Kuemmerle, 2016). Satellite image time series observations of land surface reflectance and vegetation indices, such as Normalized Difference Vegetation Index (NDVI) calculated from them, are often used for land surface change analysis as NDVI uses the spectral differences between red and near-infrared reflectance and as a result exposes the properties of ecosystem (Kirsten M. de Beurs, Henebry, Owsley, & Sokolik, 2015). NDVI-based trend analysis can assist the investigation of changes of land surface over a period of time and help to understand the mechanisms behind the observed changes. This is because NDVI is not only related to a variety of vegetation properties (structural

properties of plants, vegetation productivity) (Dubovyk et al., 2013; Forkel et al., 2013), but it can also indirectly represent the ecosystem conditions (Baldi et al., 2008). For instance, several studies used NDVI as a proxy of land cover change (Waylen, Southworth, Gibbes, & Tsai, 2014) and land dynamics (J. Chen et al., 2014), land degradation (Ibrahim, Balzter, Kaduk, & Tucker, 2015), farmland abandonment (Estel et al., 2015), and phenological changes (de Beurs & Henebry, 2010). Based on these complex characteristics of NDVI, we assume that it can be used to assess land surface dynamics over time. In the context of this study, we define land surface dynamics as the sudden or gradual transformation or modification of earth surface including vegetation, soil, water and its ecosystem functioning in the unit of time (e.g., day, month, year) including fast (e.g., land use change) and slow processes (e.g., land degradation), which can indicate the response to both anthropogenic and environmental factors (Dubovyk et al., 2013; Forkel et al., 2013; Verbesselt, Zeileis, & Herold, 2012). The detection of significantly increasing or decreasing trends is often not enough to assess the environmental impact or to be able to attribute the change to factors behind it. Abrupt changes or non-linearities may occur within the long-term time series, as the trends in complex systems usually are not monotonously increasing or decreasing (R. de Jong & de Bruin, 2012; Teferi, Uhlenbrook, & Bewket, 2015; Verbesselt et al., 2012). Furthermore, the interpretation of these abrupt changes without using additional datasets or expert knowledge is often challenging (Jamali et al., 2015). In this regard, the overall aim of this research was not only to analyze the land surface dynamics over all of Ukraine for the time period from 1982 to 2013 but also to assess underlying processes and drivers of the changes. The specific objectives were: (1) to assess long-term land surface variability, (2) to integrate data from different sensors and investigate the suitability of different methodologies, and (3) to estimate the effects of the essential environmental variables namely soil moisture, air temperature and precipitation on land surfaces. Our study is, therefore, the first study that analyzed spatiotemporal changes of land surface over all of Ukraine for the long time period of 30 years to provide integrated and spatially continuous knowledge of the changes and its triggers using remote sensing approaches.

3.2 Materials and Methods

3.2.1 Study Area

Ukraine is located in Eastern Europe in the southeastern part of the East European plain, between 44°20'N and 52°20'N latitudes and 22°5' E and 41°15' E longitude (Figure 3.1). It covers 603,550 km^2 and consists of 24 administrative units (oblast) (State Statistics Service of Ukraine). Most

of Ukraine is composed of vast plains stretching north from the Black and Azov Seas. There are also two mountainous areas in the west and south of the country, the Carpathians and Crimean Mountains, respectively. The climate in the East European Plain, the medium Ukrainian Carpathians, and the Crimean Mountains is mostly temperate continental, with hot summers ($t > 18\,°C$) and cold winters ($t < -5\,°C$); the southern coast of the Crimea has a subtropical Mediterranean climate (FAO, 2008). The area of Ukraine is divided into three main agro-ecological zones: steppe (southern and eastern regions, 40% of the area), semi-steppe (central regions) and mixed forest (north and north-west) (Smaliychuk et al., 2016; Zastavnyi, 1994) (Figure 3.1).

Despite the prevailing moderate continental climate, the study area is characterized by fairly significant differences in the humidity, temperature and length of the growing season (Shishenko & Munich, 2008). Hot and relatively dry summers, together with relatively severe winters, create good conditions for the formation of chernozems (black soils) that are highly fertile for most agricultural crops (Nazarov, Cook, & Woodgate, 2001). The average winter temperature ranges from $-8\,°C$ to $-12\,°C$. In the southern regions, the mean winter temperature is $0\,°C$. The mean summer temperature ranges from $18\,°C$ to $25\,°C$, although it can reach above $35\,°C$.

The area of Ukraine is characterized by significant regional differences in rainfall and its distribution throughout the year with a summer maximum. The largest amplitude of the volume is characteristic to the south. Most of the precipitation falls in the Ukrainian Carpathians (more than 1500 mm per year). The precipitation ranges from 650 mm (in the west) to 400 mm (in the southeast). In dry years, precipitation is significantly reduced: in the coastal areas of the Azov and Black Seas up to 100 mm, in the steppe up to 150–200 mm, and in forest-steppe up to 250–350 mm. In winter, permanent snow cover occurs almost everywhere in the country. One of the key features of the climate of Ukraine are the droughts which in recent years have increased frequency and affect large areas (Adamenko & Prokopenko, 2011; Shishenko & Munich, 2008; Skakun et al., 2015).

3.2.2 Data

Normalized Difference Vegetation Index

As a primary data source for the regional study the Global Inventory Monitoring and Modeling System (GIMMS) NDVI3g dataset was chosen as it is the only currently available dataset that spans since 1982 and includes a dense time series needed for the analysis of land surface dynamics. The GIMMS NDVI3g dataset is an improved 8 km NDVI dataset produced by the National

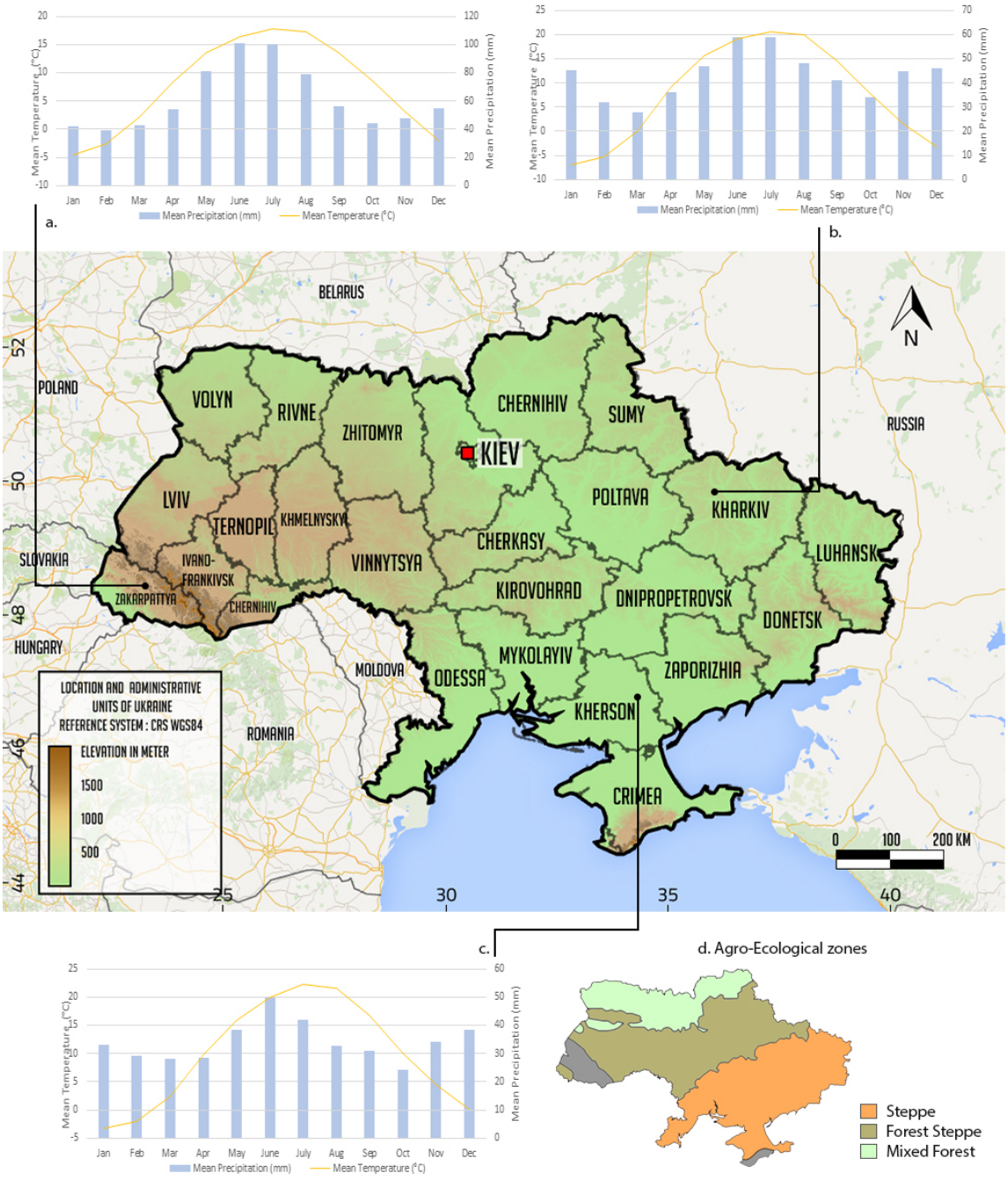

Figure 3.1: Primary remote sensing proxies for crop water stress observation (3.1d adapted from Smaliychuk et al. (2016)).

Oceanic and Atmospheric Administration (NOAA) Advanced Very High Resolution Radiometer (AVHRR) instruments that extend from July 1981 to December 2013 (Forkel et al., 2013; Pinzon & Tucker, 2014). The third generation GIMMS NDVI is a 15-day Maximum Value Composite that was acquired from seven different NOAA satellites (7, 9, 11, 14, 16, 17, 18), which have been

processed using an adaptive Empirical Mode Decomposition. NDVI3g is appropriate for long-term studies of land surface trends in vegetation, seasonality and coupling between climate variability and vegetation over the last three decades (Atzberger, Klisch, Mattiuzzi, & Vuolo, 2013; Eastman, Sangermano, Machado, Rogan, & Anyamba, 2013). The NDVI3g has different quality flags (Ibrahim et al., 2015). Based on these flags, prior to analysis, all values with reduced quality were excluded. We used pixels with minimum 75% valid data excluding interpolated observations, possible snow covered pixels. In addition, the images for the year of 1981 were also excluded to have full-year observations. The maximum value compositing approach was applied in the NDVI3g dataset.

Environmental Variables

Several studies discussed the effects of climate variability on land surface change (Kirsten M de Beurs & Henebry, 2004; Rogier de Jong, Schaepman, et al., 2013; Evans, Pitman, & Cruz, 2011). The monthly mean temperature (TMP) and precipitation total (PRE) datasets were obtained from the Climate Research Unit (CRU). The datasets cover the period 1901 to 2014 with a spatial resolution of 0.5° (Harris, Jones, Osborn, & Lister, 2014). Recent studies also show the impacts of soil moisture on vegetation at various temporal scales (Dorigo et al., 2012; Evans et al., 2011; Y. Y. Liu et al., 2011). They discuss the co-variation of NDVI and soil moisture, stating coherent trend changes (T. Chen, de Jeu, Liu, van der Werf, & Dolman, 2014). Furthermore, other authors showed that a soil moisture NDVI pixel-wise residual trend indicates land degradation (Ibrahim et al., 2015). Soil moisture influences hydrological and agricultural processes, runoff generation, drought development and other processes. A soil moisture dataset ("ESA CCI Soil Moisture," n.d.; Y. Y. Liu et al., 2011) was chosen for the study, which was a merged product of active and passive microwave soil moisture products. The dataset covering the period 1978–2013 provides daily surface soil moisture with a spatial resolution of 0.25°and depicts the soil moisture in around 2 cm layer depth ("ESA CCI Soil Moisture," n.d.). Therefore, we chose the following environmental variables precipitation, temperature and soil moisture for the analysis. In addition, we used a land cover map (Lavreniuk, Kussul, Skakun, Shelestov, & Yailymov, 2015) of 1990 as a reference (the main institutional changes happened after 1990) to characterize the possible associations of the environmental variables and NDVI in main vegetation formations: cropland, grassland, and forest, which have different seasonal characteristics and response to the disturbances (Lavreniuk et al., 2015).

3.2.3 Methods

Prior to processing, the raster time series datasets were reprojected to World Geodetic System (WGS) 84 coordinate reference system and resampled to a common 8 km grid, using a bilinear interpolation algorithm. The datasets were further smoothed with Savitzky-Golay filter as the datasets were not extremely noisy, and we intended preserving the local variations (Eklundh & Jönsson, 2015). We extracted the temporal window (1982–2013) of the environmental time series to match the same period with NDVI dataset. The water bodies and build up areas were masked out. All the analyses were conducted using R statistical software (R Core Team, 2016).

Trend Analysis

After the pre-processing of the image time series (1982–2013), we explored the trends of annually aggregated NDVI series. There are several methods described in the literature for time series analysis of satellite imagery (Dubovyk et al., 2013; Forkel et al., 2013; Verbesselt et al., 2012). The simplest and most common method is the ordinary least-squares (OLS) regression, where the main assumption is that the land surface is changing linearly and gradually over time (R. de Jong & de Bruin, 2012). The drawbacks of this method have been depicted by several authors (R. de Jong & de Bruin, 2012; Jamali et al., 2015). In particular linear regression assumes normality and independence of data (neglecting the temporal autocorrelation). To overcome this, we used the Mann–Kendall nonparametric trend test, which does not depend on the distribution of data and can be used with data with serial dependence. Tüshaus, Dubovyk, Khamzina, and Menz (2014) demonstrated the performance of trend analysis with the aforementioned method for the land surface dynamics monitoring. This non-parametric test evaluates the occurrence of a monotonic single direction trend in the time series (Tüshaus et al., 2014). Furthermore, non-stationarity (time dependency) was excluded due to a significant Augmented Dickey-Fuller test and inspection of the autocorrelation graphs and the related tests of annually aggregated time series. However, the land surface dynamics are not always a gradual process and often the changes are abrupt due to factors such as extreme weather conditions or changes in land management. In general, the changes that can be monitored using remotely sensed data can be classified as follows: (1) a seasonal or cyclic change; (2) a gradual change over time consistent in direction (monotonic); and (3) an abrupt shift at a specific point in time (Rogier de Jong et al., 2012; Verbesselt et al., 2012). To study sudden and gradual changes in land surface, the Break For Additive Season and Trend (BFAST) algorithm was used, (R Core Team, 2016) which decomposes the series into trend, seasonal and reminder components to evaluate gradual and seasonal dynamics occurring within indices derived

from satellite image time series such as NDVI (Rogier de Jong, Verbesselt, Zeileis, & Schaepman, 2013; Horion et al., 2016; Verbesselt, Hyndman, Newnham, & Culvenor, 2010). The season-trend model (i.e., linear trend and harmonic component) was fitted to pre-processed monthly NDVI time series, and the stability of the model was assessed using a test that determines the significance of structural trend breaks. As we were focusing on trajectories of the changes, rather than the number of the breakpoints, we chose the model with either 0 or 1 breakpoints. These breakpoints were assumed to catch the most influential trend shifts in the time series, which represent drastic changes in ecosystem functioning (Rogier de Jong, Verbesselt, Zeileis, & Schaepman, 2013; Horion et al., 2016). We classified the trends based on the modified methodology described by Rogier de Jong, Verbesselt, Zeileis, and Schaepman (2013). The authors used the term greening/browning for categorizing the changes based on the signal before and after the breakpoint. Instead of the above-mentioned terms, we used the concept of increase or decrease of the NDVI trends.

Correlation Analysis

We used correlation analysis to investigate the effects of essential environmental variables, namely soil moisture, air temperature and precipitation on variability of NDVI. Correlation analysis is one of the commonly used methods for assessing the associations between vegetation indices and independent variables. In the case of simple correlation, the linear relationship between two variables is determined. The disadvantage of such an approach is that the effect of other variables is ignored. For example, when the correlation between soil moisture and NDVI is studied, the impact of other factors, such as precipitation and temperature, on NDVI is disregarded. To reflect the internal relation between two variables, a partial correlation coefficient should be calculated. Partial correlation coefficients reveal the relation between two variables when controlling the impact of other variables. As a result, when two variables are both linked to the third, only the relation between the former two variables is estimated while the impact of the third variable is removed (Peng, Li, Tian, Liu, & Wang, 2015). Partial Spearman correlation is nonparametric in the form of relationship, and it is robust against outliers and invariant against monotone transformation.

3.3 Results and Discussion

Trends of NDVI Series

Figure 3.2 shows the results of the non-parametric Mann–Kendall trend analysis of annually aggregated NDVI time series from 1982 to 2013 for Ukraine. Areal statistics (Figure 3.2) depict the

occurrence of positive and negative trends in each administrative unit proportional to its area. As changes of environmental conditions are most likely to affect the land-cover classes in a different way (Rogier de Jong, Verbesselt, Zeileis, & Schaepman, 2013), we interpreted the relative influence of each factor based on the spatial context of the observed associations i.e., land cover class and the agro-ecological zone. Overall, around one-third of the area of Ukraine is characterized by significant positive trends, clustered mainly in northern and western parts, which are mostly in the relatively humid and temperature limited area with forests and forest-steppe zones. These areas are also characterized by less frequent crop cultivation and observed land abandonment processes (Estel et al., 2015). The secondary succession on the former croplands is captured by a positive trend signal in our analysis.

Around 30% of cropland is characterized by positive trends, which also indicates changes in agricultural practices. A large cluster of the positive trend was identified in the northwest from Kiev, where the Chernobyl zone is located. This area has been closed since 1986 after the occurrence of the Chernobyl disaster, which is one of the major anthropogenic disasters of the last century. Within the Chernobyl zone, active vegetation growth and environmental recovery are observed and documented (Hostert et al., 2011), which is also reflected in the results of the trend analysis. The observed positive trends in forest cover 32% of its area. This is evident in the areas such as mountainous regions in the Carpathian Mountains in the west of Ukraine and in the Crimean Mountains (Kuemmerle et al., 2009). Statistically significant negative trends were less frequent (<2% of the total area) and are mostly scattered across the country. This could probably be explained by the fact that the area was more dynamic, and, instead of a monotonic trend, land surface was varying over the entire study period. Most of the steppe zone does not reveal significant trends. The steppe zone of Ukraine, sometimes also referred to as the 'bread basket' of Ukraine, is the area where most intensively cultivated lands are located. The absence of the big clusters of significant trends within this part of Ukraine may indicate that, despite the overall socio-economic and environmental processes that have occurred in the country since 1982, these areas were continuously managed in a similar way, which has not led to noticeable land surface trends. It should be emphasized that the analysis of long-term earth observation time series is affected by several factors, such as the spatial resolution of the imagery, the level of temporal aggregation, number of observations, pre-processing steps, and the analysis method itself. The temporal resolution of the time series has an effect on the trend significance estimation. In comparison to the full-resolution time series, the use of annually aggregated data reduces the number of observations, which results in the underestimation of the trend significance. Nevertheless, annual aggregation decreases the

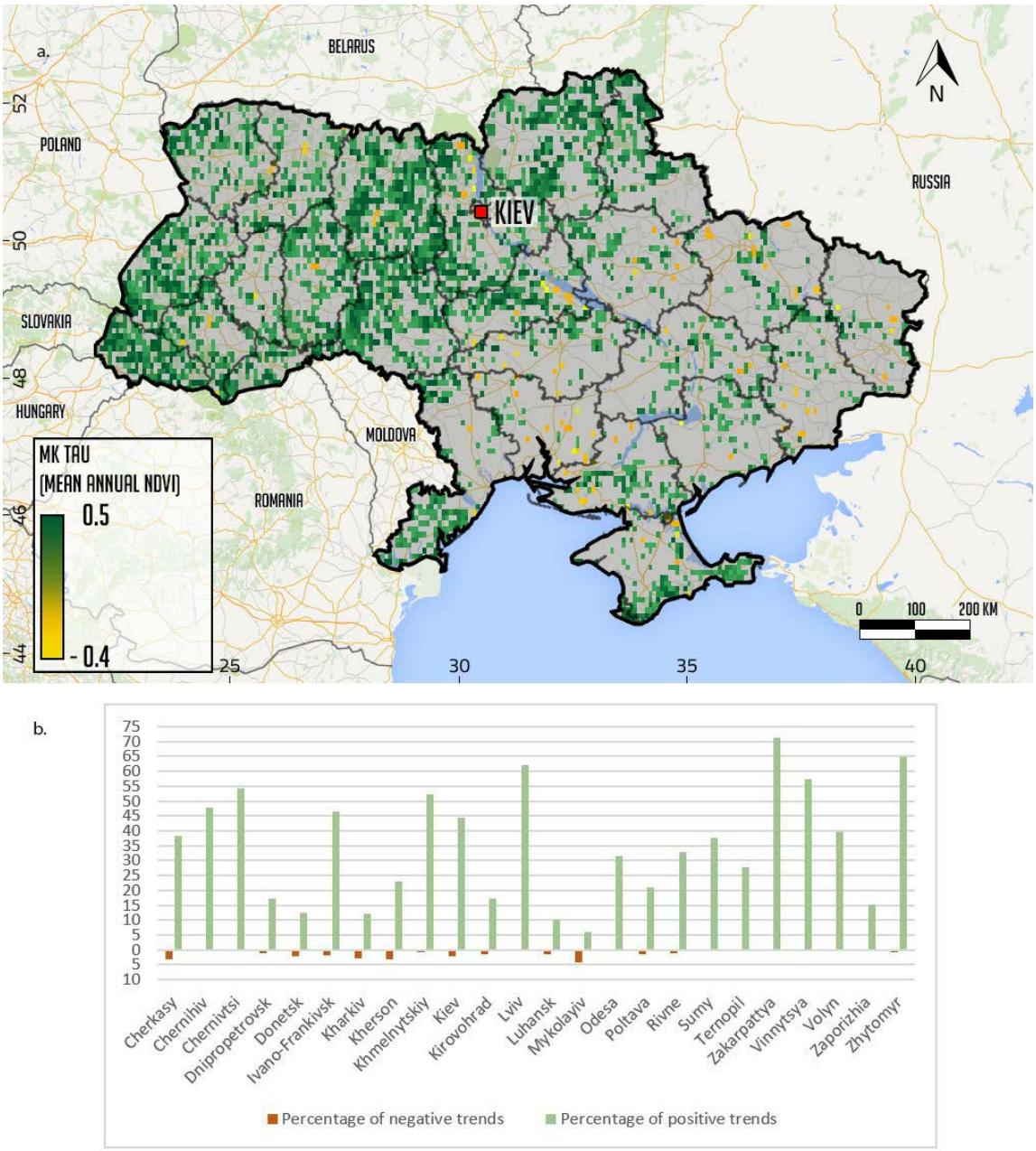

Figure 3.2: Spatial distribution of annually aggregated Normalized Difference Vegetation Index (NDVI) trends for the period 1982 to 2013 (a), and the areal statistics for each region (oblast) (b).

risk of detecting false positive trends (Forkel et al., 2013). Furthermore, the aggregation is an effective method to account for autocorrelation: dependence between successive observations in a time series (Yu Zhou et al., 2015).

Although monotonic trend analysis can reveal the general tendency of land surface changes, the trends are not always continuously increasing or decreasing but can fluctuate over time (Teferi et al., 2015). To account for these changes, a breakpoint analysis was conducted. (Figure 3.3)

illustrates the spatial distribution of change categories. Pixels with insignificant trends ($P \geq 0.05$) were masked out. For each category of land surface change, representative points were selected, and the temporal profiles of NDVI response and the observed trend were studied in detail (Figure 3.3a–d).

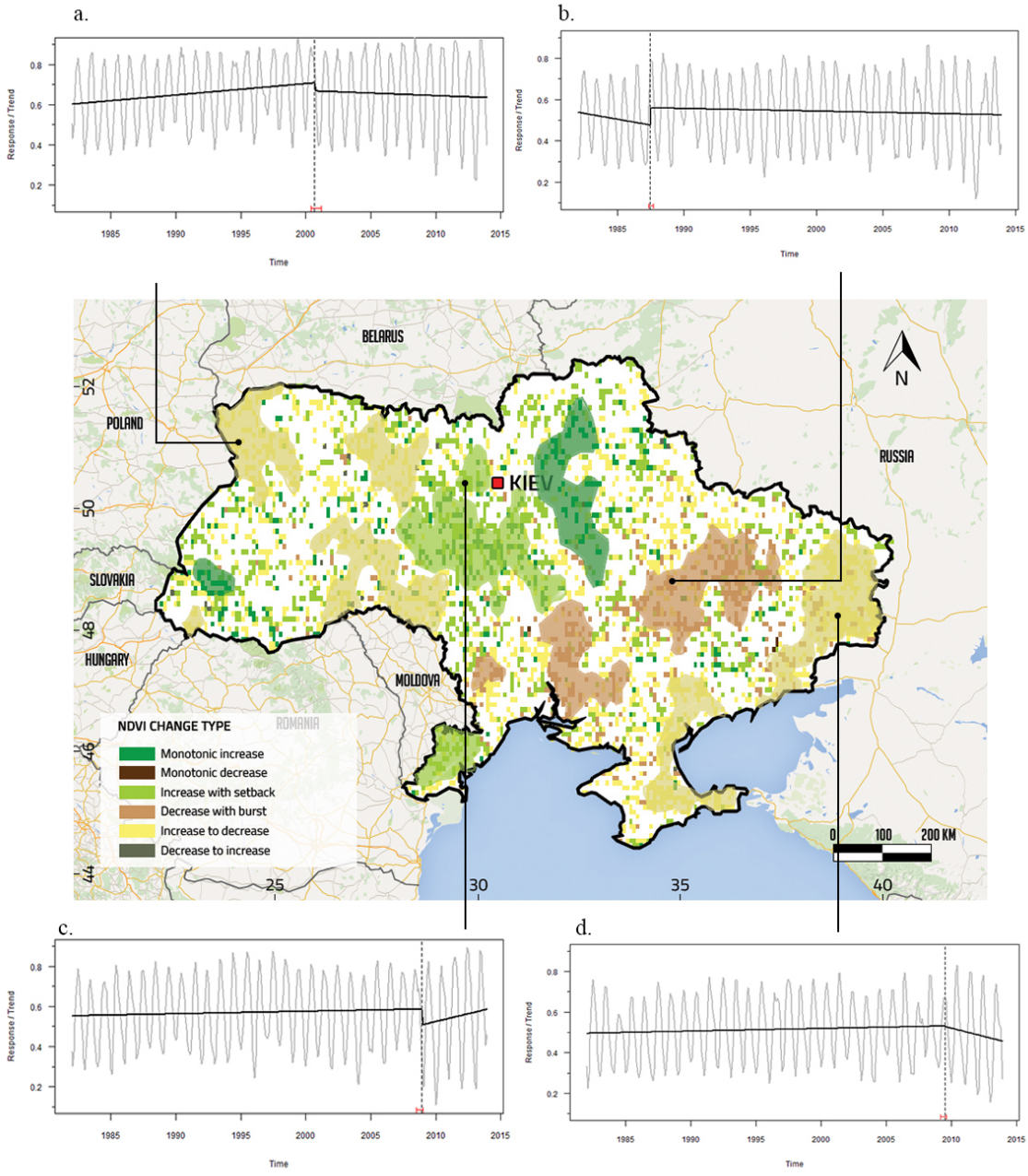

Figure 3.3: Spatial distribution of the change categories. The pixels with significant trends in both segments and significant monotonic trends are represented ($p < 0.05$). Temporal profiles show the most frequent change types. (a) Increase to decrease (b) Decrease with burst (c) Increase with setback (d) Increase to decrease

In general, NDVI varied and pixels with trend shifts prevailed (Figure 3.3). Increasing trends with the shifts is the dominant type covering 28% of Ukraine (Table 3.1). Although the hotspots of the monotonic increase can be noticed (3.67% of the area), the results of the analysis of the change type reveal a higher number of interrupted trends (i.e., increase with setback) and reversal trends (increase to decrease). The interrupted increasing trends could probably be conditioned by human interventions and by the effect of extremely dry periods (observed in 10.24% of the area). The reversal trend indicating trend change from increase to decrease stated the decline of ecosystem functioning. We suggest that these types of changes can be associated with the large socioeconomic disturbances followed by the collapse of the Soviet Union and associated processes of land abandonment after 1991 and land re-cultivation after the 2000s (Alcantara et al., 2013; Smaliychuk et al., 2016). We also evaluated the percentage of change types in each land cover class (Table 3.1)

Trend type	Cropland	Grassland	Forest
Monotonic increase	4.66	7.34	2.53
Decrease with burst	6.96	13.27	0.73
Increase with setback	11.21	24.41	7.43
Increase to decrease	18.97	44.49	10.31

Table 3.1: Percentage of change types in each land cover class.

The estimates reflect the percentage of the trend type within the dominant class, using the land cover information from the 1990 reference year. Generally, the interpretation of these trends is challenging as the trend shifts can be explained by several factors (Rogier de Jong, Verbesselt, Zeileis, & Schaepman, 2013). The reversal trend can be attributed to long-term increasing human pressures (Horion et al., 2016), particularly the cultivation of abandoned croplands, which was also observed by Smaliychuk et al. (2016). Another abundant category of change is the increasing trend with an abrupt negative change, which can be related to the extreme events such as drought. In Ukraine, frequent drought events have been observed during the last 16 years (Skakun et al., 2017). The drought in 2003 in most of the pixels was not detected as a major break and this can be explained by the fact, that in long-term series from 1982–2013, the drought did not have the biggest break in the NDVI trajectory. Furthermore, during the consecutive drought in 2007–2010, the break was not detected in the first year of the drought. The effects of droughts should be further investigated. Another challenge for the interpretation is the spatial resolution of the dataset, as one pixel of NDVI3g dataset can contain diverse land cover types, due to the fragmented landscapes in some regions and the size of the land management units (Chandler & Scott, 2011; Sutton et al.,

2008). Despite of this sub-pixel heterogeneity, the dataset is still representing the large-scale land use/land cover patterns and their spatiotemporal variance over this vast area. The validation of these trends is not straightforward because the field observations are not temporally dense and mostly were restricted to a few-time steps. In addition, the scale compatibility was another issue, as the datasets might be not representative for an 8 km grid (Rogier de Jong, de Bruin, de Wit, Schaepman, & Dent, 2011). To overcome this, we compared our results with the results of the previous studies (Alcantara et al., 2013; Baumann et al., 2011; Hostert et al., 2011; Schierhorn et al., 2013) and investigated the validity of the results by local experts.

Characteristics of the Main Time Periods of the Trend Shifts in Ukraine

To understand the land surface dynamics and the main drivers of its changes, it is essential not only to look at the spatial distribution of the trend shifts but also the timing of these changes. We classified the time of the NDVI changes in three time periods of 1982–1992, 1993–2002 and 2003–2013 as the socio-economic pressures and environmental conditions were different during these periods (Figure 3.4). According to our results, the decrease with the abrupt positive break predominated during the first period of 1982–1992 within the steppe zone of Ukraine, which is the main agricultural zone of the country. This period was the last period before the collapse of the Soviet Union and was still characterized by extensive cultivation and agricultural land expansion in the country.

During the second period (1993–2002), most of the changes occurred in the northwest of Ukraine (Figure 3.4). The first post-socialistic years were described with high abandonment rates as well as with prevailing forest disturbances. The agricultural activities were mostly affected after the collapse of the Soviet Union due to the ongoing transformation processes and structural changes in the agricultural sector at that time. Almost 70% of cropland abandonment occurred within the first 10 years of the transition from a state-command to a market-driven economy (Schierhorn et al., 2013). Since the late 1990s and early 2000s, due to the economic recovery, the re-cultivation of formerly abandoned land emerged (Schierhorn et al., 2013). The last period (2003–2013) was also associated with strong environmental impacts (i.e., droughts and extreme weather conditions) (Adamenko & Prokopenko, 2011; Shishenko & Munich, 2008). Although the effect of sensor change that affected the quality of the AVHRR data is significantly reduced in NDVI3g (Ibrahim et al., 2015; Tian et al., 2015), some research found that GIMMS3g NDVI data are still showing an inconsistency between sensors in humid, dry-sub humid, semi-arid and hyper-arid regions (Tian et al., 2015). As the AVHRR platform changes (1985, 1988, 1994, 1995, 2000 and 2004) could

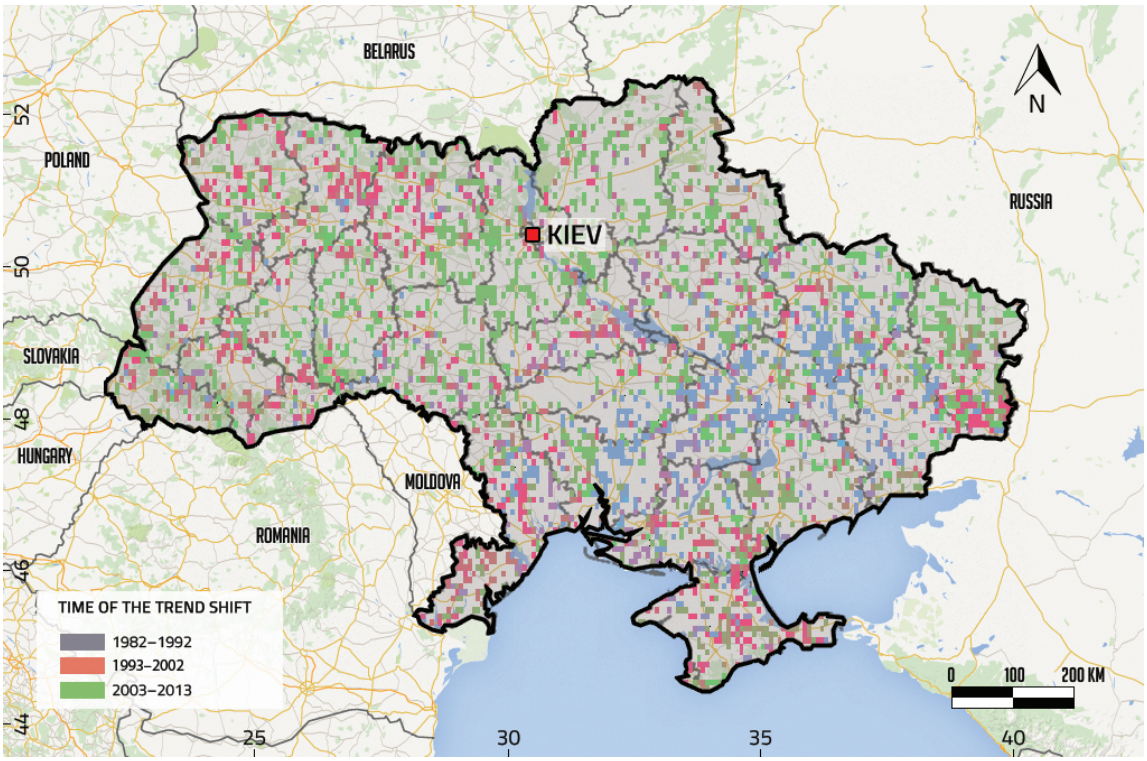

Figure 3.4: Spatial distribution of the time of the shift classified in three major time intervals.

potentially cause the breakpoints in the trends (Rogier de Jong, Verbesselt, Zeileis, & Schaepman, 2013), we have conducted the corresponding tests. We compared these changes with the frequency of the detected changes and the detected breakpoint did not show the same result, suggesting that our results are unlikely to be affected by the platform changes.

Factors of Land Surface Dynamics in Ukraine

We explored the correlations between NDVI time series and environmental variables (mean annual temperature, total precipitation and mean soil moisture) using the partial rank correlation method. Prior to correlation analysis, we evaluated multicollinearity by obtaining VIF (variance inflation factor) for each variable. Non-stationarity (time dependency) could be excluded due to a significant the Augmented Dickey–Fuller test and inspection of the autocorrelation graphs and the related tests of annually aggregated time series. As the VIF was smaller than two, we continued the partial ranked correlation analysis of the driving factors and NDVI. (Figure 3.5) illustrates the spatial distribution of the extent of the effect of each factor. We used a subtractive model for visualization, where the primary factors are illustrated with a pure color and the overlapping areas of influence are depicted by the intersection of colors.

Although the studies have discussed the impact of climatic variation on land surface changes

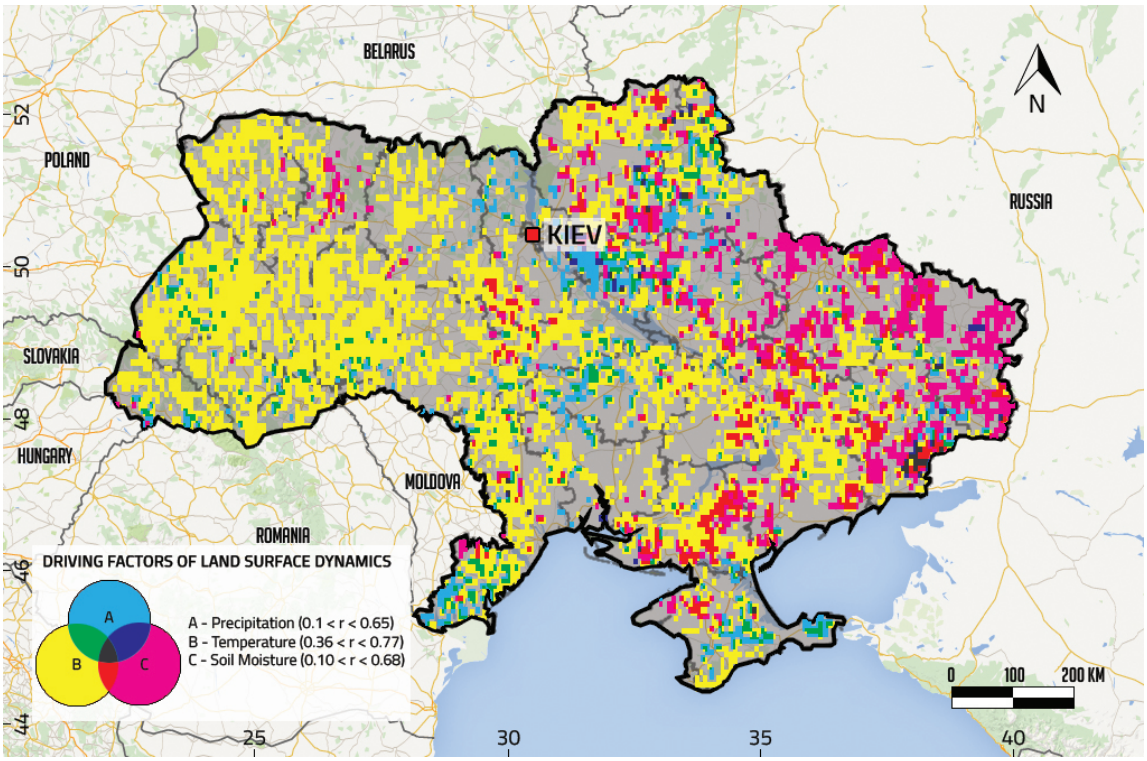

Figure 3.5: Dominant factors of Normalized Difference Vegetation Index (NDVI) change: pixel-wise correlation coefficients between NDVI and environmental variables. The gray color denotes pixels without statistically significant correlations ($p < 0.05$).

(Rogier de Jong, Schaepman, et al., 2013; Y. Liu, Li, Li, & Motesharrei, 2015; Nemani et al., 2003), very few of them have focused on the impact of environmental factors on land surface trends in Ukraine as opposed to management and land tenure factors (Adamenko & Prokopenko, 2011; Alcantara et al., 2013; Baumann et al., 2011; Hostert et al., 2011; Kovalskyy & Henebry, 2009; Schierhorn et al., 2013; Smaliychuk et al., 2016). Our results show that the changes in land surface can be partially explained by the combination of thermal and water conditions. It is important to mention, that we do not raise any causal argument for the statistical results of presented correlations. The only aim we had was to assess the effect of an estimator and describe possible associations between environmental variables and land surface changes. Among all analyzed factors, air temperature explained most of the NDVI variability (Table 3.2). The impacts of air temperature were observed in 31.5% of the area, with a positive correlation coefficient (0.36–0.77). This can be explained by the fact, that in western and northern regions, the temperature is the main limiting factor for the vegetation growth, and with the increase of temperature over the study period, the correlation becomes higher. The percentage of the area in each land cover class with NDVI/Air temperature correlation depicts that grasslands were the most sensitive to temperature.

Correlation Coefficient Range	Cropland	Forest	Grassland
0.36–0.44	20.34	10.45	41.04
0.45–0.53	16.94	9.86	34.67
0.54–0.77	8.70	4.47	15.10

Table 3.2: Percentage of the area in each land cover class with Normalized Difference Vegetation Index (NDVI)/Air temperature correlation.

Soil moisture content is influential in eastern (r = 0.68), semi-steppe, and steppe zones, covering around 12% of the area. High correlation coefficients between NDVI and soil moisture is observed in grasslands (Table 3.3). Furthermore, we observed small clusters of negative correlations between NDVI and soil moisture that might be referred to anthropogenic influences in this area and unfavourable socio-economic conditions. Finally, precipitation is a dominant factor (r = 0.65) in central regions of the country (Table 3.4). Relatively low correlation coefficients were estimated between NDVI and precipitation in forests, which were conditioned by lower water limitation compared to other classes. Again, there is a small cluster of a negative correlation between NDVI and precipitation in the northwest of Ukraine. Since it is not driven by climate variability, this could be an indicator of human-induced changes such as land transformations (Dubovyk, Landmann, Erasmus, Tewes, & Schellberg, 2015) (not represented on a map). Moreover, the results of NDVI/soil moisture partial correlation analysis show a higher number of pixels with a significant association within the study area than NDVI/rainfall. Although theoretically the precipitation is considered as an essential forcing factor for soil moisture variability, the latter is also affected by conditions such as soil hydraulic properties, land cover, evapotranspiration, and topography. This is in line with several studies (Ibrahim et al., 2015; Sohoulande Djebou & Singh, 2015) where soil moisture had better performance for the explanation of land surface dynamics. In addition, when evaluating the partial rank correlations between variables, the effect of the other confounders is eliminated by adjusting the target correlation for any other monotonic association with the variables of this study.

Correlation Coefficient Range	Cropland	Forest	Grassland
-0.55–(-0.21)	0.53	0.31	2.27
0.1–0.44	8.91	1.84	19.72
0.45–0.68	7.79	1.25	14.80

Table 3.3: Percentage of the area in each land cover class with Normalized Difference Vegetation Index (NDVI)/Soil Moisture correlation.

Although the additional datasets give insight about the processes that can affect the land surface changes, further analysis should consider the use of complementary factors and include datasets

representing anthropogenic activity. Several studies discussed the factors that affect the land abandonment in Ukraine, and they depicted that factors such as soil type, yield decrease, unfavourable socio-economic conditions and population density demonstrate a significant association with land abandonment and cultivation rate (Baumann et al., 2011; Meyfroidt et al., 2016). The observed increasing and decreasing trends and their interruptions are only partially explained by temperature, precipitation and soil moisture. Other factors—such as CO2 fertilization, agricultural management practices and the intensity of land use and fertilizer use may affect the land surface changes. To improve our analysis, this should be considered in the context of overall land surface dynamics.

Correlation Coefficient Range	Cropland	Forest	Grassland
-0.47–(-0.18)	0.32	0.59	1.02
0.1–0.44	6.24	2.01	9.53
0.45–0.65	3.64	0.59	6.01

Table 3.4: Percentage of land cover class with significant correlation coefficients Normalized Difference Vegetation Index (NDVI)/ precipitation.

3.4 Conclusions

The current study addressed the assessment of long-term land surface dynamics over a 32 -year period between 1982 and 2013 in Ukraine. The interpretation of the influences of environmental variables on the observed land surface dynamics were supplemented and improved by employing additional datasets. Fundamentally, we concluded that long-term increasing NDVI trends are widespread across the country. Decreasing trends with abrupt positive breaks predominated during the initial 1982–1992 study period within the steppe zone of Ukraine. This period is characterized by extensive cultivation and agricultural land expansion in the country. During 1993 and 2002, most of the changes occurred in northwest Ukraine. The first post-socialistic years in the country were characterized by high rates of land abandonment as well as widespread forest disturbances. Following the collapse of the Soviet Union, agricultural activities and practices were principally affected by transformational processes and structural changes in this sector. A general economic recovery has been occurring in Ukraine since the late 1990s and early 2000s. These conditions have stimulated re-cultivation of formerly abandoned land. This process has emerged mainly in the central portion of the country and is reflected by the monotonic increase and increase with a setback that is seen to predominate during the recent years of 2003–2013. Critical, high impact environmental events (including droughts and other extreme weather conditions) also occurred with an increased frequency during these years. Based on our results, we conclude that the combined

trend and breakpoints analysis captures and reflects the spatial patterns of these trends as well as describes the timing of those changes. This capability will allow increased understanding of dynamic land surface processes over extensive areas. We found that the GIMMS NDVI3g dataset was extremely useful for regional scale trend analysis. In particular, a data record spanning more than three decades enabled a markedly improved trend characterization. With respect to the effects of environmental factors on NDVI change, we conclude that partial correlation analysis is useful for determining the individual contribution of each specific environmental factor on NDVI dynamics. Correlation analysis shows that temperature accounts for approximately 30% of overall NDVI variance. Grassland and cropland environments show similar responses to the drivers, demonstrating high sensitivity to soil moisture and precipitation as well as temperature. Additional analyses should include complementary causal factors along with datasets that accurately characterize anthropogenic activity. There is also a requirement for analyses at higher spatial resolutions. This will enhance interpretation of land surface trends and provide for assessments at scales complimentary to land management practices. We are confident that this study demonstrates that the effective combination of different trend analysis techniques, integrated multiple datasets, and effective statistical modelling allows derivation of valuable, previously unavailable spatially explicit information on land surface dynamics and their causal factors. Finally, such information will enable an improved understanding of land surface processes and environmental changes ongoing over space and through time that are specific to Ukraine.

Chapter 4

A Rule-based Approach for Crop Identification Using Multi-temporal and Multi-sensor Phenological Metrics

Abstract: Accurate classification and mapping of crops is essential for supporting sustainable land management. Such maps can be created based on satellite remote sensing, however, the selection of input data and optimal classifier algorithm still needs to be addressed especially for areas, where field data is scarce. We exploited the intra-annual variation of temporal signatures of remotely sensed observations and used prior knowledge of crop calendars for the development of a two-step processing chain for crop classification. First, Landsat-based time-series metrics capturing within-season phenological variation were preprocessed and analyzed using Google Earth Engine cloud computing platform. The developmental stage of each crop was modeled by fitting harmonic function. The model's output was further used for the automatic generation of training samples. Second, several classification methods (support vector machines, random forest, decision fusion) were tested. As input data for crop classification, composites based on Sentinel-1 and Landsat images were used. Overall classification accuracies exceeded 80% when the seasonal composites were used. Winter cereals were the most accurately classified, while we observed misclassifications among summer crops. The proposed approach offers a potential to accurately map crops in the areas where in situ field data is scarce or unavailable.

4.1 Introduction

Due to a growing world population and decreasing land and water resources, there is a need for enhancing agricultural productivity to ensure food security. Accurate crop maps from Earth Observation (EO) can build the basis for agricultural monitoring and decision making at wider spatial scales (Nataliia Kussul, Lemoine, Gallego, Skakun, & Lavreniuk, 2015; Fabian Löw & Duveiller,

2014) to support sustainable agricultural land management. Improving the resiliency of food production systems, and implementing sustainable agricultural practices have been recognized as one of the most important development goals (United Nations, 2015). Spatially explicit information on the distribution of croplands and crop types can also assist accurate statistical estimation such as yield prediction and crop area estimation (Kogan et al., 2013; Nataliia Kussul et al., 2015; Pan et al., 2012) and so support policy making (Davidson, Fisette, Mcnairn, & Daneshfar, 2017). The recent advancement of satellite remote sensing, such as the free distribution of satellite archives and the availability of new sensors, gives more opportunities to derive land cover and land use (LULC) information. Also, the frequency of data acquisition is nowadays rather high, which allows not only to discriminate different crops but also to assess their growth stage. Several studies discussed the use of multi-temporal imagery for classification (Hentze, Thonfeld, & Menz, 2016; Jinxiu Liu, Heiskanen, Aynekulu, Maeda, & Pellikka, 2016; Siachalou, Mallinis, & Tsakiri-Strati, 2015; Simonetti, Simonetti, Szantoi, Lupi, & Eva, 2015; Yan, Wang, Lin, Xia, & Sun, 2015) often using vegetation indices, such as Normalized Difference Vegetation Index (NDVI), for the identification of croplands and crop types from other types of land cover (Hao, Wang, Zhan, & Niu, 2016; Marais Sicre et al., 2016; Wardlow & Egbert, 2008). Previous studies also discussed the use of knowledge-based temporal features for crop identification based on several optical sensors. These studies applied a phenology-based approach for the identification of areas cultivated with different crop types (Bargiel, 2017; Waldner, Canto, & Defourny, 2015; Zhong, Hu, Yu, Gong, & Biging, 2016). However, these multi-temporal classification approaches either rely on a high number of training data and/or cannot be applied in years without training data. Moreover, the integration of several data sources and the discrimination of crop types are still challenging as most of the studies are based on the use of remote sensing data coming from one sensor. Hence, the present study proposes an approach to automatically generate training samples based on phenological metrics derived from both optical and radar image time series. We applied this method to the study site in Central Ukraine as this region has undergone profound changes during the last decades in the extent and intensity of agricultural land use (Kuemmerle et al., 2011). For the study area, (Nataliia Kussul et al., 2015) demonstrated successful classification of the agricultural land use. However, the crop identification methods applied were relying on extensive field data collection which was further used for calibration of the classification model. Although a number of studies have addressed the use of satellite data products for crop mapping (Loosvelt, Peters, Skriver, Baets, & Verhoest, 2012; F. Löw, Michel, Dech, & Conrad, 2013; Wardlow & Egbert, 2008), there is still an ongoing discussion regarding the choice of input data. Further, when using only optical remote

sensing data, unfavourable atmospheric conditions such as cloud cover can reduce the quality of classification results (Forkuor, Conrad, Thiel, Ullmann, & Zoungrana, 2014; Joshi et al., 2016; Whitcraft, Becker-Reshef, & Justice, 2015). Therefore, analyses are needed which strives for a better understanding of the effect of type and number of input variables on classification accuracy. Such analysis should also consider an increase in amount and quality of freely distributed data especially when data from multiple sensors are combined. In our study, we thus tested the performance of several non-parametric classification algorithms (support vector machines, random forest, and decision fusion) and applied them to multi-temporal data sets. As these algorithms are widely used for classification, the comparison of these approaches is important to test their applicability for crop type mapping. In this light, the objectives of the research were: (i) to develop a two-step procedure for crop identification based on analysis of crops' within season temporal dynamics and application of non-parametric classification algorithms, (ii) to identify a favorable selection of input data derived from optical and SAR sensors, and (iii) to compare the applicability of classification methods and a training sample generation approach across years.

4.2 Study Site

We selected the Vasilkovsky district in Kiev region as the test site (Figure 4.1). This area is located in Central Ukraine in the semi-steppe zone, comprising 1184 square km. In 2015, the total sown area was 58,618.36 ha, while in 2016 it comprised only 46,092.52 ha (State Statistical Department of Kiev region, 2015, 2016). The test site is characterized by a temperate climate and a heterogeneous agricultural land use. Agricultural production in the region is highly dependent on rainfall, as the area is not irrigated. In this region, two major cropping seasons are distinguished. Winter crops are grown from October to July of the following year, whereas summer crops are grown from April to September. In this area, during one growing season, one crop is planted and after the harvest of winter crops, no other crop is planted. Although the area is located in the temperate zone, agro-climatic conditions were different during the study years. Particularly, in 2015 the weather was drier lacking rain from mid-July. Although growing conditions in 2016 were more favorable, the average temperature and precipitation deviated from the long-term mean. The agricultural field size in this area varies mostly from 30 ha to 100 ha. Small fields have a size of less than 5 ha (5% of the fields in the area) and large fields can even reach up to 250 ha. Such differences occur due to several factors such as different types of cropland tenure, ownership (agricultural holdings, household farms).

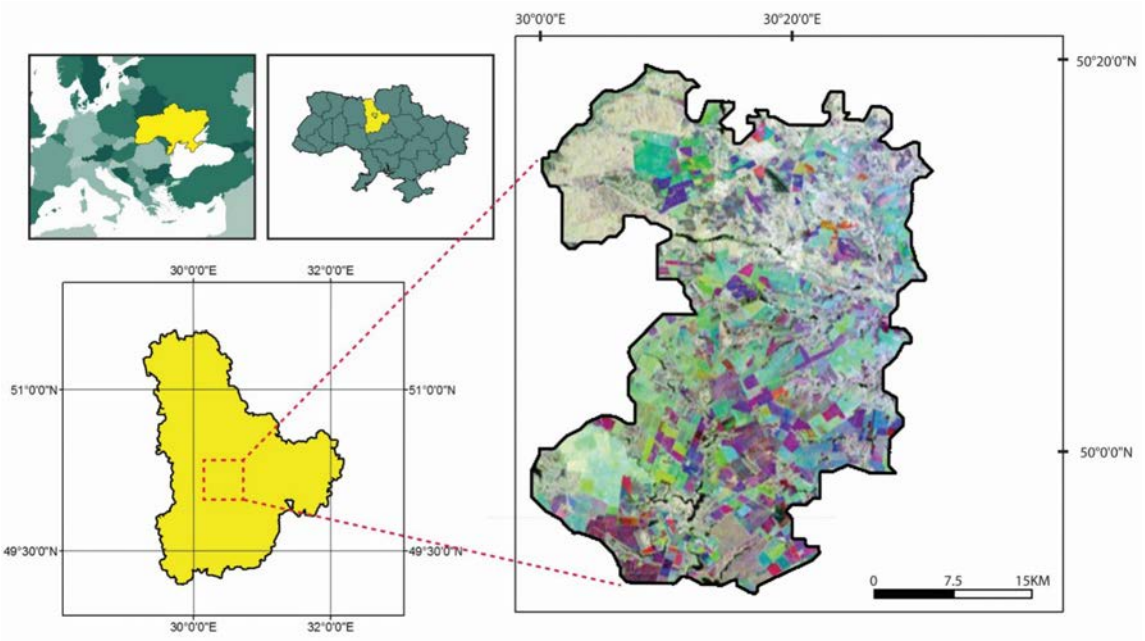

Figure 4.1: Location of the study area (Sentinel 1 multi-temporal composite, RGB bands: VH images from May, August, and October in 2016)

Wheat is the main winter cereal, which is typically planted in late September or October. The seeding date depends on weather conditions as plants start growing when temperature exceeds 1-2 °C, while the optimal temperature for growth ranges from 14 to 20 °C. The active vegetative period ends in November but starts again in the following spring (Day of the year (DOY) 60-85). Winter wheat usually reaches the flowering stage in the second part of May; and the crop is consequently harvested in July and early August (DOY 11-123) (Figure 4.2).

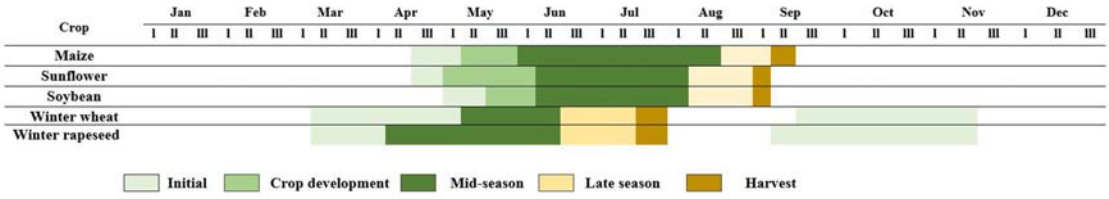

Figure 4.2: Typical crop calendar.

Besides winter wheat, other winter cereals, such as barley are also sown, but usually the cultivated area is smaller compared to winter wheat. Another common winter crop is rapeseed, which is one of the main oilseed crops grown in this area. It is also planted in fall. The distinctive flowering period is in late April, which usually lasts for 35 days. The duration of the growing season of rapeseed is around 300-320 days. Maize, soybean, and sunflower are the main summer crops cultivated in the study site. Maize is sown between late April and May: the crop reaches the peak of the

vegetative phase in July and is harvested till mid-September. Maize typically reaches the flowering stage in mid-July (DOY 190-202). Soybean is usually sown in May, reaching a flowering stage in July and maturing in August (the overall growing period is 80-240 days). Sunflower is another important oilseed crop, which exhibits similar crop development stages during the growing season: seeding is in late April, flowering in July and harvest is in early September (growing period: 95-120 days) (State Hydrometeorological Service of Ukraine, 2007). The other crops which are cultivated in this area are sugarbeet, buckwheat, oat, spring wheat and barley. However, due to relatively small area (0.88-10% of cultivated area in the study region) they were not included in the study. In the following section these classes were designated as class 'other'.

4.3 Datasets

4.3.1 Satellite Data

Landsat 8 Operational Land Imager (OLI) time series were used as the primary source of data. Top of Atmosphere (TOA) collection was accessed using Google Earth Engine (GEE) (Google Inc., 2016; Lessel & Ceccato, 2016). The Landsat archive was chosen due to its 30m spatial resolution, which is suitable to characterize land use at field level given the average field size in the study area. As the study area is in the overlapping section of two Landsat paths (181/25 and 182/25), four optical acquisitions are available per month. In figure 4.3, the selected Landsat scenes are illustrated (several Landsat scenes were excluded due to extensive cloud cover). Some of the Landsat bands, such as costal blue (Band 1), thermals (Band 10 and 11), panchromatic (Band 8) and cirrus (Band 9) were not used in the study. Following initial tests, Blue (Band 2) and Green (Band 3) bands were excluded from the classification framework as well. In addition to the optical images, Sentinel-1A C-band SAR images with VH (Vertical transmit, Horizontal receive) polarization were used (Interferometric Wide swath mode (IW), Processing level 1 high-resolution products, Ground Range Detected). As SAR backscatter is sensitive to both geometric (e.g. crop structure, roughness) and dielectric properties (permittivity, which highly depends on water content) of the targets, it provides additional information to optical data (Inglada et al., 2016; Weng, 2011). When using multi-temporal SAR data, it is important to use the data with the same viewing configuration. For this, we used the images in descending mode, and we filtered images by the orbit, as the difference in orbit might cause changes in backscattering that are not related to (bio)-physical properties of the target.

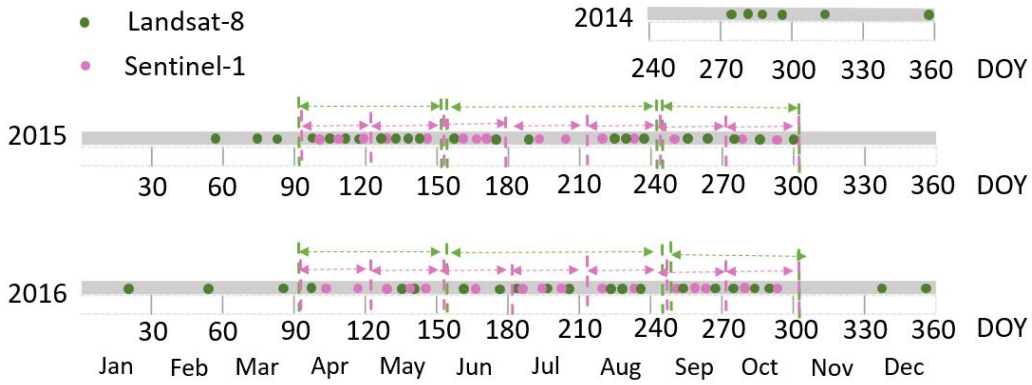

Figure 4.3: Data acquisition (dots) and the temporal window of compositing (arrows).

4.3.2 In situ Data

In situ phenological observations acquired from the State Hydrometeorological Services of Ukraine were used for the assessment of seasonality parameters derived from remote sensing. This data represents long-term observations of dates of the main phenological events for each crop. These key dates of crop development can be grouped into the following temporal classes: initial (low vegetation, beginning of emergence), development of leaves (greening up), mid-season peak and flowering, late season (grain filling and senescence) and harvest. According to the collected in situ crop phenological data, among recent years these plant growth stages generally corresponded to crop calendar. Land cover information was collected using a mobile device with the GPS during the growing season of each year. The field data collection was carried out during the entire growing season of all crops, which enabled the recognition of winter crops (cereals and rapeseed) and summer crops (maize, sunflower and soybean). The reference dataset for each crop is listed in Table 4.2.

4.4 Methods

4.4.1 Preprocessing

Prior to the analysis, remotely sensed time series went through several preprocessing steps. We filtered the Landsat data collection by the time interval corresponding to the monitoring period and to the extent of the study area using Google Earth Engine. The Fmask (Function of mask) method was applied for cloud and cloud-shadow detection in Landsat imagery (Z. Zhu, Wang, & Woodcock, 2015). Temporal SAR composites were created and, subsequently, included into the classification scheme. Prior to compositing, it is important to filter the speckle noise in SAR images.

We used GammaMap filter for this purpose (Lopes, Nezry, Touzi, & Laur, 1990) with the 7x7 kernel size. The Sentinel-1 and Landsat imagery were orthorectified to the same map projection and resampled to a common 30 m pixel resolution (Figure 4.4). The NIR and R bands of Landsat were used to compute NDVI images for each individual time step.

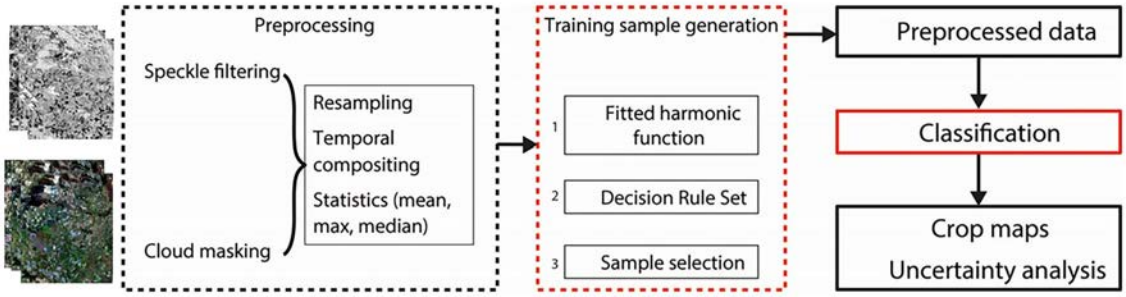

Figure 4.4: Methodological workflow.

4.4.2 Two-step approach

A two-step approach for crop identification was developed which included generation of training samples and a pixel-wise classification per se.

Training sample generation

To automatically generate training samples, a processing chain was developed to separate the main crops in the study area. First, a harmonic function was fitted to the time series of NDVI data. By fitting a harmonic function (Eq. 4.1), it has been possible to model temporal signal of NDVI as a sum of additive term and harmonic term, which were then expressed by phase and amplitude. Phase term represents the angle at which the peak occurs (time represented in radians). The amplitude corresponds to the amount of the NDVI change (Dubovyk, Landmann, Dietz, & Menz, 2016; Jakubauskas, Legates, & Kastens, 2002).

$$NDVI_t = \beta_0 + \sum_{n=1}^{\infty} A_n \cos(\frac{2\pi nx}{f} - \varphi_n) \tag{4.1}$$

where NDVIt represents the reconstructed series, A is the amplitude and ϕ is the phase of the nth harmonic term, f is the frequency and t represents the time. β_0 can be viewed as the coefficient at zero frequency (intercept), which is the average of the series. Phase and amplitude terms were further used to extract the decision rules. The phenometrics were calculated for each pixel-wise time series (Table 4.1). As the main variance in NDVI series is captured in first harmonic terms and their

additive component, we have tested our approach based on these terms. The first harmonic term represents the annual cycle while the second term captures semi-annual variation (Jakubauskas et al., 2002). We filtered the Landsat time series based on the crop calendar, which means that for winter crops (wheat, rapeseed) it was essential to use the observations from previous fall to have correct fitting. In situ observations of crop phenology were used to check their agreement with remotely sensed seasonality metrics by the comparison of key phenological dates.

Phenometrics used in the study	Description
Phase	angle in which the peak occurs
Amplitude	magnitude of peak
Mean	average of the series
Maximum Landsat-8 composite from the start of a season	pixel based maximum composite (Period 1, month 4-5)
Median Landsat-8 composite from mid-season	pixel based median composite (Period 2, month 6-8)
Median Landsat-8 composite from the end of a season	pixel based median composite (Period 3, month 9-10)
Sentinel 1 composites	VH polarized monthly temporal composites: months 4 and 5 correspond to Period 1 months 6,7,8 to Period 2 and months 9,10 to Period 3 respectively

Table 4.1: Input features used for the development of the decision rules.

Based on the harmonic regression fit, we identified the essential temporal intervals for the derivation of the Landsat composites. Using statistical aggregates such as mean, median and maximum values during each phenological stage, we generated the image composites (Table 4.1) Although all pixels in such composites were not acquired during the same day, they still represent the same phenological state of the crop. Thus, such composites from different periods of the growing season (start, mid-season, end of the season) can be further used for differentiation of crops. 'Start', 'mid-season', 'end of the season' terms correspond to period 1, period 2 and period 3 respectively and through the manuscript are used interchangeably. Afterwards we used these composites, derivatives from harmonics and the reference phenological information to determine the range of the values of the peak of vegetation index and the timing of the peak, the range values of base and mid-season NDVI values. In this way, the decision rule set was developed to separate crop types. Based on these decision rules, we generated the masks which we labeled as 'probable' class for each crop (Figure 4.6). The winter cereals (wheat, barely) were aggregated in one class due to their spectral similarities. To reduce the effect of mixed pixels in the generated crop masks, they were filtered one more time. The final training set was randomly selected each time from the crop masks. The selection of the sample points was based on the lowest standard deviation of

NDVI values, where the 'lowest' means those standard deviations that are within 95% confidence interval, derived from observed standard deviations. The number of generated training samples was proportional to the validation set. The values that were out of the range for the main crop classes, were used to generate a class labeled 'other'.

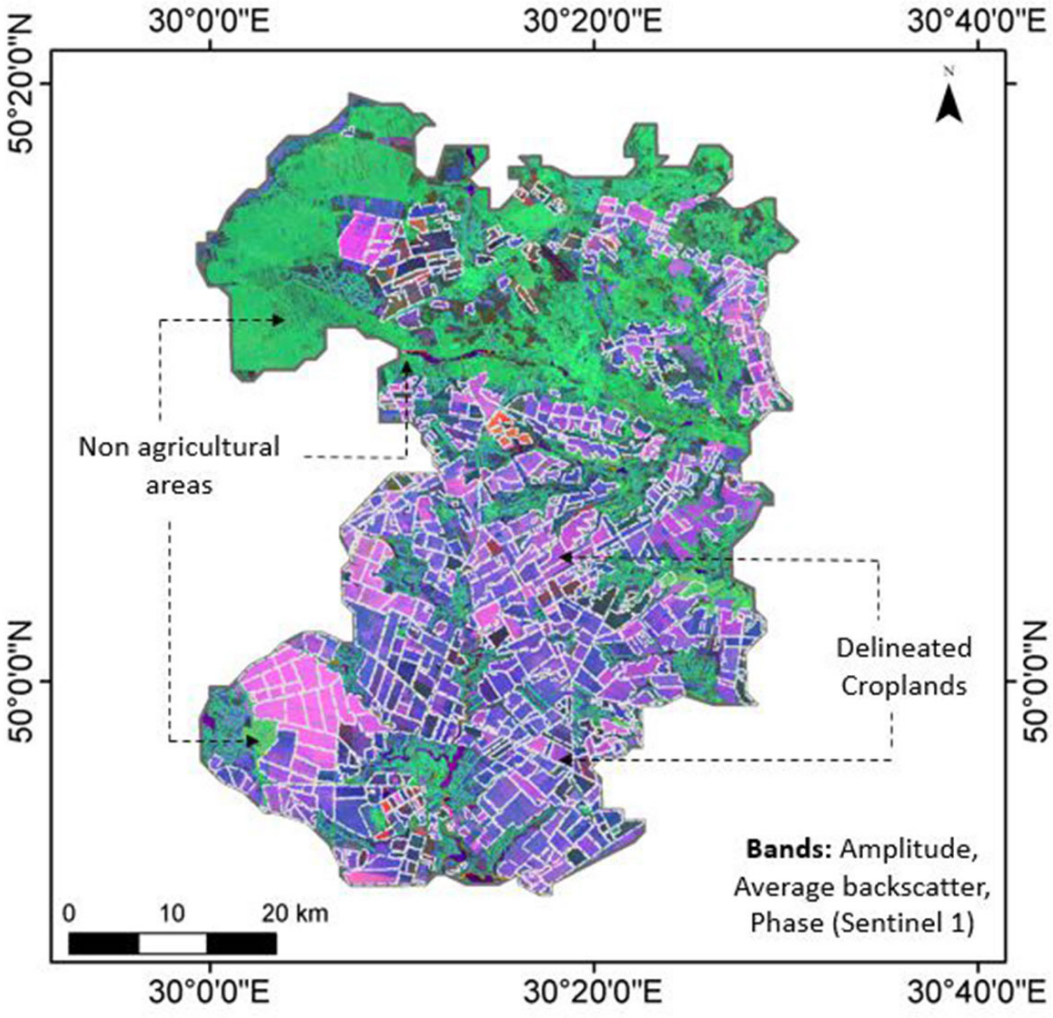

Figure 4.5: Delineation of agricultural areas.

We run image segmentation to generate field boundaries and identify only cropland areas in the study area. Elimination of non-cropped areas and generation of field boundaries was performed by the intersecting several segmentation results based on both Landsat and Sentinel-1 images. The elimination of non-cropped areas was possible when using the distinctive characteristics of harmonic derivatives of different land cover classes such as masking the areas with low yearly average (zero harmonic component) for bare land and high values for the forest. Another assumption used for the

delineation of cropped areas was the higher amplitude compared to non-cropped areas (Figure 4.5). In the map we can clearly differentiate non-cropped areas, illustrated in green, and cropped areas in the shades of purple. The visible differences in the cropped area are due to characteristic distinctions in temporal metrics of different crop types.

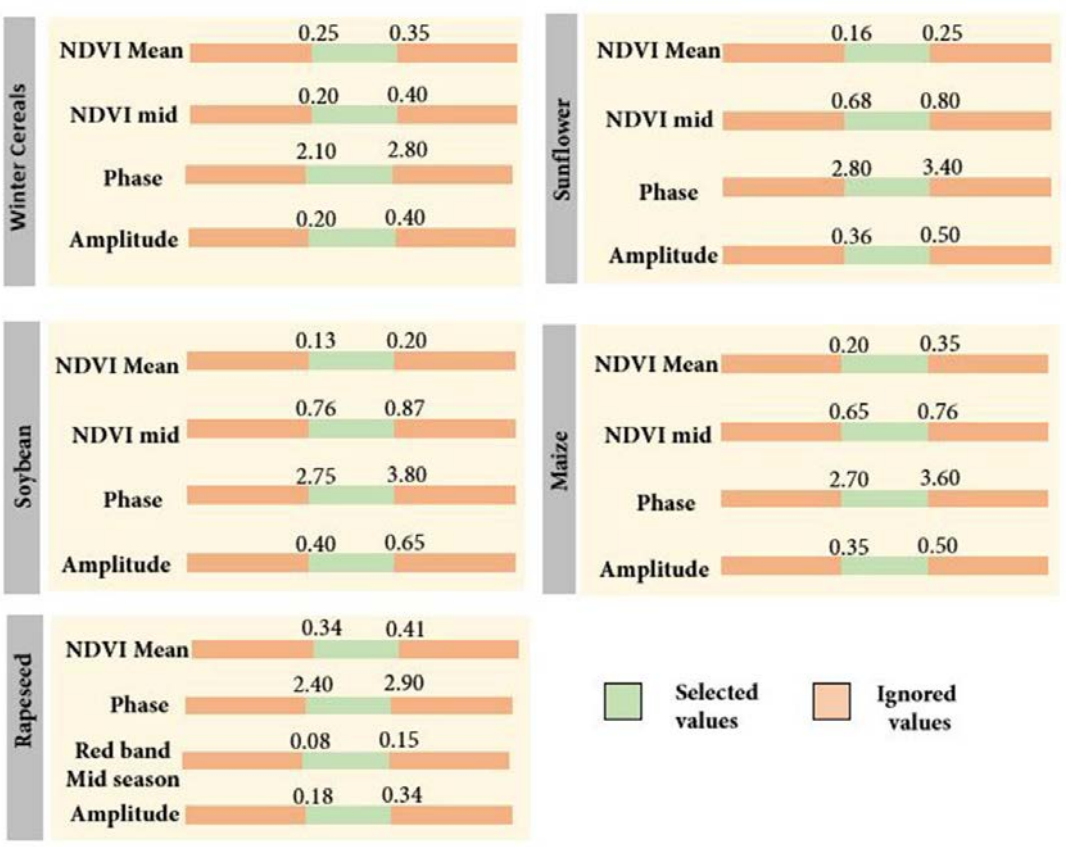

Figure 4.6: The rule set used for sample generation (NDVI mid is the NDVI estimated from the mid-season composite).

Classification

The second step in the classification procedure was the selection of the features that can improve the class separability and the training of the classifier. The main input features for the classifier were six spectral bands of Landsat, NDVI, derived from three temporal composites, and Sentinel-1 monthly composites (Table 4.1). We tested three machine-learning algorithms for pixel-based classifications Random Forest (RF), Support Vector Machine (SVM) and one decision fusion approach. The first classification algorithm employed was the Random Forest which is an ensemble machine learning technique that combines multiple trees (Breiman, 2001). One of the advantages of the RF is that the increase in the number of trees does not result in over-fitting (Hao, Zhan, Wang, Niu, & Shakir,

2015; Ozdarici Ok, 2012). We have selected the optimal number of trees in the ensemble as 500. For each scenario of classification, the square root of the number of features was used for generation of the trees at each node. Support Vector Machine was the second method applied for classification, which uses higher dimensional features space for a class separation (G. M. Foody & Mathur, 2004). SVM is a non-parametric method, and the parametric distribution of the input data is not required. SVM is reported to work well with small training datasets (Mathur & Foody, 2008). For the SVM test we used Radial basis function kernel (RBF). The third classification approach was based on decision fusion by combining the results of several classifier algorithms (Kittler, Hatef, Duin, & Matas, 1998), similar to the method proposed by (Waske & Benediktsson, 2007). Two classifier algorithms (here: RF and SVM) were trained based on randomly selected feature subsets. Whilst Waske, van der Linden, Benediktsson, Rabe, and Hostert (2010) recommended 20-30% of all input features to get accurate results, such a low number of features decreased classification accuracy in our study. Hence, the subsets were created by randomly drawing 75% of all input variables. This process was repeated 50 times, based on recommendation of Waske et al. (2010) and initial tests in our study. Through this procedure, we created 100 outputs (50 by the RF, and 50 by the SVM) which were 100 land cover maps. These 100 maps were then combined using a majority vote (Fabian Löw, Conrad, & Michel, 2015), and as a result, one final map was the output from the decision fusion (Figure 4.7).

4.4.3 Accuracy Assessment

The accuracy of the initial crop masks and final crop maps was assessed based on confusion matrices (Congalton, 1991), calculated with the independent validation set collected during the field visits (Table 4.2). From confusion matrices, we derived overall accuracy (OA), as well as producer´s (PA) and user´s (UA) accuracy. We used McNemar's test (Giles M. Foody, 2004) for the comparison of the classification results. Further, we calculated the area of each crop class and compared it with the official agricultural census statistics (State Statistical Department of Kiev region, 2015, 2016). For the spatially explicit representation of uncertainty of crop maps, we divided the training data into multiple overlapping collections by randomly selecting each time 75% of data. Afterwards we trained the classifier with each subset, classified the input with each classifier. After generation of the classification results, we have normalized the values of pixels in each array to a common scale and estimated the variance of classification for each pixel. All the analyses were carried out with the use of R (R Core Team, 2016) and GEE (Google Inc., 2016).

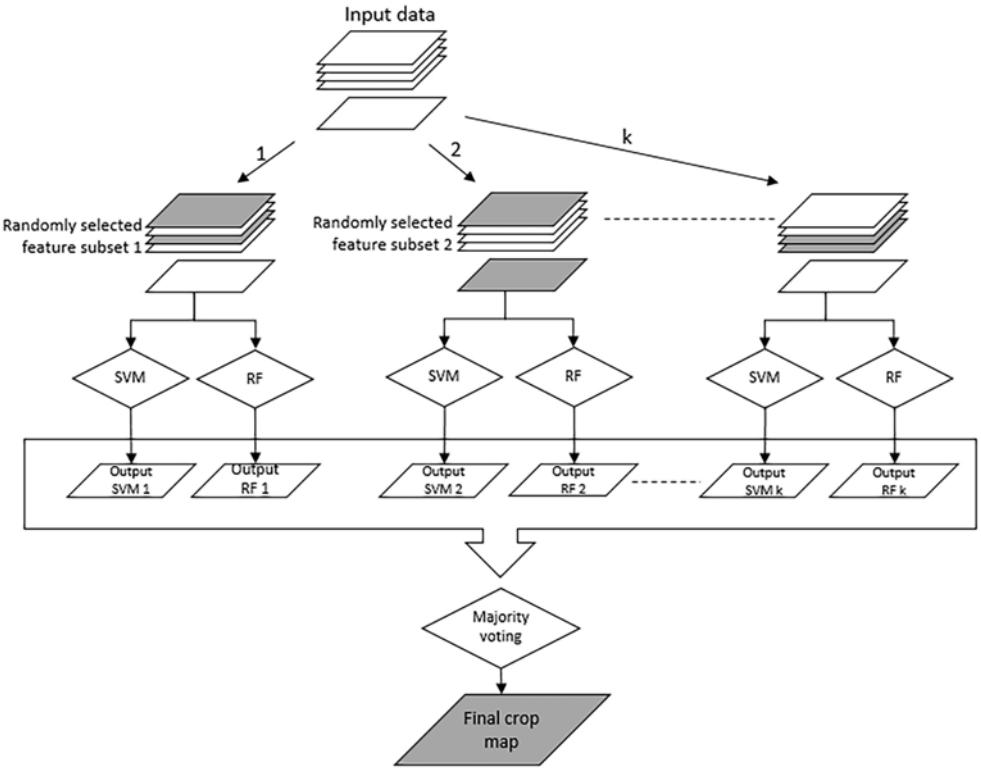

Figure 4.7: The workflow for decision fusion approach.

	2015		2016	
Class	**Training**	**Validation**	**Training**	**Validation**
Winter Cereals	19	19	20	23
Winter Rapeseed	7	7	5	4
Maize	18	20	20	19
Sunflower	7	8	13	13
Soy	20	21	19	19
Other	10	6	7	6

Table 4.2: The samples used for training and validation

4.5 Results and Discussion

According to the approach described in the previous section, crop maps were produced using one of the supervised algorithms (RF, SVM, and DF) and different input time series derived by single Landsat or Sentinel-1 sensors and their combination. The study site was characterized with different agricultural landscapes and its crop variability therein (Figure 4.8). As SVM resulted in accuracies lower than 75%, we did not consider it for further analysis. Crop maps indicated that the general patterns of crop distribution were similar when using different classification methods. An exception

were fields in the southwestern region of the study area, which were classified in 2015 as 'winter cereal' when using decision fusion, whereas with random forest those fields were assigned to the class 'other'. Based on a visual inspection of the generated crop maps we found out that several fields of the same crop were in the direct neighborhood or in the close distance. In general, we can observe that, the output using different input data (Landsat or Sentinel-1 sensors plus their combination) was similar for several fields. Particularly, this is visible for 'winter cereal' class, where the area in the disagreement class comprised 4-14% of the classified 'winter cereal' area. The explanation for this could be the fact that winter cereals have distinctive temporal characteristics which can be detected in both SAR and optical temporal composites. The disagreement was higher for summer crops, which can be explained by their spectral similarities and the allocation of these fields to different classes during several classification tests (Figure 4.9, class 'disagreement among different scenarios' represented in red). For instance, soy had higher portion of pixels with higher disagreement among the classifiers, reaching up to 33% with DF and 41% with RF in 2016. Furthermore, looking at the accuracy metrics (Table 4.3), we can observe, that with the elimination of the input variables, PA and UA for crops such as soy decrease respectively. The reason for this is that with less data it is harder to distinguish the summer crops which have similar development throughout a growing season.

We compared the results when using three seasonal composites from Landsat-8 and Sentinel-1 using McNemar's test. The difference between the classification results of RF and DF was statistically significant in both years (for 2015 χ^2: 4.5; p=0.034 and for 2016χ^2: 5; p=0.025). Similar results were observed in the study of (Hao et al., 2015; Fabian Löw et al., 2015) who report that the fusion approach had better results. Among the classification algorithms tested, DF performed the best in terms of OA using both Landsat and Sentinel as input data (88% in 2015 and 85% in 2016) and resulted in more accurate crop maps with an increase in OA of 2-6% over the RF classification's accuracy. DF yielded acceptable accuracies (>80%) when using optical and SAR data separately as well. The only exclusion was the SAR based classification of 2016, where the OA was 78% which was close to the desired accuracy metric. This can be due to the fact that the map produced based on DF was a product of several classification results based on combination of the classifiers. In addition to the traditional accuracy assessment methods, we have also visualized pixel-based uncertainty of classifications (Figure 4.10). In general, the variance was higher when using RF, whereas with DF we can observe good agreement of class allocation among multiple classification results.

We have evaluated the efficiency of training sample generation by assessment of the accuracies of

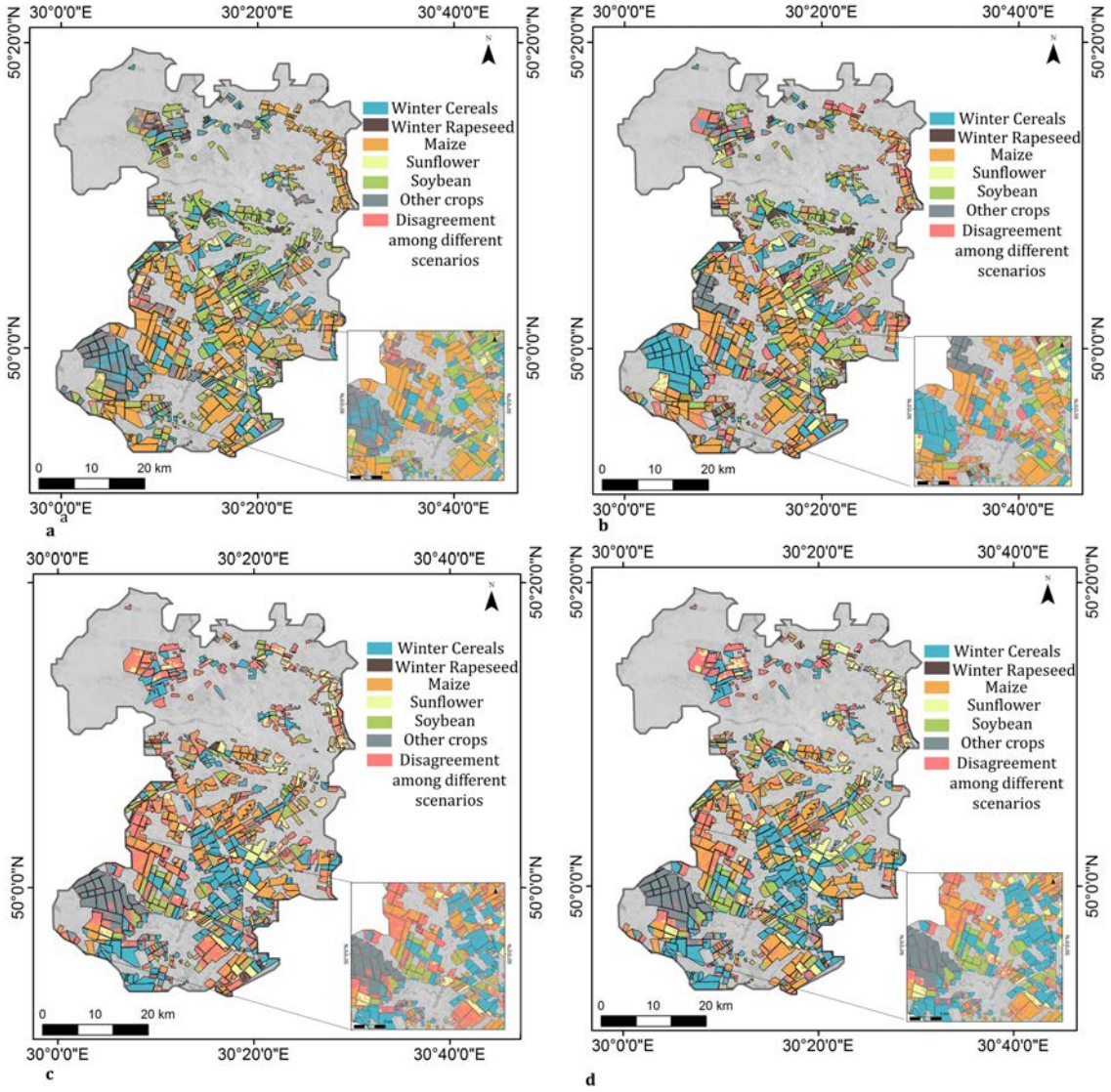

Figure 4.8: Crop maps for 2015 obtained using a) Random forest b) Decision fusion and 2016 obtained using c) Random Forest d) Decision fusion with the input data from Landsat-8 and Sentinel-1 composites from start, mid and end of the growing season.

the 'possible crop masks' with the independent validation data. For both years, the accuracies were high for winter crops (80%), whereas lower accuracies were found for soybean and maize (60%). This lead us to infer that the masks should be further filtered and only the samples which exhibited low standard deviation were selected for final classification.

Overall, results indicate that the temporal patterns of crops can be modeled with harmonic function especially when using the first and second components. For summer crops, the main variation was derived using only first harmonic component as they exhibited a strong unimodal behavior. In contrast, to derive the best fit for winter crops, we used the function generated from

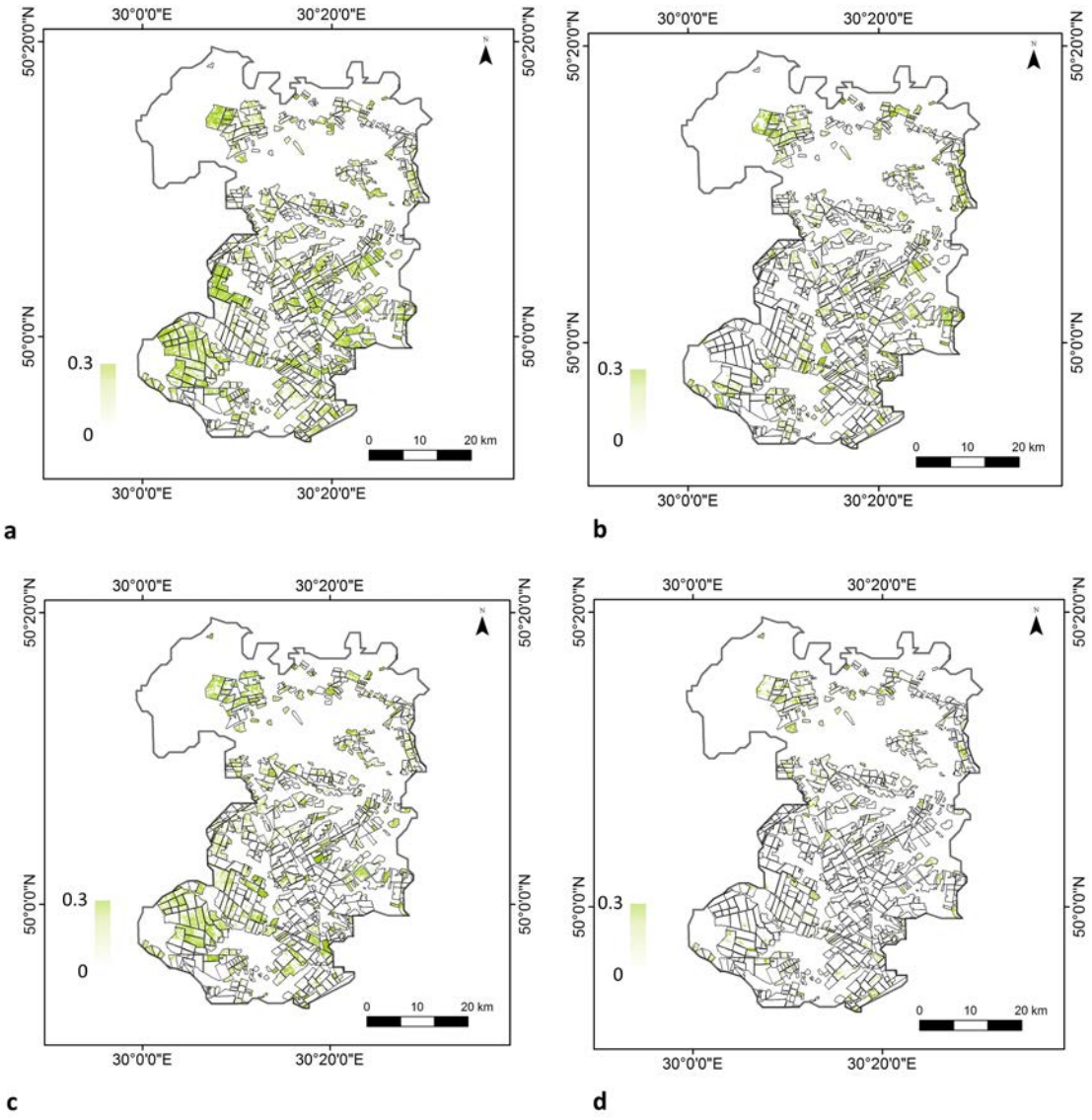

Figure 4.9: The uncertainty of classification results using a) Random forest b) Decision fusion and 2016 obtained using c) Random Forest d) Decision fusion with the input data from Landsat-8 and Sentinel-1 composites from start, mid and end of the growing season.

the first and second harmonic components. These crops are usually planted in fall of the previous year and due to their distinct phenological development, the second component is characterized with substantial variability.

4.5.1 Per-class Separability

In general, the winter cereal class was most accurately classified, whereas we observed misclassifications with maize and soybean classes. This could be explained by the fact that winter cereals exhibit distinctive development stages and early growth, which make them easily separable from

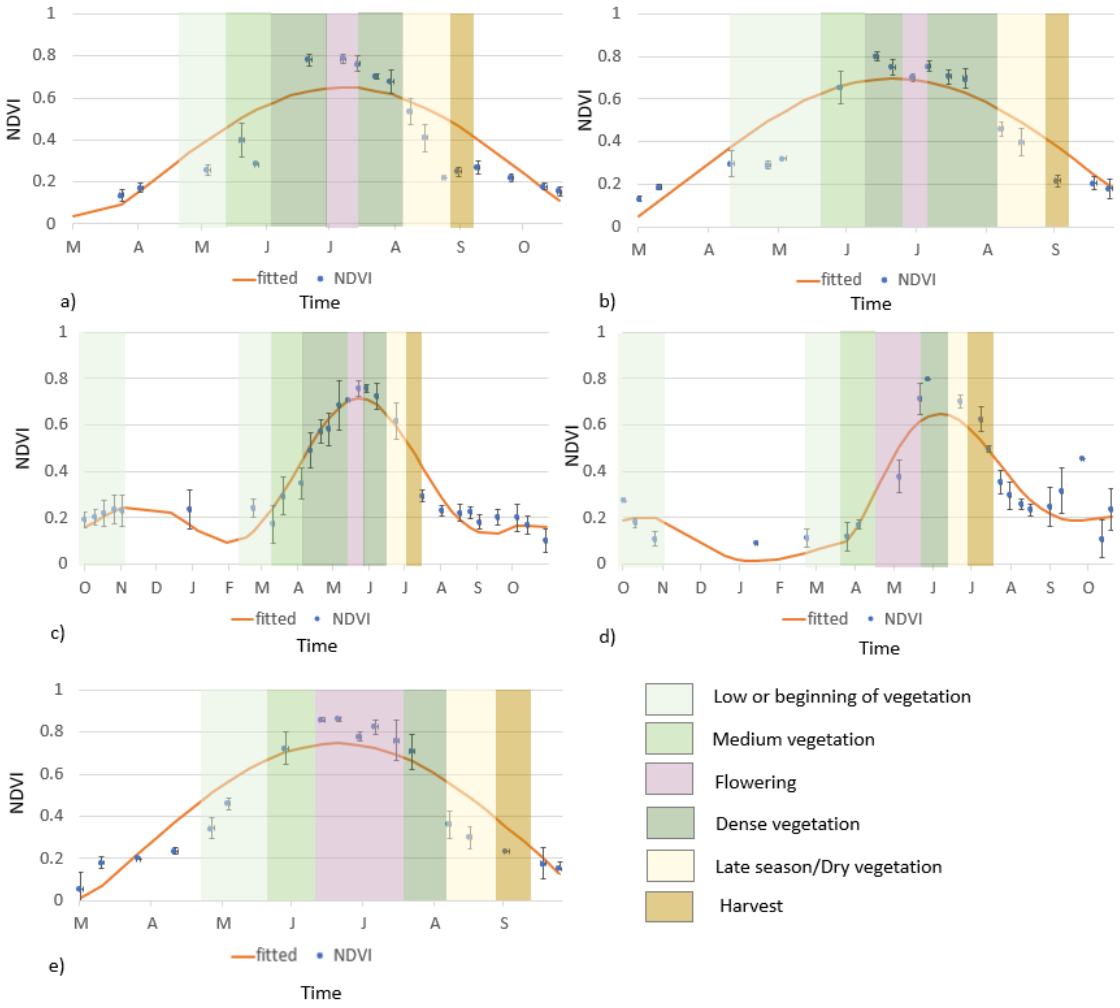

Figure 4.10: Temporal profiles of the main crops. a) sunflower, b) maize, c) winter cereals, d) winter rapeseed, e) soybean (Error bars are illustrating the standard deviations and the temporal windows show the phenological phases).

spring crops. In the case of spring/summer crops, we observed misclassifications between maize and soybean in 2015. In 2016, sunflower was misclassified with maize. Soybean also exhibited slightly lower accuracy and was misclassified together with maize and sunflower. Relatively poor classification results for soybean (both accuracies (Table 4.3) and the areal estimates (Figure 4.11)) can be explained by confusion with other summer crops. The comparison of the sown areas derived from classification results and the official agricultural census statistics published by the State Statistical department of Kiev region (Figure 4.11) showed that the area estimated for each class was in acceptable agreement with reference agricultural census statistics and the deviation for four crops was ranging from 7% - 35%. We observed large error estimates among spring crops which can be accounted to misclassifications between them. We observed the lowest accuracies in the class

other and winter rapeseed. This could be the result of high heterogeneity of the class as it includes several summer crops, which have different spectral response. Another reason for this could be the relatively small number of training samples compared to the rest of classified crop classes. The estimated area for winter rapeseed was significantly larger than recorded in the official statistics.

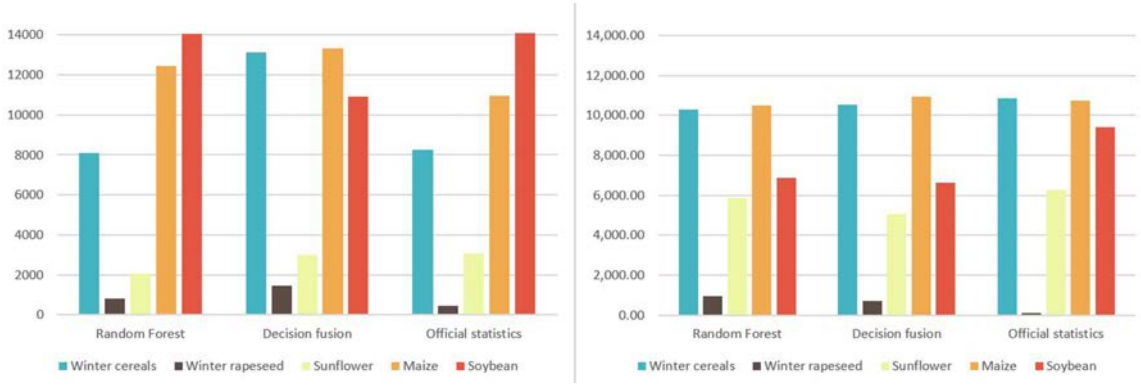

Figure 4.11: Crop area (ha) estimated according to the classification and official statistic.

4.5.2 Evaluation of Input Features

To check the effect of selected input features for the classification, we applied a backward elimination approach, and estimated the decrease of prediction accuracy due to the exclusion of some input variables. The most successful classifications were conducted using Landsat bands along with NDVI and monthly backscatter composites. The integration of both Landsat features (spectral bands, NDVI) and Sentinel-1 based composites at multiple time steps is advantageous. Overall, these results are in line with several studies (Fontanelli et al., 2014; N. Kussul et al., 2015) where the integration of optical and SAR data improved crop identification. These results demonstrate the applicability of Landsat time-series and fitted harmonic function for the derivation of phenological features. When adding Sentinel-1 composites, the cropped areas were quantified with higher accuracies. The integration of multispectral and SAR data improved the classification accuracy by 2 - 5%. The increase in class-specific accuracies was observed in both studied years for winter cereals. In addition, there was an improvement for the separation of spring/summer crops (Table 4.3). We have also noted the increase in overall accuracies when using several temporal composites. Despite this, with mono-temporal analysis, acceptable results can be achieved, if using mid-season composites (Period 2). Mono-temporal classifications from early season and end of the growing season resulted in significantly lower accuracies. To achieve high separability among crops, the use of imagery from at least two periods within the crop growing season is required (Figure 4.12).

The use of temporal composites was justified, as when averaging different images, we decreased the contribution of speckle which resulted in within-class variance decrease and easy separation of the crops. In case of optical imagery, composting enabled the creation of cloud free images covering the study area. It is worth mentioning, that the use of GEE profoundly decreased the time for data access and analysis, as it was possible to use the satellite time series from repository and run computationally intensive pixel-wise analysis using google's distributed power.

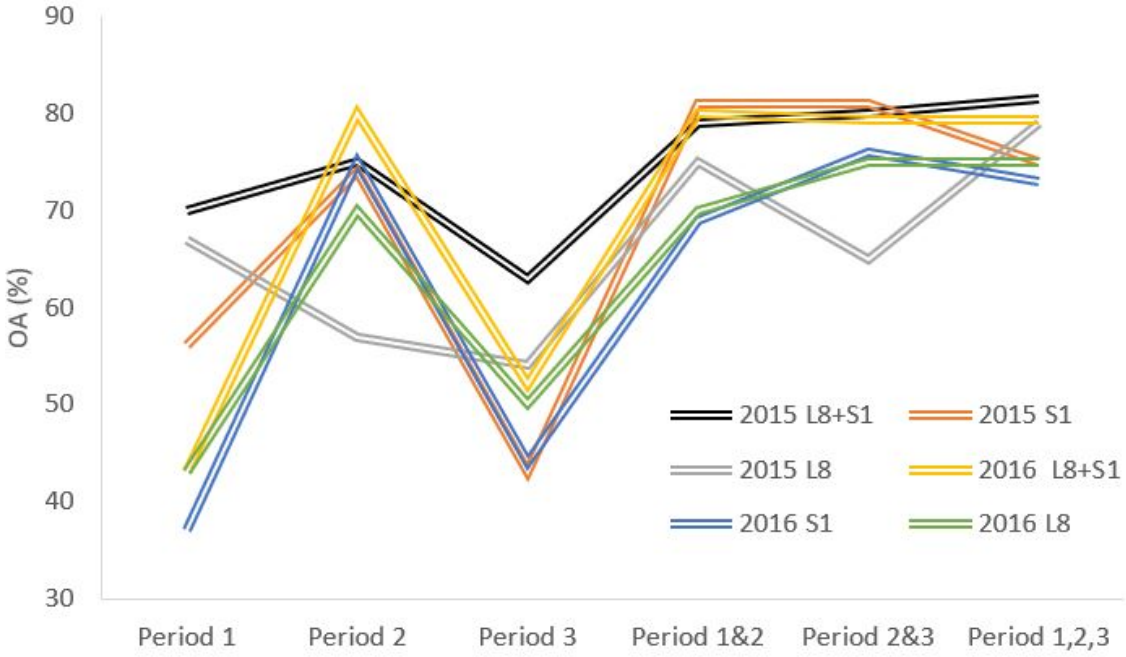

Figure 4.12: Classification accuracies using different scenarios: L8 corresponds to Landsat-8 data, S1 to Sentinel-1 data, L8+S1 corresponds to combined use of data from both Landsat-8 and Sentinel-1 and OA corresponds to overall accuracy.

	Decision fusion (All Landsat 8+Sentinel-1composites)							Decision fusion (All Landsat-8 composites)							Decision fusion (All Sentinel-1 composites)					
Time	OA	Winter cereals		Maize		Soybean		OA	Winter cereals		Maize		Soybean		OA	Winter cereals		Maize		Soybean	
		PA	UA	PA	UA	PA	UA		PA	UA	PA	UA	PA	UA		PA	UA	PA	UA	PA	UA
2015	88	86	100	82	95	94	80	83	90	94	70	95	93	66	81	95	100	63	95	90	47
2016	85	90	86	90	100	93	71	82	86	82	90	95	100	71	78	84	95	77	70	65	71
	Random forest (All Landsat 8+Sentinel-1composites)							Random forest (All Landsat-8 composites)							Random forest (All Sentinel-1 composites)					
Time	OA	Winter cereals		Maize		Soybean		OA	Winter cereals		Maize		Soybean		OA	Winter cereals		Maize		Soybean	
		PA	UA	PA	UA	PA	UA		PA	UA	PA	UA	PA	UA		PA	UA	PA	UA	PA	UA
2015	81.4	89	89	80	85	78	85	79	88	84	80	80	77	80	75	100	100	60	70	66	66
2016	79.3	90	86	69	90	87	66	75	75	81	79	95	100	66	73	100	95	63	70	57	71

Table 4.3: Accuracy measures of area dominant crops using different classification approaches and data.

4.5.3 Considerations and Outlook

The mapping of different crop types based on temporal variation is a demanding and complex process. First, several factors influence the process of crop identification. Individual fields can be managed with different seeding and harvesting times for the same crop species, which in turn has an impact on spectral signatures. Second, different crops can have analogical stages of development throughout a growing season. This can introduce a bias to the selection of training samples and classification. The timing and frequency of image acquisition influence the accuracy of the derived sample set, as it has a significant effect on the fitting accuracy and subsequent estimation of phenological parameters (Eklundh & Jönsson, 2016; Kuenzer et al., 2015; Wardlow & Egbert, 2008). An important aspect of this approach is that crop development throughout the growing season highly depends on several factors such as temperature, the amount and temporal distribution of precipitation that can vary from year to year. This variation plays a key role in the development of the decision rules of several years. One solution for this was making the range of values in decision rule set quite wide, but with the consideration that too large range can lead to lower classification accuracies. Another solution was creation of the composites and fitting the harmonic function, which removed sharp differences and noise in time series due to atmospheric conditions and cloud cover. Although the development of the decision rule set was straightforward for winter crops due to distinctive spectra-temporal characteristics, the identification of summer crops was challenging due to spectral similarities of these crops. For spatial upscaling and transferring of this approach to other areas, the variation in phenological development from one region to another should be considered. For this, in situ data of phenology, the knowledge of crop development and the integration of the weather data may lead to accurate results for large area classification.

4.6 Conclusions

In the presented paper, we discussed the delineation of main crop types in the central region of Ukraine using multi-source remote sensing data. We have proposed and evaluated a two-step approach that constitutes of training sample generation based on harmonic regression, random forest and decision fusion classification. The approach developed and tested herein has the potential for cases especially when field data are insufficient. We have also demonstrated the potential use of optical and SAR data for the rule-based training sample generation and subsequent crop classification in complex cropping systems. The derivation of key phenological and temporal metrics enabled the creation of image composites that allow mapping the crop types accurately. In addition,

we demonstrated that the harmonic fit and derived metrics can be very useful for representation of the seasonal variations of crops. The obtained results confirmed the feasibility of the herein developed two-step approach for crop mapping in the study area in Ukraine. Overall accuracy exceeded 80% when seasonal composites were used. Among the crop species, the class of winter cereals was the most accurately identified, while we observed misclassifications between soybean and maize. We showed that class separability is depending on the selected features and their temporal distribution of the input data. The integration of multispectral and SAR data improved the classification accuracy. The method was tested for two years which enabled us to study the effect of inter-annual meteorological differences on crop phenological development that in turn, impacts crop classification results. Based on our results, we recommend the use of seasonal composites in a two-step approach of classification to create accurate crop maps over several years. Overall, our remotely sensed crop patterns were confirmed by quantitative (via accuracy assessment and comparison with state crop statistical data) and qualitative tests including agroecological knowledge of local experts. Therefore, we concluded that the proposed approach could be implemented in the areas where field observations are not available or scarce.

Chapter 5

Local Scale Agricultural Drought Monitoring with Satellite-based Multi-sensor Time-series

Abstract: Globally, drought constitutes a serious threat to food and water security. The complexity and multivariate nature of drought challenges its assessment, especially at local scales. We aimed at assessing spatio-temporal patterns of crop condition and drought impact. For this, we used time series from optical (Landsat, MODIS) and SAR (Synthetic Aperture Radar) data to identify the main characteristics of agricultural droughts in Ukraine at the spatial scale of field management units. Indicators were derived based on optical (Normalized Difference Vegetation Index (NDVI), Normalized Difference Moisture Index (NDMI), Land Surface Temperature (LST), Tasselled cap indices) and Sentinel-1 (backscattering intensity and relative surface moisture) data. We used logistic regression to evaluate the drought-induced variability of remotely sensed parameters estimated for different phases of crop growth. The parameters with the highest prediction rate were further used to estimate thresholds for drought / non-drought classification. The models were evaluated using the area under the receiver operating characteristic (ROC) curve. The results revealed that not all remotely sensed variables respond in the same manner to drought conditions. Growing season maximum NDMI and NDVI (70-75%) and SAR derived metrics (60%) reflect specifically the impact of agricultural drought. These metrics also depict stress affected areas with larger spatial extent. LST was a useful indicator of crop condition especially for maize and sunflower with prediction rates of 86% and 71%, respectively. The developed approach can be further used to assess crop condition and to support decision making in areas which are more susceptible and vulnerable to drought.

5.1 Introduction

Increasing crop production and resilient agriculture are essential to meet the rising food demand. To close the gap between potential and actual yield, it is critical to understand how climate extremes impact crop condition in a spatially explicit and scalable manner. Crop production changes, and particularly crop loss related to weather variability have always been of interest for farmers, governments, and decision makers who aim to reduce these impacts triggered by natural disasters and extreme events, in order to take actions for mitigation and to support food security in general (Kogan et al., 2013). One of the extreme events having an impact on crop production are droughts which bear food and water security concerns globally (Sadegh et al., 2017). Drought is a complex slow-onset natural disaster which can, with regard to its impact, last over a notable period of time (weeks to months) (Mishra et al., 2015; L. Zhang, Jiao, Zhang, Huang, & Tong, 2017). Although, there is no universally accepted definition of drought, it is most commonly characterized with a precipitation deficit (Wardlow, Anderson, & Verdin, 2012). It significantly alters several sectors, including water quantity and quality and influences food, water, and energy security and can subsequently have broad socio-economic effects.

In the past decades, several studies discussed the derivation of drought-related metrics based on hydrological variables such as precipitation and soil moisture. To have a drought indicator, often hydrological variables were used to estimate the extent of an anomaly or difference from a reference. The resulted indicators are then used to quantitatively assess and categorize drought severity (AghaKouchak et al., 2015). One of the first indices developed was the Palmer Drought Severity Index (PDSI) (Palmer, 1965) which enabled the assessment of relative drought severity. Another widely used drought metric is Standardized Precipitation Index (SPI) (Guttman, 1998). However, as evapotranspiration (ET) also plays a major role in agricultural water stress and crop production, the standardized precipitation evapotranspiration index (SPEI) was developed (Vicente-Serrano, Beguería, & López-Moreno, 2009).

Remote Sensing (RS) data has been widely used to monitor drought impact and to derive parameters along with climatological indices. Its main advantage is the availability of temporally and spatially continuous information over large areas. This is an advantage for monitoring of vegetation condition on large scale compared to in situ measurements which can be costly, labour intensive and limited to rather smaller areas. Optical RS data has been used to explore the link between photosynthetic rate and optical properties of the plant leaves by estimation of vegetation indices. The most commonly used vegetation indices are the Normalized Difference Vegetation Index (NDVI)

and Enhanced Vegetation Index (EVI) which indicate the vegetation condition through the ratio of near-infrared and visible bands. Specifically, data obtained from Advanced Very High-Resolution Radiometer (AVHRR) and Moderate Resolution Imaging Spectroradiometer (MODIS) were often used for calculating drought indices. One of the conventional approaches is the derivation of the Vegetation Condition Index (VCI), which uses NDVI or EVI of the current time relating it to long-term minimum and maximum. Another drought relevant indicator derived from remotely sensed time series is the Vegetation Health Index (VHI), which incorporates both NDVI and brightness temperature (BT) data. VHI, in particular, has been found efficient in determining the empirical probability of agricultural drought occurrence (Kogan, 2019).

Fewer studies have focused on high-resolution data derived from sensors such as Landsat due to a lack of dense time series needed for drought impact monitoring. Besides the frequent use of NDVI (Karnieli et al., 2010; Klisch & Atzberger, 2016; van Hoek, Jia, Zhou, Zheng, & Menenti, 2016) further studies explored the sensitivity of other VIs to vegetation condition change, such as indices incorporating the shortwave infrared (SWIR) band. Notably, it was demonstrated that MODIS based NDWI, derived from NIR and SWIR bands, is more sensitive to the onset of drought stress compared to commonly used NDVI (Gu, Brown, Verdin, & Wardlow, 2007). Furthermore, NDVI and NDWI were later integrated into Normalized Difference Drought Index (NDDI) (Gu et al., 2008). In general, the integration of several data sources such as remotely sensed indices, climate, land cover has been discussed to be more effective in vegetation stress monitoring, because multisensor data makes it possible to assess adverse impacts of droughts. One of the examples is VegDRI derivation where the satellite and climate based drought indicators are combined with other biophysical information such as ecoregions and elevation (Wardlow et al., 2012). Although there are examples of multivariate drought analysis (Enenkel et al., 2016; Wardlow et al., 2012; Wu, Qu, & Hao, 2015), there is still a need for the use of multisource high resolution data. The integration of remotely sensed information from optical, infrared and microwave portions of the spectrum could provide valuable, complementary information regarding drought severity (Xiang Zhang, Chen, Li, Chen, & Niyogi, 2017). Synthetic aperture radar (SAR) applications for crop monitoring have only been used rarely as compared to optical data. The reasons for this include limited availability of freely distributed datasets, the absence of large-area acquisitions and the need for more comprehensive data processing compared to optical data. So far, few studies have used dense SAR time series data for crop monitoring (Moran et al., 2012; Schroeder et al., 2016). Some studies have demonstrated the use of microwave sensors for vegetation monitoring in general, such as Metop Advanced SCATterometers (ASCAT), Soil Moisture Ocean Salinity (SMOS) mission

and Soil Moisture Active Passive (SMAP), but the spatial resolution of these datasets is coarse. Only recently, finer resolution SAR data, such as Sentinel-1 data has been used to assess the sensitivity of backscatter to crop dynamics (Urban et al., 2018; Veloso et al., 2017; Vreugdenhil et al., 2018). In order to derive methods using dense time series of SAR and optical data, there is a need to study their temporal behavior for a variety of widely cultivated crops. As backscatter is affected by water content and roughness of land surface (i.e. soil, leaf and stem moisture content, geometry and structural properties such as size and orientation) it may be sensitive to drought (Schroeder et al., 2016). Recent studies reported fluctuations in crop production related to extreme weather conditions in Ukraine. It was reported to have more intense and frequent droughts in recent years (Adamenko & Prokopenko, 2011; Kogan et al., 2013; Skakun et al., 2015). This climate fluctuation reduced summer crop production by up to 75%. Furthermore, there were reports on increasing frequency of extreme events with severe drought in 2003, 2007, 2015 and 2017 (Adamenko & Prokopenko, 2011; Ivits, Horion, Fensholt, & Cherlet, 2014). Skakun et al. (2015) quantified agricultural drought-risk in Ukraine using VHI. However, continuous monitoring of croplands throughout the growing season is needed, to identify the key characteristics of drought hazard at a finer scale. The knowledge about start, severity, duration and spatial extent of the affected areas would improve our understanding of drought characteristics which would in turn support the decision-making and actions aimed at mitigating drought effects at the spatial scale of field management units. Drought impact increases when the lack of precipitation is coupled with heat waves enhancing the vegetation's evaporative stress (Ahmadalipour, Moradkhani, Yan, & Zarekarizi, 2017). In the context of this study, we aimed at understanding the impact of moisture scarcity and increased evaporative demand due to heat stress. In this regard, the overall aim of this research was to study the possibility of the use of high-resolution remotely sensed time series for observing drought impact. Specifically, we aimed (i) to investigate features derived from optical and SAR imagery for drought impact monitoring, (ii) to study the temporal variability of time-series during the growing season under drought and non-drought conditions and (iii) to investigate the spatial variability of drought impact and the agreement of drought characteristics derived from different sensors.

5.2 Materials and Methods

5.2.1 Study Area

Three study cites were selected in the Kiev region: Bila Tserkva, Mironivka and Yagotin districts (Figure 5.1). Agricultural fields and cultivated areas comprise more than 70% of the area in each district (State Statistical Department of Kiev region, 2015). Primary crops grown in these regions are winter wheat, maize, soybean, and sunflower (Nataliia Kussul, Mykola, Shelestov, & Skakun, 2018). The agricultural production is highly associated with favourable meteorological conditions, as rainfed agriculture is predominant in these regions. In dry years, precipitation significantly reduces from 400 mm to 170 mm during the growing season.

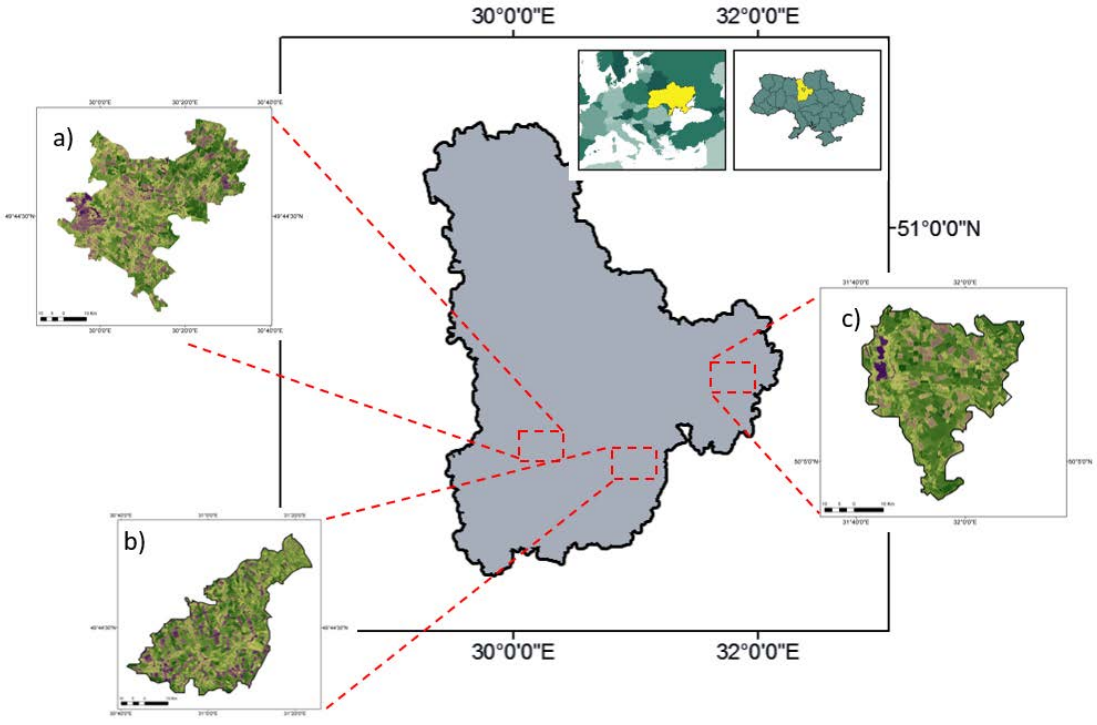

Figure 5.1: Study Areas: a) Bila Tserkva, b) Mironivka c) Yagiton districts.

During four growing seasons, suboptimal hydrological conditions were observed in 2015 and 2017 (Figure 5.2). Topography in this area is mostly flat with in the range of 0- 2%. The soils in the area are mostly chernozems (Black soils), which are rich in organic matter and highly fertile.

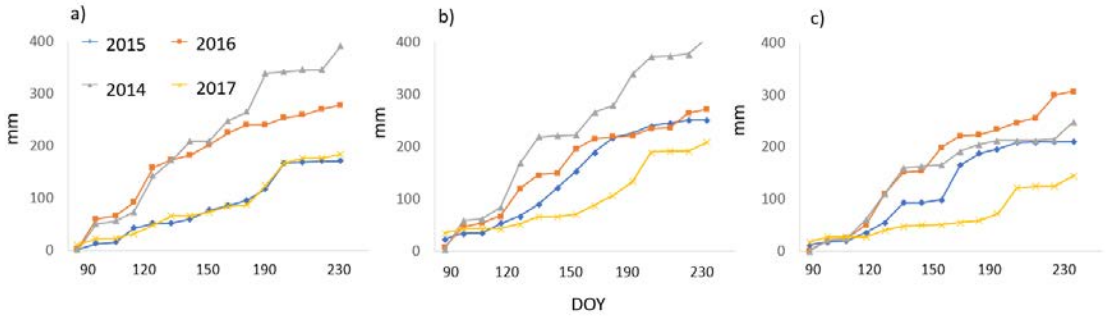

Figure 5.2: Precipitation during the main crop growth period between April and September in a) Bila Tserkva, b) Mironivka c) Yagiton regions.

5.2.2 Data

Satellite Imagery

Our analysis focused on the 2014 –2017 period, which was determined by the availability of datasets encompassing consecutive growing seasons with different hydroclimatic conditions. 30m-Landsat-based (L8) time series metrics that capture the seasonal variations of crops were acquired and analyzed using Google Earth Engine (GEE) cloud computing platform (Gorelick et al., 2017) . The number of valid observations of optical data series might have been reduced due to poor atmospheric conditions and cloud cover. For this reason, we used observations from MODIS with 250 m resolution to integrate it with Landsat and to test improvements (Feng Gao, Wang, & Masek, 2013). Cross-polarized Sentinel-1 C-band SAR images (S1) were also used due to their sensitivity to the attributes of a target surface such as dielectric properties and roughness (Schroeder., 2016). In order to test the interoperability of Sentinel-2 (S2) data with previously discussed data collections, we integrated Level-1C (L1C) TOA data which is also available in GEE data catalog. Although the data was available for only two growing seasons, S2 imagery was still used in the analysis to test the comparability of data from different optical sensors.

Additional Data

A suite of ancillary data was also compiled and used to link quantitatively crop condition and crop growth dynamics with different factors. These datasets consisted of agrometeorological observations along with land use maps. The agrometeorological data (e.g., temperature, precipitation, in situ phenological observations) were acquired from the State Hydrometeorological Services of Ukraine. In addition, we used land use maps of the study area from 2014 to 2017 provided by Space Research Institute (SRI) of the National Academy of Sciences of Ukraine (NASU) (Nataliia Kussul et al.,

2018). Additionally, in-situ observations of drought-impacted fields were acquired comprising 20 fields from 2015, 19 fields for 2017 and 14 fields from 2016 non-drought conditions from Bila Tserkva district.

5.2.3 Methods

The workflow for crop condition monitoring and estimation of drought characteristics was based on the analysis of relevant metrics derived from Sentinel-2, Landsat-8 and backscatter time series based on Sentinel-1 (Figure 5.3).

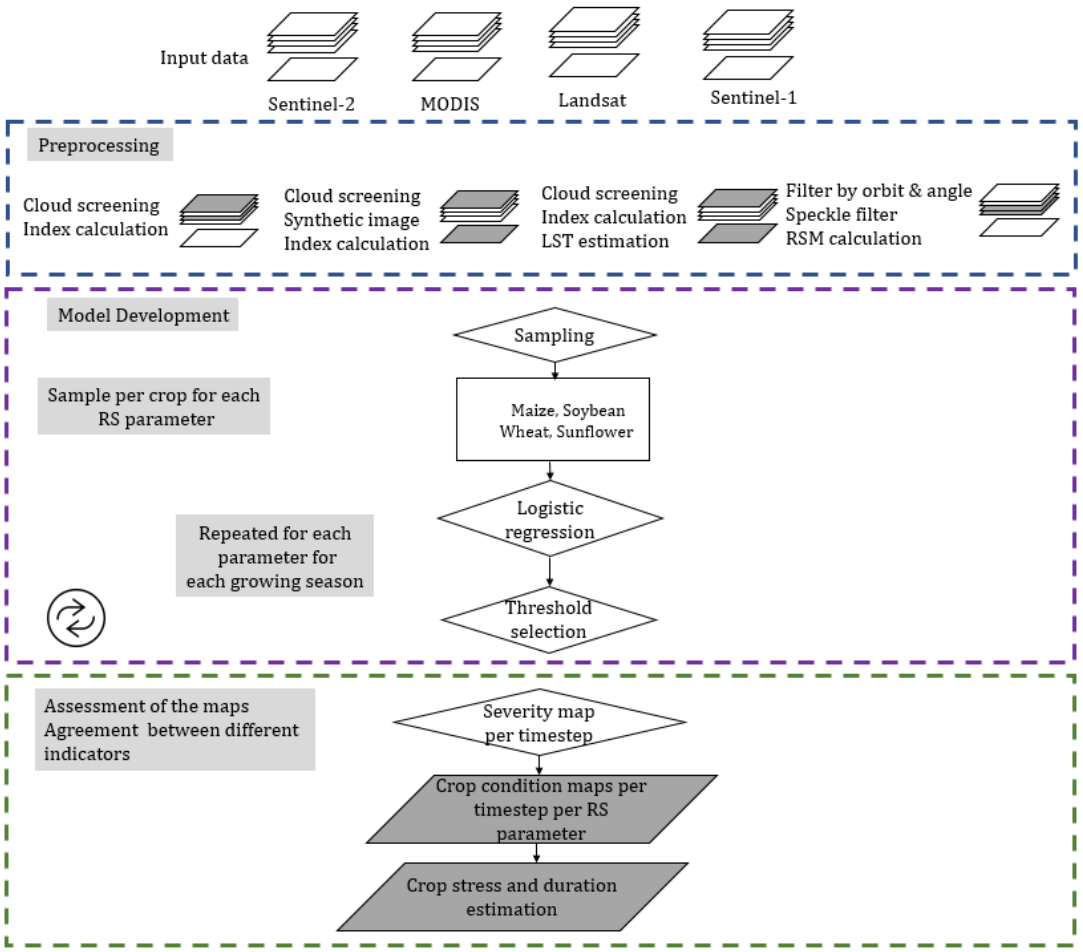

Figure 5.3: Workflow for drought induced crop condition monitoring, where RS stands for Remote Sensing, LST for Land surface Temperature, RSM for Relative surface moisture.

Pre-processing

To overcome the frequently missing data in Landsat time series due to cloud cover we used MODIS and Landsat data to predict synthetic Landsat imagery for timesteps when MODIS was available. The primary selection criterion of Landsat and MODIS data pairs was their acquisition date. Both images should be acquired with the shortest temporal delay (Feng Gao et al., 2013). With the closest pair we predicted synthetic Landsat image based on pixel-wise linear regression (M. He et al., 2018). Prior to analysis, Fmask (Function of mask) (Z. Zhu et al., 2015) and cloud-mask flags were used for clouds and cloud shadow detection in the Landsat and MODIS imagery. For Sentinel-2 time series we used the QA60 bitmask band which contains cloud information to mask out opaque and cirrus clouds. In addition, we used modified Temporal Dark Outlier Mask method which was applied to Sentinel-2 observations (Housman et al., 2018). The Sentinel-1 σ_o time series analysis was carried out following pre-processing of the SAR imagery such as geometric correction, radiometric normalization, speckle noise reduction. The data was pre-processed by GEE (GEE API, Sentinel-1 Algorithms) following the steps implemented in the Sentinel-1 toolbox. The pre-processing included thermal noise removal, radiometric calibration, and terrain correction. To reduce the impact of differences in viewing geometry and the orientation of the radar beam, the ascending and descending overpasses were used separately. For each location we further filtered images by the orbit, as the difference in orbit and incidence angles can induce changes in backscattering that are not related to geometric or dielectric properties of the target. To further reduce the effects of incidence angle variations on the backscatter, we eliminated observations with very shallow and steep incidence angles. We applied GammaMap filter to reduce speckle with the 7x7 kernel size.

Derivation of RS Parameters

Following the pre-processing of each image collection, we derived parameters based on vegetation index time series, such as NDVI and NDMI. NDMI was estimated based on NIR and SWIR. Landsat based NDVI was further used to derive information on the timing of green-up, senescence and length of the growing season. These metrics were derived by estimating the DOY (day of a year) of the first NDVI observation during the growing season, which had lower/higher values than a defined threshold. Besides the aggregation of these metrics throughout the crop growth period (maximum, amplitude) as a proxy of overall condition, we studied crop condition at specific growth stages. For this, we calculated local changes of VIs within 20-day and the ratio of S1 backscatter change. Taking into consideration the frequency of different observations, 20-day interval was chosen, as this window allowed to capture changes in data acquired with all sensors (i.e. Landsat with 16-day observation,

Sentinel-2 with 12-day observation). To investigate thermal conditions of the vegetation, we used single channel method to derive LST based on Landsat imagery. NDVI-based surface emissivity information was used (Jimenez-Munoz & Sobrino, 2010). Another metric that we investigated was the Landsat based tasseled-cap transformation (TCT). TCT is an empirical transformation that captures critical physical characteristics of vegetation, mainly we used the wetness which is mostly linked to a combination of moisture conditions and vegetation structure. Relative surface moisture was estimated using the minimum and maximum backscatter values observed over the study period, which is considered to be equivalent to the dry reference (5th percentile) and wet reference (95th percentile) (Urban et al., 2018; Wagner, Lemoine, & Rott, 1999). Thus, crop condition was described by several metrics derived from Landsat (NDVI, NDMI), the combined use of Landsat and MODIS (NDVI), Sentinel 2 and Sentinel 1 (Table 5.1).

Indicator	Sensor
Normalized Difference Vegetation Index	L8, S2, L8+MOD
Normalized Difference Moisture Index	L8, S2
Backscatter	S1 (VH, VV)
Relative Surface Moisture	S1 (VV)
Tasseled-cap wetness	L8
Land surface temperature	L8
Phenometerics (green up, senescence, length, amplitude)	L8

Table 5.1: Main RS indicators tested for agricultural drought monitoring, where L8 stands for Landsat 8 observations, S2 for Sentinel 2, S1 for Sentinel-1 and L8+MOD for Synthetic Landsat products.

Model Development

We used logistic regressions to further examine crop condition and subsequent classification of drought impact in three disturbance levels based on the comparison of parameters from different conditions. The models were tested based on 20 samples per crop/per region derived for the growing seasons. The only exception was soybean, for which the number of samples was less (28 observations less than the other crops), as in 2014, 2016 and 2017 we were unable to find representative fields (based on size, uniform cover) in our study areas. The initial drought events were identified based on historical studies and in situ weather data. 2015 and 2017 were known to be drought years that affected large areas. Additionally, non-drought years were represented by the years 2014 and 2016 (Figure 5.2). One of the challenges for the comparison is the estimation of relevant thresholds that discriminate between drought and non-drought conditions, as well as varying levels of drought impact level, namely low, moderate and severe as they can be different among different

crop type, location, and season. Typically, a relative VI value or a deviation of a VI value from a baseline is used as an indicator of drought. Due to crop rotation and subsequent year to year crop changes in our study area, instead of comparing the indices derived from different years at the same location, we compared the condition of the respective crop from different locations in different years. The output of the regression was used to evaluate the drought-induced variability of remotely sensed parameters. The variables with the highest prediction rate were further used to estimate the thresholds for drought/non-drought classification. The models were evaluated using the area under the receiver operating characteristic (ROC) curve. For each variable which yielded in a statistically significant result ($p< 0.05$) and satisfactory prediction accuracy, we derived a value at which the parameter discriminated drought and non-drought conditions. Based on these values, crop specific thresholds for three levels were subsequently estimated. Based on the consecutive drought occurrence during the growing season, the length of the drought was estimated. Finally, we evaluated the results derived from different parameters with the in-situ field data from 2015-2017.

5.3 Results and Discussion

Comparing the Parameters Extracted from Different Sensors

Remotely sensed time series were used to derive indicators from a single data source (Landsat, Sentinel-1, and Sentinel-2) or fused series (Landsat/Modis) and to assess drought-induced properties during 2014-2017. Among the variables tested in this study, NDMI, LST, and SAR based relative moisture index had a significant impact on the prediction of drought occurrence. The accuracy of different models varied based on region, crop of interest and remotely sensed derivatives. In general, within all models, maize was affected the most compared to other crops, that showed lower values in impacted areas. This can be explained by the fact that crops are characterized by different sensitivity to water-deficiency during each phenological phase (Xiang Zhang et al., 2017). NDVI and NDMI from different sensors exhibited similar results (i.e. AUC, prediction rate) for positive and negative predictions when applying the logistic model. Particularly, NDVI and NDMI accuracies ranged between 50-70% and 52-75% respectively. These results are in line with other studies and can be conditioned with the properties of SWIR that reflect changes in water content. The lowest accuracies were observed for soybean, with a ROC value of 0.57 which can be conditioned by a lower number of samples. The MODIS/Landsat based methods, were less accurate compared to results derived from Sentinel-2 and Landsat. One possible explanation is the

higher intrapixel heterogeneity at the MODIS scale, which results in underestimation of drought impact. As a result, best MODIS/Landsat based models produced satisfactory results, with a ROC value of 0.72. Local parameters (e.g. short-term maximum, amplitude within a month) describing within seasonal changes, especially those from mid growth period, were sensitive to drought as well. The only constraint for this was the decreasing number of samples, due to masked values in the optical data set. LST was significantly higher for crops with unfavourable conditions during the mid-season of 2017. This was observed for maize and sunflower with the highest ROC values 0.86 and 0.79, respectively. As a result, the drought affected fields could be discriminated (Figure 5.4). This is in agreement with several studies reporting that the period around anthesis is particularly sensitive to heat stress in nearly all crops (Luo 2011). The link between vegetation indices and LST is attributed to changes in the proportion of vegetation cover and moisture conditions, showing that surface temperature can quickly increase with drought stress (Johnson, 2014).

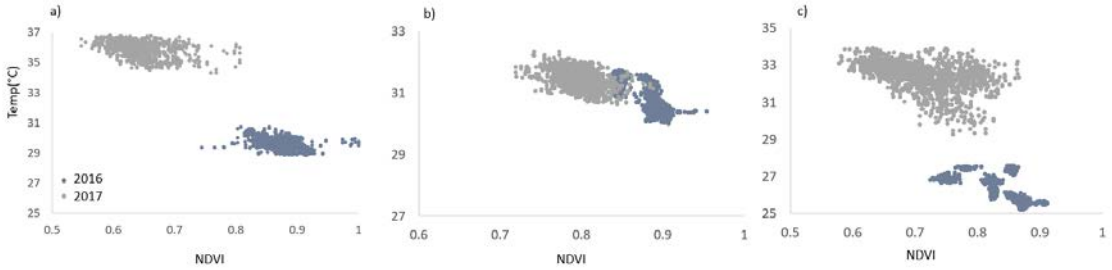

Figure 5.4: NDVI/LST scatterplots for a) maize, b) soybean and c) sunflower during the mid-growing season derived from Landsat-8.

Although we observed differences in the length of growing season among drought and non-drought years, they were not statistically significant. Furthermore, tasseled cap wetness did not yield in statistically significant results and so this was not used for further analysis. Including SAR input variables into the logistic model resulted in satisfactory performance with a ROC value of 0.65 and an accuracy of 60% only for maize. The best results were acquired from observations during the tasselling and silking period.

Temporal Variability of RS Metrics During Drought and Don-drought Years

Two major drought occurrences differing in intensity, timing, duration and location were examined over the three study sites in Ukraine between 2014-2017. Our results illustrate that optical time series, including NDVI, MDMI, play a primary role in determining drought occurrence.

The most pronounced and significant changes were observed during the peak growing season and corresponded to anthesis and ripening stages of summer crops (Figure 5.5). The NDVI

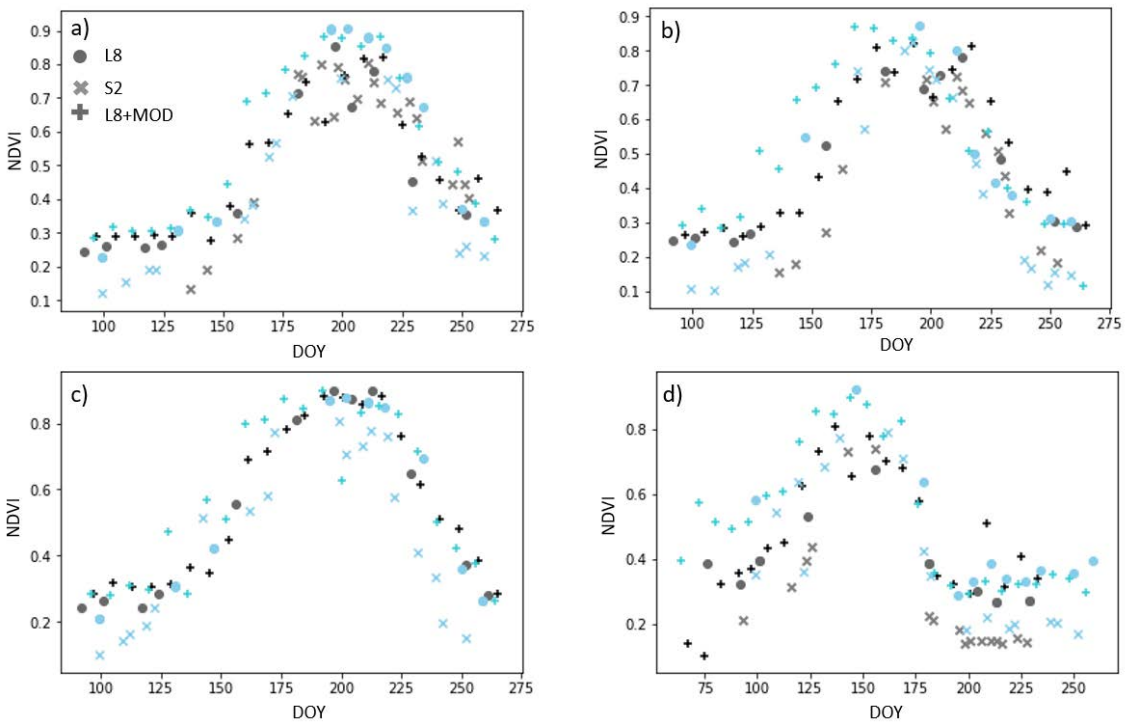

Figure 5.5: Time series of NDVI derived from optical sensors for a) Maize, b) Sunflower, c) Soy, d) wheat with blue depiction non-drought conditions (2016) and black drought conditions (2017).

derived from different sensors in general was similar for both drought and non-drought conditions. The local amplitudes of NDVI were high in drought-affected fields reaching a value of 0.4. When using SAR backscattering signal, we observed higher fluctuations of intensity in drought-affected fields of maize. For the other crops the backscattering intensity was highly variable. This was most prominent for wheat. Particularly, lower backscatter during the non-drought condition was observed, which can be caused by increased attenuation. Backscattering intensity is a function of the geometry and the dielectric properties of a crop. Throughout the growing season, crop height and water content are changing, so it is difficult to decompose drought factors. Crops' growth period is visible as an increase in reflectivity in the VH band (Figure 5.6). Backscatter generally increases as water content in vegetation increases. Similarly, backscatter intensity decreases with the decline of wet biomass, which could be observed in this study at the end of the growing season.

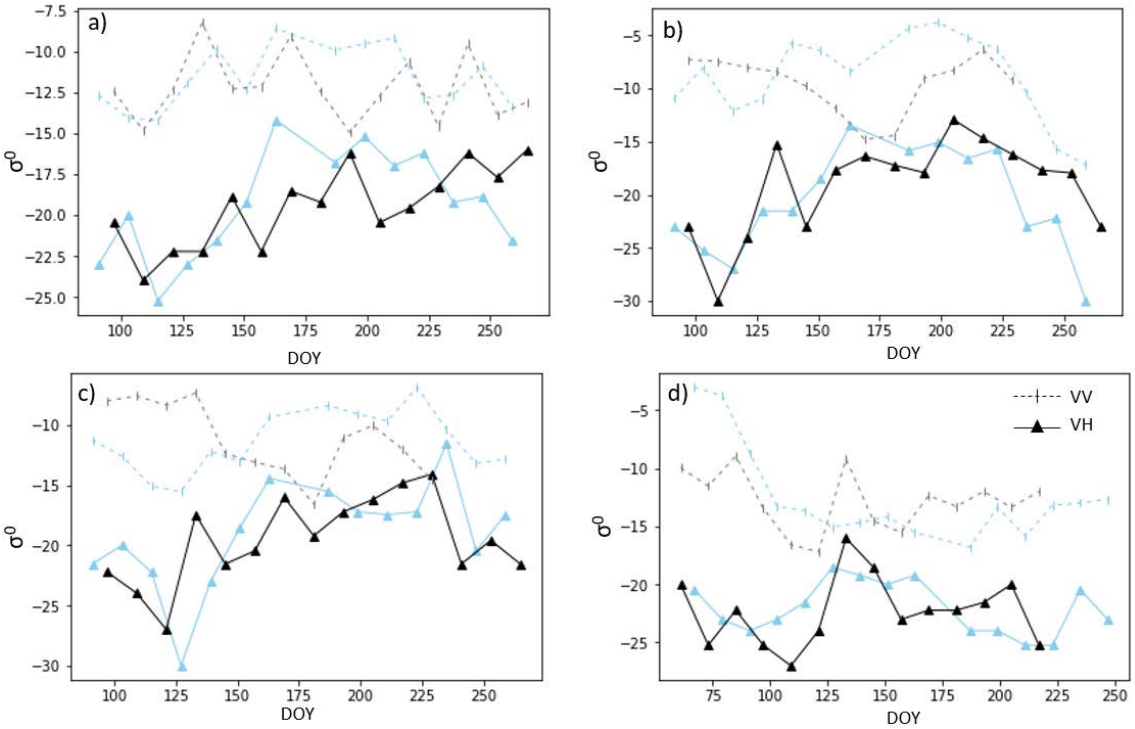

Figure 5.6: Time series of backscattering coefficient for a) Maize, b) Sunflower, c) Soy, d) wheat with blue depiction non-drought conditions (2016) and black drought conditions (2017).

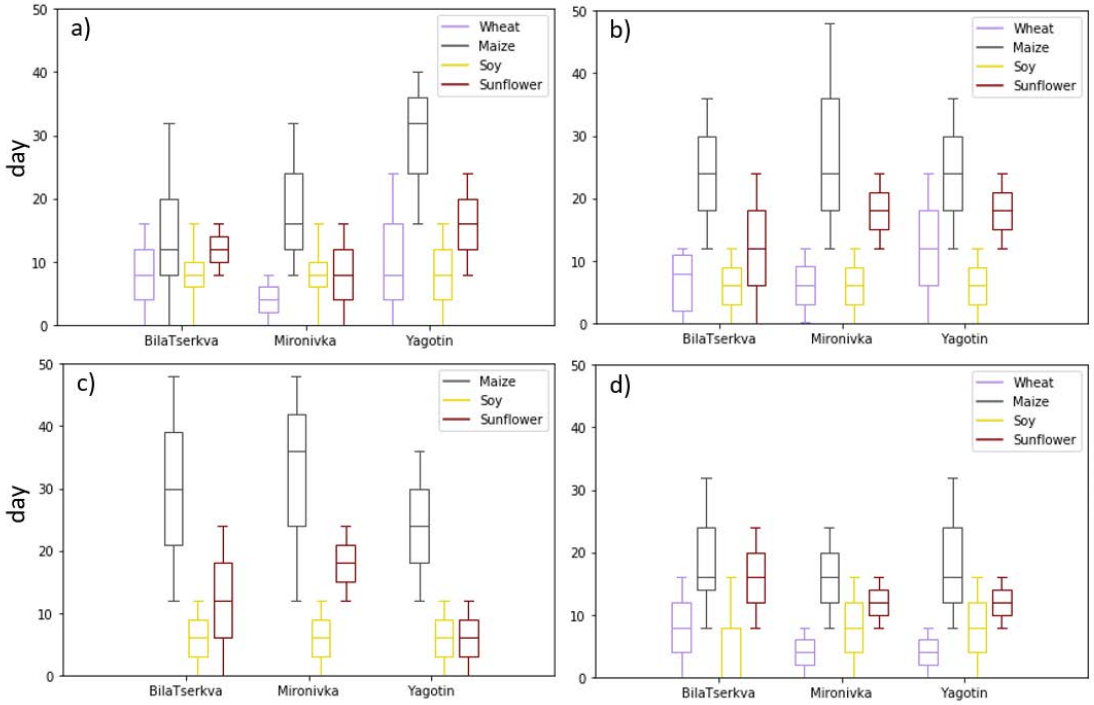

Figure 5.7: Length of the drought estimated in 2017 from a) Landsat NDMI b) Sentinel 2 NDMI, c) Sentinel 1, d) L8+MOD NDVI.

The sensitivity of VV backscatter to soil moisture in maize (Figure 5.6a) can be explained by larger row spacing on maize fields. Because of this, bare soil is visible and VV backscatter is not attenuated by vegetation and can be still affected by soil moisture. Similar results have been reported by other studies (Vreugdenhil et al., 2018). In this study, the maximum drought duration identified varied among different drought indicators (Figure 5.7). Based on our analysis, the maximum drought duration appeared to be higher in the SAR based variables than in the optical indices. Maize was the most sensitive to a drought of one month occurring in July, which corresponds to silking and reproductive stages. This agrees with other studies, where NDVI was evaluated for maize response to drought (R. Wang et al., 2016). For wheat we observed high sensitivity particularly in June. Even though we observed large areas of wheat with suboptimal water conditions in 2015, this was not reflected in the yield statistics which did not depict a drastic yield decrease. This might be explained with the recovery of the crop due to sufficient rainfall and optimal thermal conditions during the subsequent stages of crop growth. For further understanding of the winter wheat response to drought hazard, the study of conditions during the winter months is still needed. One of the limiting factors for the estimation of drought duration was the temporal frequency of remotely sensed observations. This was critical for cases when periods of precipitation deficit were shorter than the revisit time of the sensor, and as a result drought induced changes were not fully depicted by the indicator. Our results indicate, that VIs were not sensitive to drought stress at early growth stages. For all crops we observed the impact of drought stress and the start of the drought close to the flowering stage. Although considered as moderately drought tolerant, we observed drought impacted sunflower fields in three regions.

Spatial Distribution of Drought Impact

For each of these drought events, the corresponding areas being affected by recurrent drought events were mapped. Our results indicate areas that were affected by drought when using different indicators for different crops ranging from 20% (for soybean) to 44% (maize) in 2017. In general, areas affected by drought varied for different crops. We observed the highest affected areas for maize, for both 2015 and 2017, whereas the areas for other summer crops (sunflower and soy) comprised 23-30% of the cultivated area. These estimates were different compared to the tests on non-drought years, where areas under sub-optimal conditions were less than 10%. The only exception was soybean, in which we observed approximately 16% of the cultivated area under severe, moderate and mild stress, although the year of 2016 exhibited more favourable conditions. Depiction of these false positive stressed areas can be caused by different management practices and

cultivar change which were not examined in this study. The drought impacted areas as derived from remotely sensed crop condition variables also differed with time (Figure 5.8). In the case of 2015, we identified larger affected areas at the end of the growing season, whereas in 2017, the drought impact could be observed at earlier stages of the growing season. In general, derivatives from optical sensors reported similar timing of the start of drought. In a contrary, SAR derived onset of crop stress appeared 12 – 24 days earlier than those derived from optical data. Coupled with the declined precipitation during the growing season as well as reduced crop yields, this indicates that drought-induced properties of time series can be characterized based on temporal metrics. Temporal features showed that different crops experience different intensities of drought impact (Figure 5.9). Moreover, the described drought-induced properties were more prevailing in different regions of the study, opposed to local management differences, which would be allocated to specific smaller areas. The agreement maps based on peak growing season (July) for maize show that in the majority of the fields the indicators have more than 50% agreement for 2017. This shows that data from different sensors indicate a similar condition for the crop and are comparable, thus further integration of the datasets is feasible (Figure 5.10). Whereas for 2015, both the detected drought impacted fields and the agreement between five indicators is less, which can be conditioned by the later onset of the drought. The major environmental drivers that affected crop productivity were used to assess the results of the study. Firstly, we checked the total precipitation during the critical stages of the growing season (April-August) which was 50- 180 mm less. However, precipitation was not evenly distributed during the growing season, and there were periods without rain during start-mid July. The examination of yield of several crops showed that the yields in different regions of the study area decreased significantly in 2017. Mainly, for soybean 26-30% decrease, sunflower yields were 17-26% less, maize 16-40% and wheat yield decreased by 20-33%. The yield losses in general were less in 2015, especially for wheat and sunflower comprising 7-10% compared to non-drought years. Nevertheless, in 2015 maize and soy had 20% yield decrease.

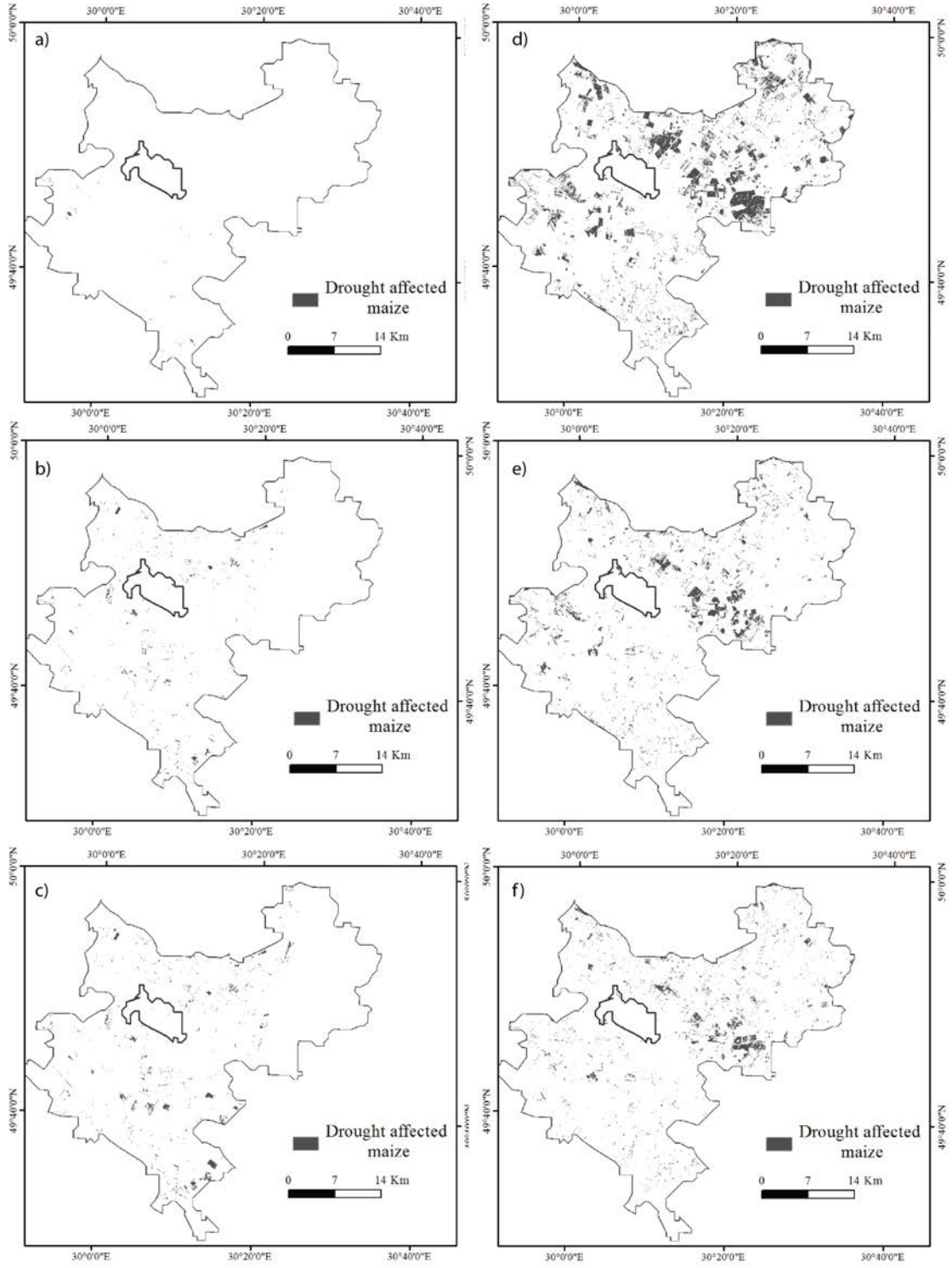

Figure 5.8: Spatially explicit drought mapping series based on Landsat time series in June, July and August during two sub-optimal growing seasons a)-c) in 2015 and d)-f) in 2017.

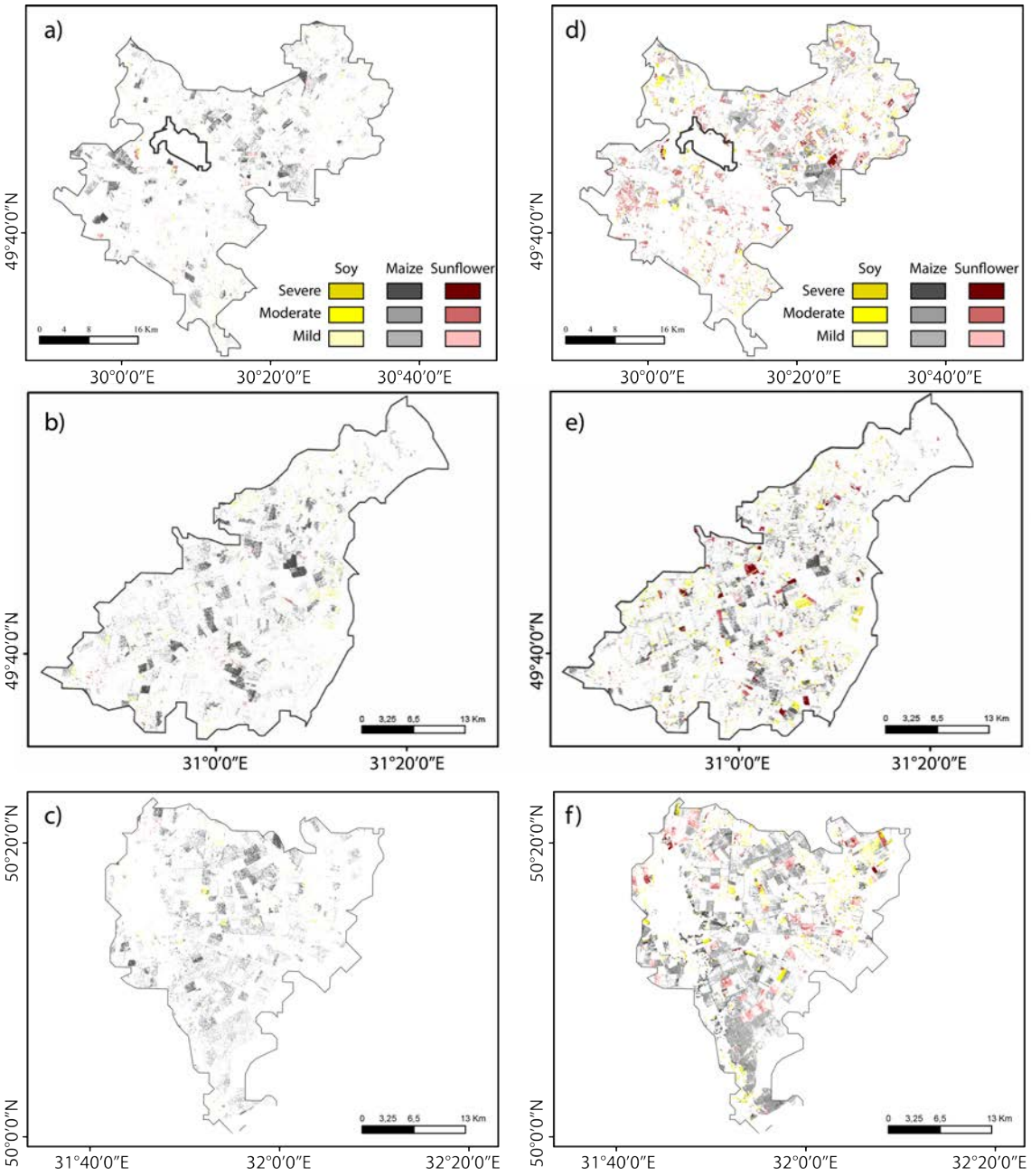

Figure 5.9: Drought impacted crops in 2017 derived from a)-c) Sentinel 2 NDMI and d)-f) Sentinel 1 during peak of the growing season (July).

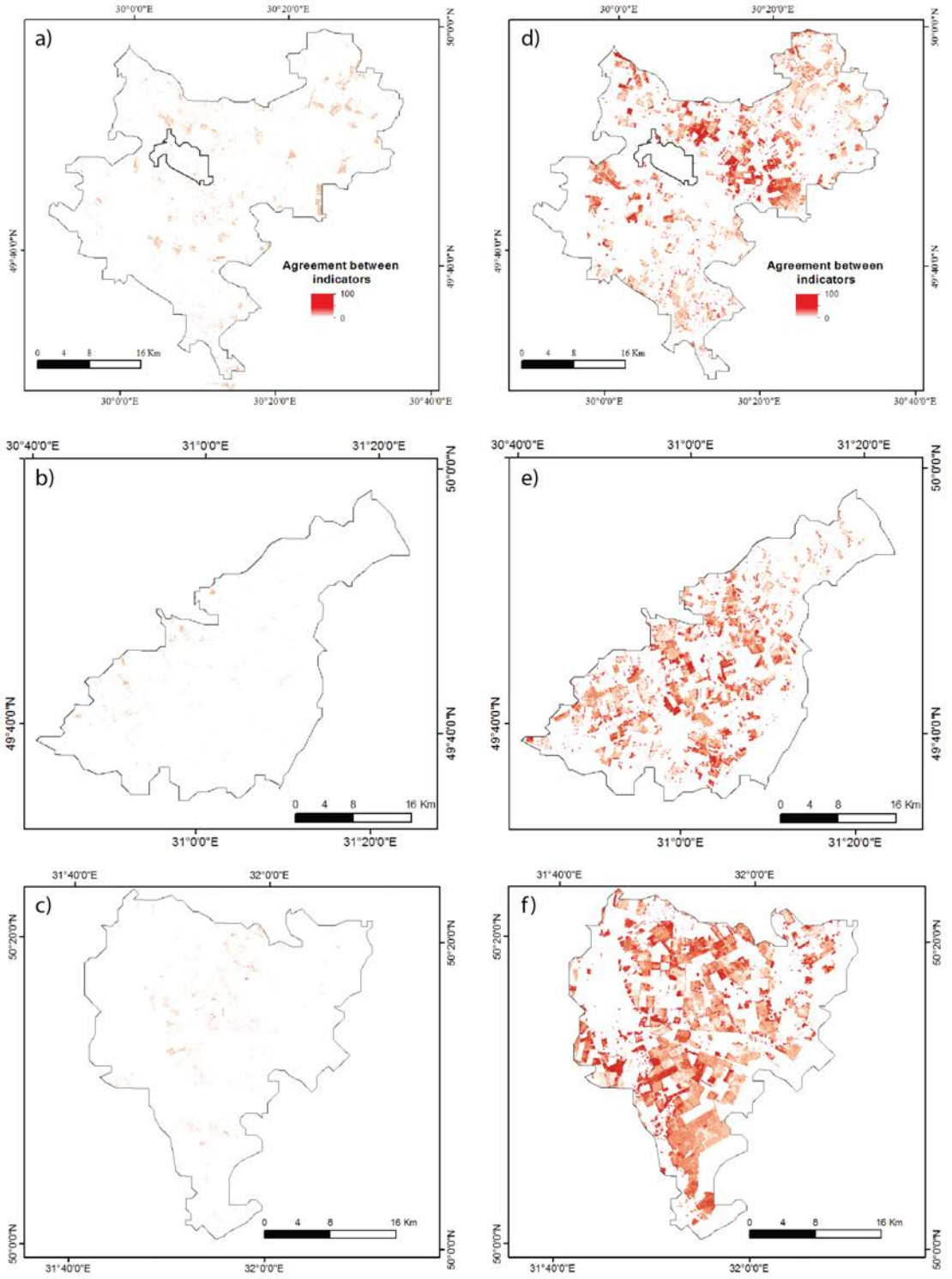

Figure 5.10: Percentage agreement between different indicators a)-c) in July 2015 (LST, S1, L8 NDMI, L8 NDVI, MOD+L8 NDVI) and d)-f) 2017 (LST, S1, L8 NDMI, S2 NDMI, MOD+L8 NDVI).

Although the results of the logistic model show sufficient accuracy (70%) and estimated drought

impacted fields were in good agreement with field data (correct allocation in drought/non-drought class for 75% of the fields with optical data), there is still need for larger validation datasets. Furthermore, certain factors may have contributed to some uncertainties in the estimates of the drought impact and timing. In general, agricultural land cover is characterized by substantial variations within relatively short time intervals. Even though some of these variations might have been caused by agricultural practices, plant disease, cultivar change, we were able to detect the drought induced changes in crop condition. Another issue is the integration of parameters such as soil moisture which would be verified based on in situ measurements. Calibration of models and ET derivation can further improve our understanding of vegetation stress and overall dynamics during the growing season. Nevertheless, our results contribute to the general understanding of climate-induced variations in crop condition by quantifying spatial and temporal variability in drought for major crops in three study areas. Considering that instead of controlled field experiment, the study was conducted in a real environment, assuming the uncertainties, such as cloud cover, this study highlights the feasibility of crop condition monitoring at a farm management scale in different areas. Such spatio-temporal understanding allows us to identify both where and when drought-induced properties can be observed with satellite remote sensing, as well as how sensitivity to drought has evolved over time, which can help guide drought response and mitigation at field, county, state, and national levels. Approximately 45% of the cropping areas were associated with the sub-optimal condition in the key stages of the growing season. These results can be used for development of agricultural management strategies in order to mitigate impacts of droughts on agricultural production.

5.4 Conclusions

The current study introduces new sets of parameters for crop condition monitoring and demonstrates the potential of the optical and SAR data to assess crop conditions at spatial scale that can support decision-making. The combined use of SAR data, multispectral Sentinel-2, and with existing Landsat and lower resolution MODIS time series provides opportunities for applications in crop monitoring and derived variables are sensitive to drought-related stress in croplands. Landsat and Sentinel-2 NDMI estimated higher drought induced effects compared to the other metrics. On the other hand, SAR metrics characterize relatively larger drought duration. The derived drought induced crop condition is influenced by crop type and a timing of the drought. Specifically, we observed summer crops under severe vegetation stress. The findings show that moisture index, SAR

backscatter, and land surface temperature could explain drought occurrence and impact level on crop. These dense time series can be further used for crop water use estimation and near real time crop water requirement estimation. The advancement of large area soil moisture and ET estimation can further improve operational crop water management. The methods demonstrated here can be applied to other areas requiring early warning of food shortage or improved agricultural monitoring to ensure greater sustainability within the agriculture sector.

Chapter 6

Vegetation Monitoring with Satellite Time Series: an Integrated Approach for User-oriented Knowledge Extraction

Abstract: Climate change, food insecurity and limited land and water resources strengthen the need for operational and spatially explicit information on vegetation condition and dynamics. The detection of vegetation condition as well as multiannual and seasonal changes using satellite remote sensing, however, depends on the choice of data including length and frequency of time series. Thus, this contribution focuses on the derivation of the optimal remotely sensed data for vegetation monitoring and extraction of relevant metrics. Time series of satellite data from Landsat-8, Sentinel-1/2, and MODIS were used to identify characteristics of vegetation at different spatiotemporal scales. We derived parameters, such as maximum and amplitude based on vegetation index time series, as well as Land Surface Temperature (LST). Along with optical data, we used backscattering intensity over consecutive vegetation growing seasons. The analysis was carried out using Google Earth Engine, a cloud computing platform which allows to access various data archives and conduct data-intensive analysis. Taking advantage of this platform, we developed a web-based application named GreenLeaf. The application is computing metrics and plotting time series, based on parameters defined by the user. The derived vegetation condition parameters provide sufficient information to detect vegetation change. In addition, the images acquired from near-coincident dates provide similar information over continuous surfaces. The developed application contributes to the use of satellite data and the simplification of data access for users with limited remote sensing experience and/or restricted processing power. Aiming at providing this knowledge to stakeholders can further support decision making on multiple scales.

6.1 Introduction

Vegetation is one of the essential elements of the terrestrial biosphere and is a crucial component for land-cover and climate-related studies. Accurate and continuous monitoring of vegetation is vital to assess the overall ecosystem conditions. Changes in vegetation cover, both of natural and anthropogenic origin, have broad impacts on critical environmental processes including Earth's energy balance, water cycle, and biogeochemical processes (Eastman et al., 2013; B. He, Chen, Wang, & Wang, 2015). Furthermore, timely monitoring of vegetation condition, such as the spatially explicit information on heat and drought stress, growth stage can be critical for decision makers (Mishra et al., 2015). Thus, quantifying such changes is necessary to address a number of critical issues such as the assessment of ecosystem dynamics, global carbon budget, sustainable land use and the vulnerability of natural and human systems. Earth Observation (EO) data collected by different sensors can be a useful supplement to ground-based observation, providing spatial and temporal information for vegetation monitoring over large areas. These data, collected from different sensors, often have different spatial and temporal characteristics. Several studies showed the use of time-series of coarse resolution data, such as from the Advanced Very High-Resolution Radiometer (AVHRR) to extract information on vegetation change and condition (Dubovyk et al., 2015; Fensholt et al., 2015; Klisch & Atzberger, 2016; Miao, Ye, He, Chen, & Cui, 2015). Moreover, the use of moderate to high-resolution sensors such as the Moderate-resolution Imaging Spectroradiometer (MODIS), Landsat and RapidEye has been shown as well (Elste, Glässer, Walther, & Götze, 2015; Fisher & Mustard, 2007; Parplies et al., 2016; Simonetti et al., 2015; Sonnenschein, Kuemmerle, Udelhoven, Stellmes, & Hostert, 2011). Often the activity of vegetation systems has been quantified with the use of vegetation indices (VI), derived from specific combinations of the spectral bands. The use of indices such as the Normalized difference vegetation index (NDVI), or other spectral indices based on optical data has been shown to be effective not only for short-term analysis but also for long-term change characterization (Bradley, Jacob, Hermance, & Mustard, 2007; Rogier de Jong et al., 2011; Fensholt et al., 2009). VIs has been often used for tracking subtle changes in time series, capturing specific vegetation conditions, growth or stages of degradation (Venteris, Tagestad, Downs, & Murray, 2015; Yagci, Di, & Deng, 2015). Besides widely used optical data, data coming from active sensors have also been used for analysis of vegetation dynamics (Fontanelli et al., 2014). Especially the launch of Sentinel-1 and the availability of dense time series of Synthetic Aperture Radar (SAR) data provide more opportunities for tracking temporal and spatial variability of vegetated areas (Imperatore et al., 2017; Reiche et al., 2018).

The growing variety and the increasing volumes of available information make effective data handling of high importance, particularly for tracking vegetation dynamics over several time scales. Nevertheless, recent advances in cloud-based remote sensing pose a challenge to scientists to make the data available for parties outside academia (e.g. policy makers, international donors, NGOs). The latter, lacking advanced technical expertise, are given an opportunity to efficiently use the data, monitor and evaluate ecosystems and implement relevant changes if necessary. There are a number of applications targeting remotely sensed data processing, visualization and download, such as Sentinel Hub ("Sentinel-hub EO-Browser") , Landsat look ("LandsatLook Viewer"), where simple visualization of different composites and time series is possible. Other applications focus on specific applications such as sediment mapping("Lower Mekong Basin Suspended Sediment Monitoring"). One of the advanced applications available is ClimateEngine ("On-Demand Cloud Computing and Visualization of Climate and Remote Sensing Data") where besides simple visualization users can derive several climatological and remote sensing variables, and calculate anomalies. However, ClimateEngine offers more coarse scale parameters, and finer scale derivates such as Landsat based land surface temperatures, Tasseled cap indices, along with data manipulations such as thresholding, multitemporal compositing is not integrated. Thus, this contribution focuses on (i) the derivation of the optimal data and indicators for vegetation monitoring (ii) identification of characteristics of vegetation at different spatiotemporal scales and (iii) the integration of these products in an easy to access web application for large-scale information extraction.

6.2 Materials and Methods

6.2.1 Data and Tools

Time series data from Landsat-8, Sentinel-2, MODIS, and Sentinel-1 were used to identify characteristics of vegetation at different spatiotemporal scales. The data were accessed and analyzed using Google Earth Engine (GEE). It is an advanced cloud computing platform for processing global-scale satellite imagery. GEE provides access to satellite products which are organized in image collections which make the combined use of these datasets possible (Sidhu, Pebesma, & Câmara, 2018). The Landsat Surface Reflectance (SR) time series were selected (Robinson et al., 2017) as the primary source of data as this dataset is corrected for atmospheric and illumination/viewing geometry effects and are the highest levels of image processing available for Landsat data. Landsat SR products contain pixel data quality flag information indicating clear, snow, cloud or shadow conditions, as determined by the CFMask algorithm (Foga et al., 2017). These quality flags were

used to eliminate low-quality pixels with possible cloud and shadow contamination. In addition, Landsat top of atmosphere (TOA) collection was used within the framework for calculating Land surface temperatures and Tasseled cap indices. In this study, we used the MOD09Q1 surface reflectance (8-day composite, 250 m resolution). This product comprises the best (low view angle, the absence of clouds, lowest aerosol loading) observations in near-infrared (NIR) and Red spectral bands collected during an eight-day period, with corrections for atmospheric influences applied. While daily NDVI could be calculated directly from the MODIS daily surface reflectance product (MOD09GQ), the clouds and cloud shadows, high view angled can significantly affect the usability of the daily products. The 8-day product was screened for low-quality pixels using the quality flags. In order to test the interoperability of Sentinel-2 (S2) data with previously discussed data collections, we integrated Level-1C (L1C) TOA data which is also available in GEE data catalog. We used the QA60 bitmask band which contains cloud information to mask out opaque and cirrus clouds. Finally, we integrated SAR data acquired by Sentinel-1, which uses microwaves that can penetrate through cloud and haze, thus, can provide better temporal coverage (Hütt, Koppe, Miao, & Bareth, 2016). This is particularly useful for tracking subtle changes in vegetation cover during a growing season. Unlike optical sensors, SAR can provide more frequent data, as the density of time series derived from optical sensors can be significantly affected by atmospheric conditions.

6.2.2 Methods

A multi-scale framework was developed with the aim to derive remotely sensed metrics over main vegetation formations. For the pilot study, we investigated distinct agricultural regions in Central Ukraine. Nevertheless, the metrics used can be derived for broader regions. Following the preprocessing of each image collection, we derived parameters based on vegetation index time series, such as NDVI, Normalized Difference Moisture Index (NDMI) and tasseled-cap transformation (TCT) (Table 6.1).

RS indicator	Description
NDVI	Landsat, MODIS, Sentinel-2
NDMI	Landsat, Sentinel-2
TCT	Landsat
Land surface temperature	Landsat/MODIS
SAR backscatter	Sentinel-1

Table 6.1: Remote Sensing Time Series Variables.

To investigate the thermal conditions of the vegetation, we used single channel method to derive Land surface temperature (LST) based on Landsat imagery. As the algorithm requires surface emis-

sivity information from external sources we used NDVI-based emissivity estimated from Landsat red and near-infrared bands (Jimenez-Munoz & Sobrino, 2010). Another metric that we have investigated was the Landsat based tasseled-cap transformation. TCT is an empirical transformation based on linear combinations of the original bands. The design of the transformation and the use of different bands highlight inherent data properties that capture critical physical characteristics of vegetation, mainly the brightness captures variation in overall reflectance and is related to soil and albedo; greenness is related to variability of vegetation, and the wetness is mostly linked to a combination of moisture conditions and vegetation structure (Wegmann et al., 2016). MODIS based NDVI at 250 m resolution were integrated into this approach to account for potential surface variations in NDVI that can occur between the Sentinel-2 and Landsat acquisitions. All remotely sensed metrics were summarized for specific vegetated systems and the time series were derived for the different periods of the growing season. Furthermore, having a purpose to compare the data coming from different sensors, we investigated the impact of the differences in observation time. To quantify changes in vegetation, we used two approaches: bi-temporal change detection and anomaly identification. For bi-temporal change detection, specific images or composites were selected based on remote sensing-derived variables. For anomaly identification, reference is calculated for a specified region and time period. This reference defines the initial condition of the selected area. This is followed by the definition of the test period which is compared with the baseline calculated using monthly time-series.

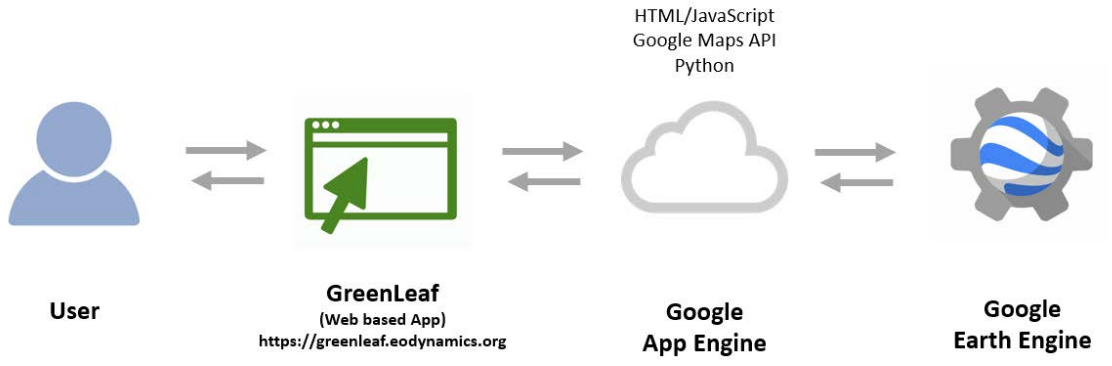

Figure 6.1: The infrastructure for spatial application development.

Taking advantage of the cloud computing platform, we developed GreenLeaf, a web-based application using Google developer tools to have an integrated platform for accessing discussed indicators and tools. The backend of the app is written in Python, using the Google Earth Engine Python library to interface with GEE servers. The frontend, is developed using HTML and CSS for the

user interface, and Javascript for interaction. The app is hosted on Google App Engine, which enables a high disponibility (Figure 6.1).

6.3 Result and Discussion

While the web app is available for a worldwide application, we used it for a specific pilot area in Central Ukraine. Figure 6.2 shows the selected parameters for this particular region of interest. It can be seen, that the spatial features are generally similar, with a distinct difference in vegetated and non-vegetated areas. We could also observe clear differentiation of individual fields especially in metrics derived from high-resolution data. This differentiation is robustly represented in multitemporal composites derived from Sentinel-1 as well. This is due to the fact that the SAR backscattering signal is mainly affected by canopy structure (such as the size, shape, and orientation of plant tissues), water content of canopy, as well as the roughness and moisture of the underlying soil (Forkuor et al., 2014). TC wetness and LST also give valuable information about moisture stress and thermal condition of vegetation. Specifically, we can observe higher NDVI values in densely vegetated areas, which correspond to areas with high TC wetness and low LST values respectively. The notable link among the variables derived from different sensors, specifically the lower NDVI and corresponding lower wetness can indicate water scarcity or vegetation at the end of the growing season.

The use of temporal composites makes it possible to create cloud-free images covering the study area. Furthermore, the composites spanning over a specific period of growing season (Figure 6.2) can be a proxy of overall ecosystem productivity. In case of SAR imagery, multitemporal composites highlight the changes during the growing season, as when averaging different images, we decreased the contribution of speckle which resulted in within-class variance decrease and easy separation of the vegetation. The temporal variability of VIs derived from different sensors was examined for the study area (Figure 6.4). Time series derived from different sensors showed a generally consistent pattern of a mid-summer peak during the growing season (April-September), though with some differences in peak timing and value. This difference is mainly caused by the lack of data during the growing season due to atmospheric condition and thus limited number of cloud-free observations. Vegetation progress varies by location. We can observe distinct differences in seasonal variation between forests and agricultural areas. Another distinct pattern is the consistent lower values of S2 derived NDVI. This can be explained by the fact, that S2 product is TOA, and compared to other products with applied atmospheric correction, has lower values. The profile and magnitude

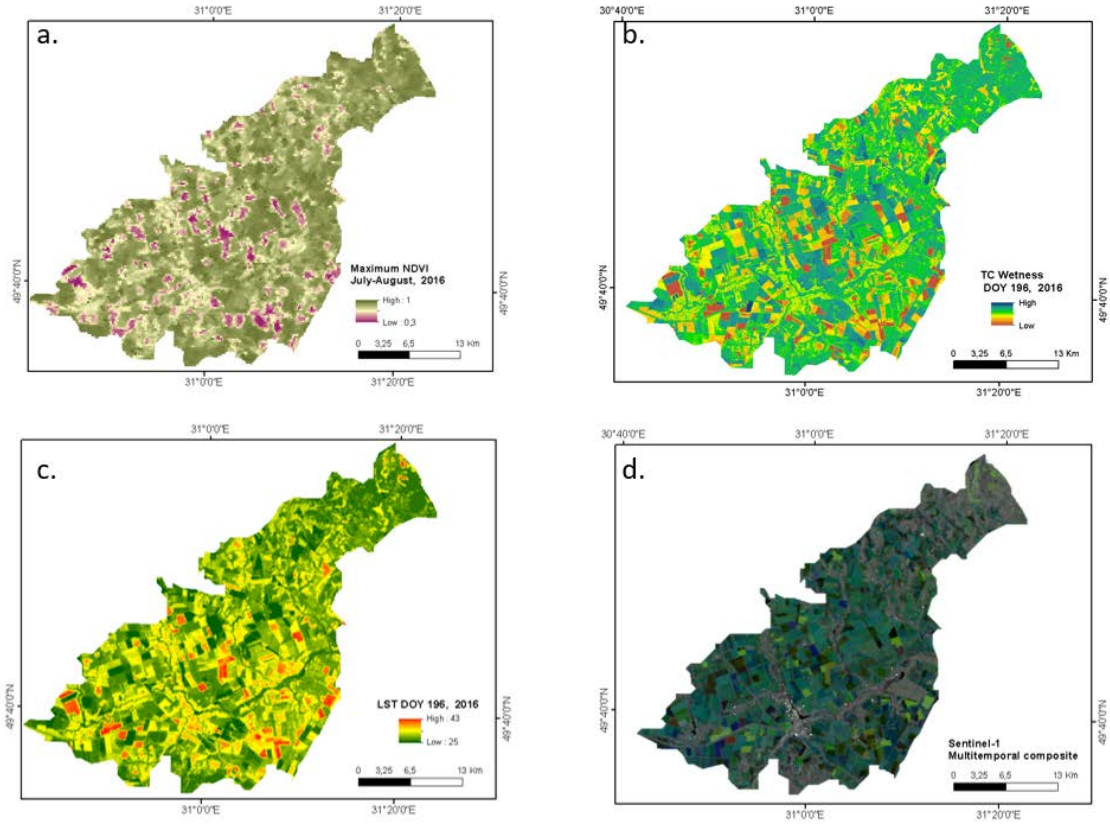

Figure 6.2: Examples of derived parameters. (a) Seasonal image composite spanning during peak growing season, (b) TC wetness derived from Landsat, (c) LST derived for specific DOY (day of the year) (d) multitemporal composite from Sentinel-1.

of the curve and NDVI variations are essential indicators of vegetation growth. Additionally, in heterogeneous landscapes, the 30 m Landsat NDVI product better reflects the spatial variability of the underlying land cover. Similar temporal patterns can be observed in SAR time series (Figure 6.3d). During the growing season, both VH and VV increases because of the volume scattering of vegetation. As a result, SAR and optical data both reproduce crop growth cycles and can be used synergistically in order to have a dense time series. The derived metrics and the time series can be an input for land cover classification as well as it can be used in biophysical and agro-economic models. It is essential to mention, that reference data are needed to validate further/explain the spatiotemporal variability of remotely sensed indicators.

In general, we can see good agreement of MODIS and Landsat (Figure 6.4), for the areas of interest bigger than 5 ha. When smaller areas of interest are selected, we can see the impact of the mixed pixels. The values are in good agreement, with high correlation coefficients equal to 0.7 (Figure 6.4a). The agreement is lower in cases of the absence of a cloud-free Landsat-8 image. In case if the images are not available within a few days of the MODIS acquisition we can observe

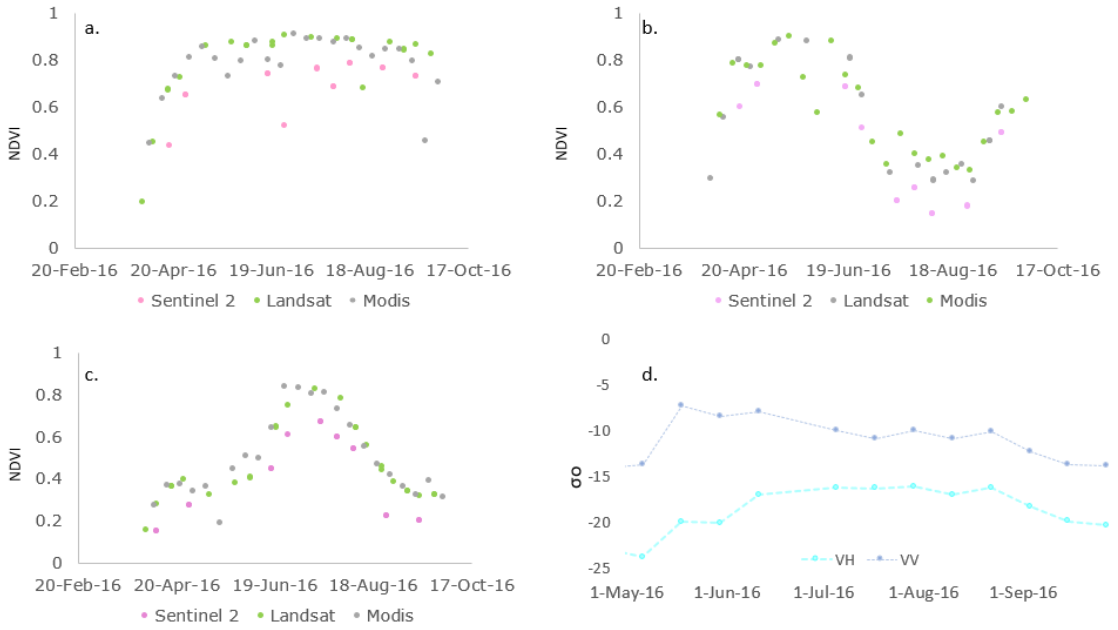

Figure 6.3: Time series of NDVI for (a) Forest, (b) winter crop, (c) summer crop and (d) Backscattering coefficient (σ_o expressed in decibels) over an agricultural area.

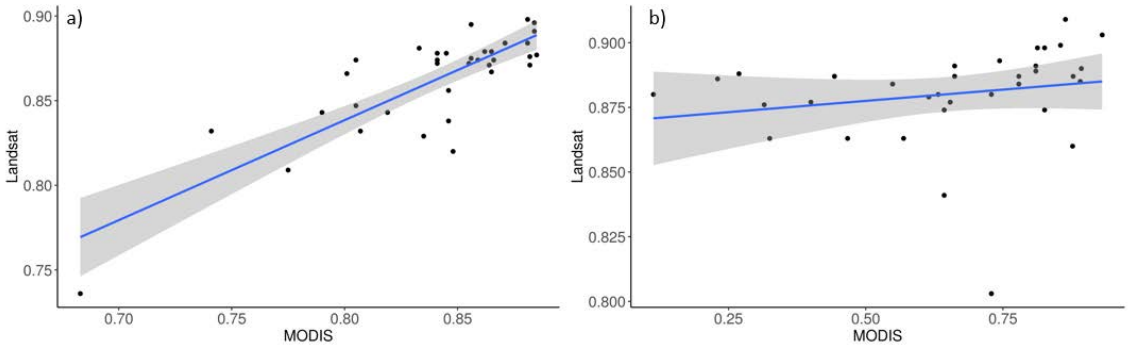

Figure 6.4: Scatterplots showing (a) minor differences for the acquisitions which are days apart (Landsat 11.07.2016; MODIS 13.07.2016) (b) differences with bigger acquisition interval (Landsat 27.06.2016; MODIS 03.07.2016).

higher variability (Figure 6.4b).

Finally, in order to integrate this information in a single vegetation monitoring tool, we developed a web-based application using Google App Engine: GreenLeaf. The application is computing metrics (minimum, maximum, mean, change between time1 and time2, detection of the anomalies from baseline) and plotting the time series graph, based on parameters defined by the user: Date range, preferred product and location/area of interest. The users can add specific thresholds (e.g., NDVI $>$ 0.5), and mask only agricultural areas based on decision rule set and temporal variability of the surface (Ghazaryan et al., 2018) and derive parameters regarding the start of the vegeta-

tion stress and severity (Figure 6.5). Further development of the app supposes upscaling of these products.

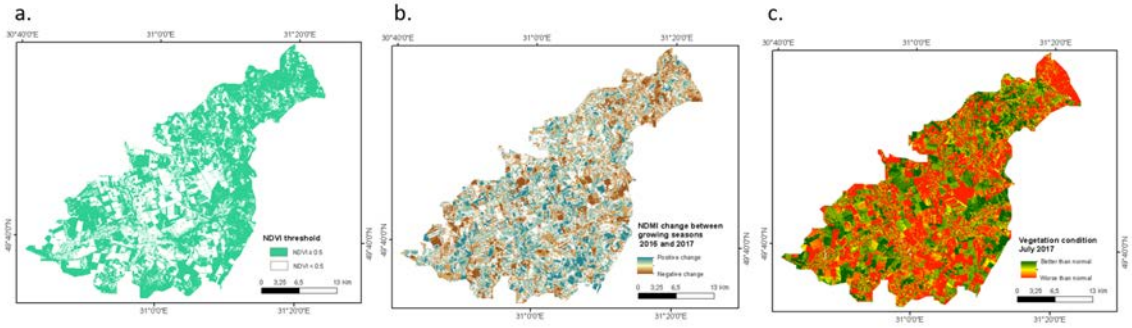

Figure 6.5: (a) Vegetated and non-vegetated areas based on a threshold of Sentinel-2 NDVI, (b) Changes detected using Landsat based NDMI between two years, c) NDVI anomaly image estimated based on Landsat data collected in July 2017 compared to the reference mean NDVI for this time-step between 2013 and 2016.

The use of web-based applications, along with big data on the cloud enable provision of customizable geospatial tools and products. The user is able to define either spatial or temporal parameters (or both), change the used algorithms or visualization parameters. With this approach, the access to geospatial operations is no longer restricted to expert users, but it is also available to others. The developed web-app, accessible online at https://greenleaf.eodynamics.org can be used for both large and small-scale analysis (Figure 6.6). The presented methodology is suitable especially for areas where in situ data is scarce and can be used for analyzing vegetation dynamics such as monitoring agricultural management and intensification, heat and drought stress and tracking deforestation. Future development of the tool will include algorithms for deriving phenometrics such as start, end and the duration of the growing season.

6.4 Conclusions

In this study, we evaluated the spatiotemporal variation of vegetation based on data derived from several sensors. Recently, with the development of new sensors, the time-series data with high spatial and temporal resolutions have become available for VI time-series analysis. These time-series, in addition to temporal information about the vegetation phenology and changes, contain valuable information about the spatial patterns of vegetation distribution. The different sensors each have comparative strengths and weaknesses, but their overall performance was similar for tracking temporal variability over homogeneous areas. With respect to spatial resolution 250 m MODIS data were not always sufficient for differentiating vegetation variability in heterogeneous

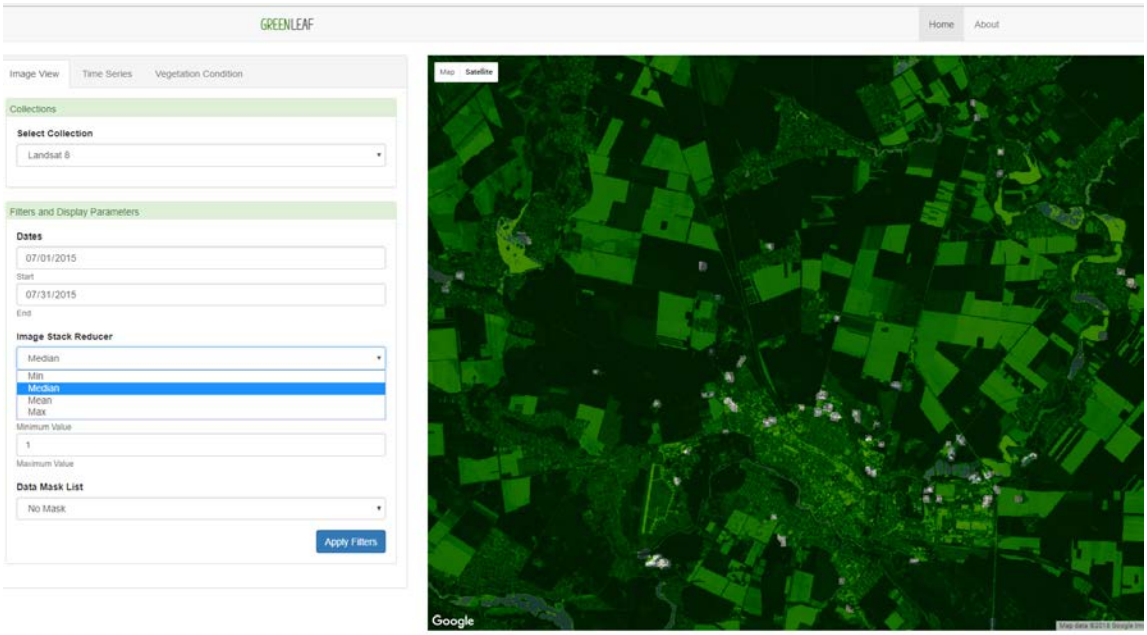

Figure 6.6: A screenshot of the developed GreenLeaf tool.

landscapes. Landsat has greater capabilities for tracking variation at finer spatial resolutions. Further, with imagery derived from Sentinel and Landsat, it was possible to detect small-scale heterogeneity within fields on agricultural land. By choosing an adequate number of images, further composites based on multi-temporal statistics can be created. GreenLeaf contributes to the use of the satellite data products and the simplification of data access for users with limited remote sensing experience and/or restricted processing power. In the presented study for the pilot area it was demonstrated how the data could be used in order to quantify vegetation change and condition; this evidence-based information can be a base to spatial planning, implementation of interventions in vulnerable areas or other policy decisions.

Chapter 7

Synthesis

7.1 Summary

During the last several decades, Ukraine experienced multiple changes, such as the collapse of Soviet Union, which, in turn induced land surface changes. The nature of the changes was different ranging from land abandonment, land productivity decline to changes in cropping practices (Kuemmerle et al., 2011; Schierhorn et al., 2013). Besides the socioeconomic changes there were several reports regarding ongoing environmental changes such as the increasing frequency of droughts and heat waves (Adamenko & Prokopenko, 2011; Kogan et al., 2013) which also had an impact on agricultural production (Kogan, 2019). The primary objective was to enhance our understanding on patterns of land surface changes through exploiting the potential of multimodal RS time series. Throughout this thesis, the use of time series observations and the applications of different algorithms were tested to pursue several research questions and/or to enhance current methodologies for the derivation of metrics describing the land surface and its dynamics. Under progressive climate change and transformations in land use such metrics are necessary to support data-driven land management decisions. It has been shown that the use of such features produced insightful results for characterizing vegetation state and its condition, such as those presented in Chapter 3, 4, 5 and 6. A variety of datasets and methods were used to address the research questions of this thesis. Regarding the first aim, coarse scale NDVI dataset was used together with a variety of time series analysis methods to assess the vegetation changes and to quantify the impact of environmental factors on vegetation variability. To tackle the second aim related to crop mapping Landsat and Sentinel-1 data were used. The use of several non-parametric classifiers was addressed in relation to their performance for crop mapping. Regarding the third aim, focusing on drought impact assessment, we have comprehensively studied crop condition with the use of several optical

and SAR time series metrics. In order to ensure the data access and transferability of results, we have integrated different datasets, derived metrics, and tools in a web application.

7.2 To What Extent can the Variation of NDVI be Explained by Environmental Conditions?

Long-term vegetation variability and the impact of environmental factors were studied for a thirty-year time span in Ukraine. The observed patterns of land surface changes were different depending on the land cover and the period. Increasing NDVI trends are widespread across the country from 1982 to 2013. The output of breakpoint analysis gave more information on land surface dynamics and possible triggers of it. For instance, large areas with trend shifts were observed in northwest Ukraine during 1993 and 2002. The first post-socialistic years in the country were characterized by high rates of land abandonment as well as widespread forest disturbances. Following economic recovery around the early 2000s, re-cultivation of formerly abandoned land emerged. The mentioned processes were reflected by the monotonic increase and increase with an abrupt break in NDVI time series that is seen to predominate during the recent years of 2003–2013. Overall, the AVHRR time series spanning more than three decades enabled an improved trend characterization. Partial correlation analysis is generally useful for determining the individual contribution of each specific environmental factor on NDVI dynamics. Among the analyzed factors, air temperature explained most of the NDVI variability. The impacts of air temperature were observed in 30% of the area. Grasslands and cropland exhibited similar responses to the drivers, demonstrating high sensitivity to soil moisture and temperature. Although AVHRR data showed a big advantage of long-term time series, the coarse spatial resolution of this dataset highlights the need for more detailed analysis. At the same time, Landsat offers a long-term data record, with 30m spatial resolution whilst the analysis of the data can be time and resource consuming. Nevertheless, with the cloud computing technologies, it is possible to implement similar time series and breakpoint algorithms on higher resolution data. Because of the distributed computational power, it was possible to run this computationally intensive processes. To highlight this, Landsat based linear trends were computed (Figure 7.1) and the three decadal record of 30m resolution data was used for national scale monitoring of land surface changes. Similar patterns of predominant greening as presented in Chapter 3 can be observed, nonetheless, the interpretation of the results for specific study cases is more straightforward, as the changes can be observed at land management scale.

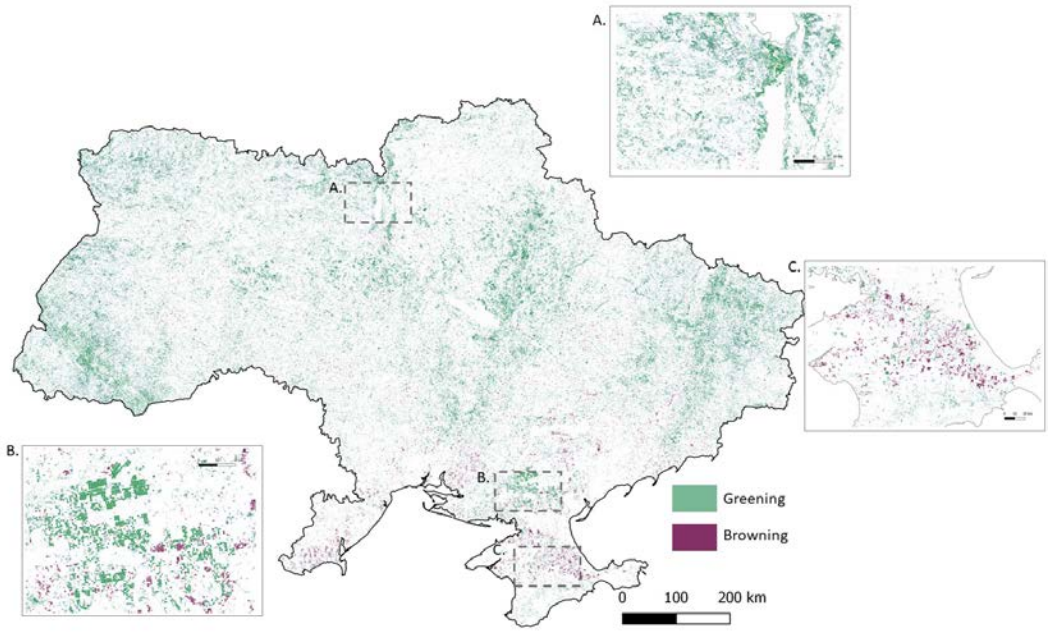

Figure 7.1: National scale long-term NDVI trends based on Landsat (1982-2018) a) Greening in Chernobyl area, b) Productivity increase in irrigated cropland and c) Decline due to farmland abandonment in Crimea.

7.3 How Can the Vegetation Seasonality Derived from Remote Sensing Contribute to Agricultural Monitoring?

The possibility of main crop type mapping with limited field level information in the central region of Ukraine was assessed using Landsat and Sentinel-1 time series. We have tested the potential use of optical and SAR data for the rule-based training sample generation and subsequent crop classification in complex cropping systems. The derivation of critical temporal metrics enabled the creation of image composites which represent the cropping patterns more adequately. In addition, we demonstrated that the harmonic analysis and derived metrics could represent the seasonal variations of crops. It was shown that selected input features have an impact on class separability. Specifically, the data availability during critical growth stages has a crucial impact on the classification results. The use of Landsat and Sentinel based composites were also highlighted (Chapters 4 -6). Recent studies suggested the use of composites (Griffiths, van der Linden, Kuemmerle, & Hostert, 2013) not only for well-known data products such as MODIS (E. Vermote, 2015) but for Landsat like sensors. The main advantage of aggregation of the data within a specific period is that when averaging different images, the contribution of speckle was decreased which resulted

in within-class variance decrease and easy separation of the crops. In the case of optical imagery, compositing enabled the creation of cloud-free images covering the study area. The integration of multispectral and SAR data improved the classification accuracy by 2% for 2015 and 5% for 2016. The method was tested in two years which made it possible to study the effect of inter-annual meteorological differences. Besides the RS datasets, a crucial role for crop classification had the additional agroecological data (e.g., phenological observations, crop status during different growth stages). Integration of other ancillary data such as soil type, crop rotation regulations and the integration of additional information over large areas can further improve the classification results. For example, with the aggregation of decision rules, the algorithm can be applied over the whole country. Figure 7.2 shows the 30m resolution map of delineated winter crops on a national level.

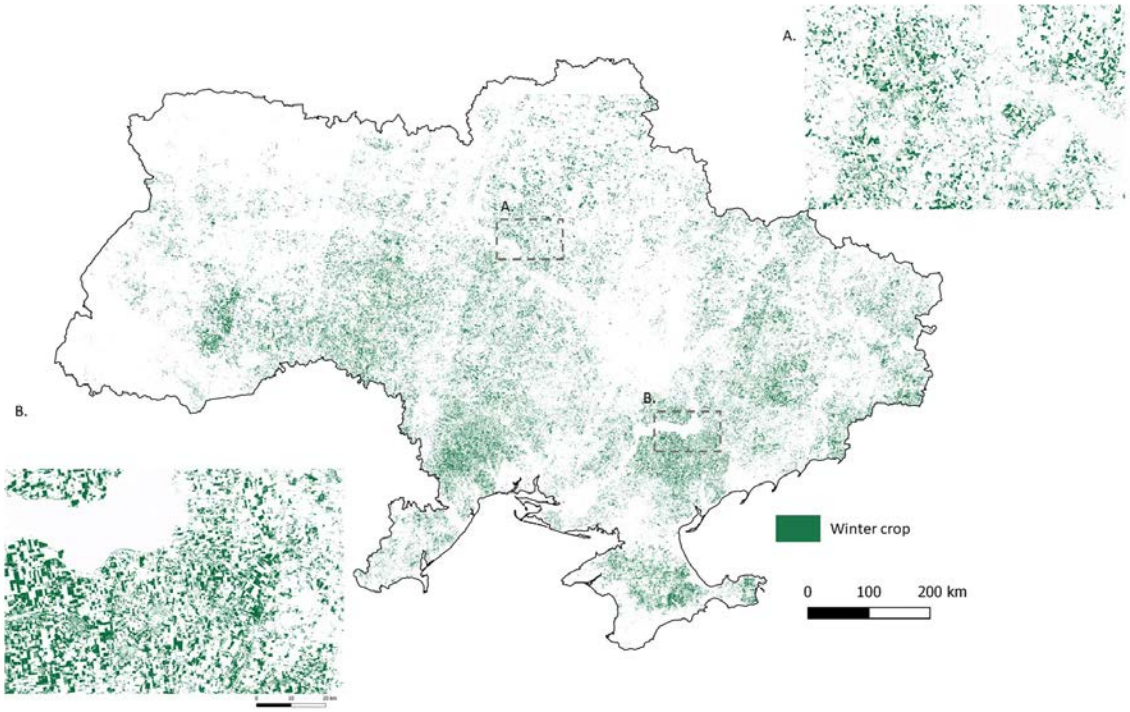

Figure 7.2: National scale winter crop mask derived from Landsat and Sentinel-1 images for 2017.

Based on the results, the use of seasonal composites in a two-step approach of classification to create accurate crop maps over several years is recommended. The approach developed and tested here has the potential for cases especially when field data are insufficient and can be further developed for upscaling to larger areas.

7.4 How much Information Can be Derived from Time Series to Study Crop Condition?

Compared to the crop classification, crop condition monitoring and identification of timing and severity of the vegetation stress is often a challenge as different crops have diverse spectral responses under different hydroclimatic conditions. The increasing number of freely distributed remotely sensed time series gives opportunities to monitor intra-seasonal changes in croplands and track subtle changes in time series, which can be induced by extreme events such as droughts. The use of time series from optical and SAR data to identify the main characteristics of agricultural drought was discussed. Indicators were derived based on optical (Landsat-8, Sentinel-2, MODIS) and SAR data. We used logistic regression to evaluate the drought-induced variability of remotely sensed parameters. We found out that growing season maximum NDMI and NDVI (70-75%) and SAR derived metrics (60%) reflect specifically the impact of agricultural drought. These metrics also depict stress affected areas with a larger spatial extent. LST was a useful indicator of crop condition especially for maize and sunflower with prediction rates of 86% and 71%, respectively. The results showed that drought-induced properties of time series could be characterized based on featurization and temporal dynamics of time series and combined use of several indicators.

7.5 How Can the Multi-source Data and Analysis Methods be Used for Vegetation Monitoring at Different Scales?

Remotely sensed imagery is an important data source for different decision makers as the data can be further used to forecast of crop production, measure and manage land use intensity. To make the results accessible for a wide range of users a web application has been developed, where users can derive satellite-based data products such as vegetation indices, SAR backscatter time series without coding or image processing for a defined area of interest and a preferred period. The computation is running on Google Cloud servers (using Google Earth Engine) and the results are returned to the user via the interactive interface. The application is computing metrics (minimum, maximum, mean, change between time1 and time2, anomalies) and extracting the time series graph, based on parameters defined by the user. The user can define either spatial or temporal parameters or both, change the used algorithms or visualization parameters. This will further contribute to the use of the data and will simplify data access for users with limited remote sensing experience, or with limited processing power. With this approach, access to geospatial operations is no longer restricted to expert users, but it is also available to others. Overall, we can observe changes in

remote sensing analysis approaches. Along with access to data from MODIS and Landsat, the launch of new satellites, such as the Sentinel constellation, give new opportunities for timely and accurate monitoring of land surface dynamics. More opportunities also arise from the private sector, such as PlanetScope constellation operated by Planet (Houborg & McCabe, 2018), where global high-resolution data are now available at very high temporal frequency i.e. daily. The approaches towards land surface analysis are also changing with the increasing amount of analysis-ready data (Giuliani, Chatenoux, Honeck, & Richard, 2018; "U.S. Landsat Analysis Ready Data (ARD) | Landsat Missions," n.d.), cloud computing, multi-temporal and multi-sensor analysis (Figure 7.3). Especially with algorithms such as deep learning, integration of different data sources gives more opportunities for accurate data products such as indicators and spatially explicit statistical output. Moreover, the output is changing from static maps, which capture the land surface state for one timestep (e.g. land cover maps), to the generation of dynamic output defined by the users' needs (Azzari & Lobell, 2017).

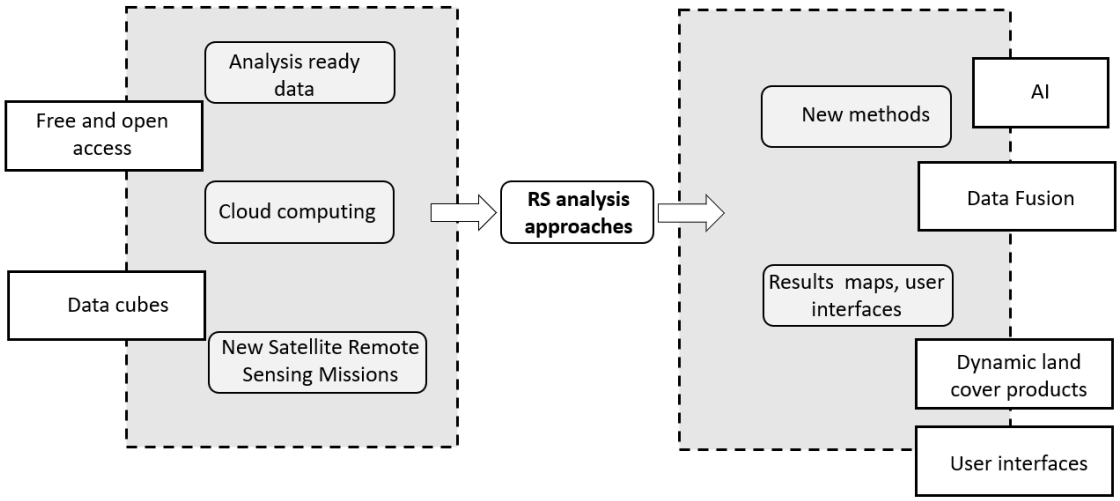

Figure 7.3: Conceptual representation of changes in remote sensing (RS) research and output generation highlighting the impact of freely accessible multisensor data, cloud computing and Artificial Intelligence (AI).

7.6 The Impact of the Resolution and Sensor

Besides the transferability of models and upscaling, the impact of the spatial resolution of imagery is a crucial aspect that can affect the accuracy of the derived land surface parameters. Several sensors introduced in the previous chapters (AVHRR, Landsat, MODIS, Sentinel-1, and Sentinel-2) – with

high, medium, and low spatial resolution have weaknesses and strengths when it comes to mapping and monitoring land cover changes. Landsat offers high-resolution data starting from the 1980s, although the data quality varies with cloud cover. In the case of MODIS, with reasonably regular time series, it is only available from the 2000s. Furthermore, MODIS offers less spectral bands with finer spatial resolution. Depending on the application, one or the other sensor might be a better choice. Consequently, different satellite sensors are not equally suitable for different applications such as vegetation monitoring, crop specific condition monitoring especially in heterogeneous landscapes. For example, dense time series (e.g., MODIS) are necessary for detailed phenology analysis, but at the same time, annually spaced Landsat like composites might be enough for tracking long term vegetation changes as a result of changes in management or political decisions and conversion. With the integration of Copernicus data, time series with both high temporal and spatial resolutions can be accessed. This highlights the need for the synergistic use of multi-scale data.

Chapter 8

Conclusions

This thesis provides a comprehensive assessment of land surface changes at different spatiotemporal scales based on multi-source remotely sensed datasets. Through the studies on country and local scale, essential gaps were addressed in the understanding of vegetation changes, drought stress impacts on crops and crop classification based on optical and SAR data. This was achieved by the application of several algorithms for time series trend and change detection, and machine learning techniques for land cover characterization. It was demonstrated how different data could influence remotely sensed change detection and its characterization. In general, it was shown that Earth Observation provides a comprehensive data source for repeated, large-scale analysis of both long- and short-term land surface changes.

Important outcomes of the thesis are:

- Integration of multiple datasets allows derivation of valuable, spatially explicit information on overall vegetation status and dynamics, and the potential causes of land surface changes. Coarse-resolution input data (NDVI, environmental data) yielded sufficient results at the national level. High-resolution input data is required for local scale analysis and for interpreting the seasonal dynamics and spatially explicit quantification of impacts of extreme events (drought stress) in heterogeneous agricultural landscapes.

- The remotely sensed patterns of crop growth confirm agroecological knowledge and presented approaches of crop identification. Furthermore, crop condition monitoring can be implemented in areas where field observations are unavailable or scarce. Temporal context of the remotely sensed data through time series and temporal composites was valuable and necessary for interpretation of vegetation change especially in dynamic agricultural setting. Nevertheless, it is still crucial to have representative in situ datasets (e.g. crop calendars, drought

occurrence databases) for calibration of the models and validation of the remotely sensed derivatives.

- The data fusion results outperform single sensor analysis for crop type classification and condition monitoring. Especially the integration of SAR data was shown to be useful for improved crop classification. Furthermore, it can be concluded that integration of optical, microwave and thermal information extends knowledge of crop-specific drought impacts.

- The use of a web-based application, along with big data on cloud enables provision of customizable geospatial tools and products showing the possibilities of scaling up of the results and implementation of the algorithms in other areas.

In addition to suggestions for future work presented at the ending of each chapter of the thesis, the following considerations are proposed.

- Regarding the country level analysis, additional factors along with datasets that accurately characterize anthropogenic activity should be considered. The study was relying on AVHRR based NDVI data. Other variables such as Net Primary Productivity (NPP) and LAI can further improve the understanding of vegetation variability.

- Regarding field-level crop type mapping, the use of dense time series should be highlighted to harness the temporal footprint of different land cover types. Although in chapters 3, 4 and 5 we have demonstrated examples of combined usage of the data, the studies bring up the necessity of the creation of harmonized data cubes. For example, Sentinel-2 integration with Landsat can dramatically increase the temporal frequency of data for dense time series analyses (Chastain et al., 2019; Claverie et al., 2018). These data can further be used for not only crop type identification but also products such as cropping intensity and crop rotation violations.

- The use of deep learning algorithms for classifications can further improve the results such as better discrimination of certain crop types. Recently, deep learning algorithms, such as Deep Neural Networks (DNNs) and the Convolutional Neural Networks (CNNs), demonstrated great potential for various applications compared to other machine learning algorithms (Cai et al., 2018; X. X. Zhu et al., 2017). Integration of deep learning with cloud processing can further enable large-scale analysis (d'Andrimont, Lemoine, & van der Velde, 2018).

- In addition, future research may also focus on investigating the potential of optical and SAR sensors for the derivation of finer scale biophysical parameters and estimates such as soil moisture, LAI and large scale observation on functional trait detection. Furthermore, remotely sensed time series and derived parameters can be used not only for drought monitoring but also prediction and early warning and forecast.

Overall, it was demonstrated that the effective combination of different trend analysis techniques, integration of multiple datasets, and effective statistical modeling allows derivation of valuable, spatially explicit information on overall vegetation status and dynamics, land (vegetation) degradation, crop stress and the potential causes of these changes. This information can be used as an input for different models and can support the decision making for sustainable land management.

References

Adamenko, T., & Prokopenko, A. (2011). Monitoring Droughts and Impacts on Crop Yield in Ukraine from Weather and Satellite Data. In F. Kogan, A. Powell, & O. Fedorov (Eds.), *Use of Satellite and In-Situ Data to Improve Sustainability* (pp. 3–9). NATO Science for Peace and Security Series C: Environmental Security. doi:10.1007/978-90-481-9618-0_1

AghaKouchak, A., Farahmand, A., Melton, F. S., Teixeira, J., Anderson, M. C., Wardlow, B. D., & Hain, C. R. (2015). Remote sensing of drought: Progress, challenges and opportunities. *Reviews of Geophysics*, *53*(2), 2014RG000456. doi:10.1002/2014RG000456

Ahmadalipour, A., Moradkhani, H., Yan, H., & Zarekarizi, M. (2017). Remote Sensing of Drought: Vegetation, Soil Moisture, and Data Assimilation. In V. Lakshmi (Ed.), *Remote Sensing of Hydrological Extremes* (pp. 121–149). Springer Remote Sensing/Photogrammetry. doi:10.1007/978-3-319-43744-6_7

Alcantara, C., Kuemmerle, T., Baumann, M., Bragina, E. V., Griffiths, P., Hostert, P., ... Radeloff, V. C. (2013). Mapping the extent of abandoned farmland in Central and Eastern Europe using MODIS time series satellite data. *Environmental Research Letters*, *8*(3), 035035. doi:10.1088/1748-9326/8/3/035035

Alparone, L., Aiazzi, B., Baronti, S., Garzelli, A., Aiazzi, B., Baronti, S., & Garzelli, A. (2015). *Remote Sensing Image Fusion*. doi:10.1201/b18189

Anyamba, A. (2011). Historical Perspectives on AVHRR NDVI and Vegetation Drought Monitoring.

Araya, S., Ostendorf, B., Lyle, G., & Lewis, M. (2017). *Remote Sensing Derived Phenological Metrics to Assess the Spatio-Temporal Crop Yield Variability*. doi:10.4236/ars.2017.63016

Atzberger, C. (2013). Advances in Remote Sensing of Agriculture: Context Description, Existing Operational Monitoring Systems and Major Information Needs. *Remote Sensing*, *5*(2), 949–981. doi:10.3390/rs5020949

Atzberger, C., Klisch, A., Mattiuzzi, M., & Vuolo, F. (2013). Phenological Metrics Derived over the European Continent from NDVI3g Data and MODIS Time Series. *Remote Sensing*, *6*(1), 257–284. doi:10.3390/rs6010257

Azzari, G., & Lobell, D. B. (2017). Landsat-based classification in the cloud: An opportunity for a paradigm shift in land cover monitoring. *Remote Sensing of Environment*. Big Remotely Sensed Data: Tools, Applications and Experiences, *202*, 64–74. doi:10.1016/j.rse.2017.05.025

Baldi, G., Nosetto, M. D., Aragón, R., Aversa, F., Paruelo, J. M., & Jobbágy, E. G. (2008). Long-term Satellite NDVI Data Sets: Evaluating Their Ability to Detect Ecosystem Functional Changes in South America. *Sensors*, *8*(9), 5397–5425. doi:10.3390/s8095397

Ban, Y. (Ed.). (2016). *Multitemporal Remote Sensing: Methods and Applications* (1st ed. 2016 edition). New York, NY: Springer.

Bargiel, D. (2017). A new method for crop classification combining time series of radar images and crop phenology information. *Remote Sensing of Environment*, *198*, 369–383. doi:10.1016/j.rse.2017.06.022

Baumann, M., Kuemmerle, T., Elbakidze, M., Ozdogan, M., Radeloff, V. C., Keuler, N. S., ... Hostert, P. (2011). Patterns and drivers of post-socialist farmland abandonment in Western Ukraine. *Land Use Policy*, *28*(3), 552–562. doi:10.1016/j.landusepol.2010.11.003

Bégué, A., Arvor, D., Bellon, B., Betbeder, J., De Abelleyra, D., P. D. Ferraz, R., ... R. Verón, S. (2018). Remote Sensing and Cropping Practices: A Review. *Remote Sensing*, *10*(1), 99. doi:10.3390/rs10010099

Bhandari, S., Phinn, S., & Gill, T. (2012). Preparing Landsat Image Time Series (LITS) for Monitoring Changes in Vegetation Phenology in Queensland, Australia. *Remote Sensing*, *4*(6), 1856–1886. doi:10.3390/rs4061856

Bradley, B. A., Jacob, R. W., Hermance, J. F., & Mustard, J. F. (2007). A curve fitting procedure to derive inter-annual phenologies from time series of noisy satellite NDVI data. *Remote Sensing of Environment*, *106*(2), 137–145. doi:10.1016/j.rse.2006.08.002

Breiman, L. (2001). Random Forests. *Machine Learning*, *45*(1), 5–32. doi:10.1023/A:1010933404324

Cai, Y., Guan, K., Peng, J., Wang, S., Seifert, C., Wardlow, B., & Li, Z. (2018). A high-performance and in-season classification system of field-level crop types using time-series Landsat data and a machine learning approach. *Remote Sensing of Environment*, *210*, 35–47. doi:10.1016/j.rse.2018.02.045

Chandler, R., & Scott, M. (2011). *Statistical Methods for Trend Detection and Analysis in the Environmental Sciences*. John Wiley & Sons.

Chang, N.-B., & Bai, K. (2018). *Multisensor Data Fusion and Machine Learning for Environmental Remote Sensing* (1 edition). Boca Raton, FL: CRC Press.

Chastain, R., Housman, I., Goldstein, J., & Finco, M. (2019). Empirical cross sensor comparison of Sentinel-2A and 2B MSI, Landsat-8 OLI, and Landsat-7 ETM+ top of atmosphere spectral characteristics over the conterminous United States. *Remote Sensing of Environment*, *221*, 274–285. doi:10.1016/j.rse.2018.11.012

Chen, J., Wan, S., Henebry, G., Qi, J., Gutman, G., Sun, G., & Kappas, M. (2014). *Dryland East Asia: Land Dynamics amid Social and Climate Change*. Walter de Gruyter.

Chen, T., de Jeu, R. A. M., Liu, Y. Y., van der Werf, G. R., & Dolman, A. J. (2014). Using satellite based soil moisture to quantify the water driven variability in NDVI: A case study over mainland Australia. *Remote Sensing of Environment*, *140*, 330–338. doi:10.1016/j.rse.2013.08.022

Claverie, M., Ju, J., Masek, J. G., Dungan, J. L., Vermote, E. F., Roger, J.-C., ... Justice, C. (2018). The Harmonized Landsat and Sentinel-2 surface reflectance data set. *Remote Sensing of Environment*, *219*, 145–161. doi:10.1016/j.rse.2018.09.002

Congalton, R. G. (1991). A review of assessing the accuracy of classifications of remotely sensed data. *Remote Sensing of Environment*, *37*(1), 35–46. doi:10.1016/0034-4257(91)90048-B

Cristóbal, J., Jiménez-Muñoz, J. C., Prakash, A., Mattar, C., Skoković, D., & Sobrino, J. A. (2018). An Improved Single-Channel Method to Retrieve Land Surface Temperature from the Landsat-8 Thermal Band. *Remote Sensing*, *10*(3), 431. doi:10.3390/rs10030431

d'Andrimont, R., Lemoine, G., & van der Velde, M. (2018). Targeted Grassland Monitoring at Parcel Level Using Sentinels, Street-Level Images and Field Observations. *Remote Sensing*, *10*(8), 1300. doi:10.3390/rs10081300

Davidson, A. M., Fisette, T., Mcnairn, H., & Daneshfar, B. (2017). Detailed crop mapping using remote sensing data (Crop Data Layers). *Handbook on remote sensing for agricultural statistics*, 91–117.

de Beurs, K. M. [Kirsten M.], Henebry, G. M., Owsley, B. C., & Sokolik, I. (2015). Using multiple remote sensing perspectives to identify and attribute land surface dynamics in Central Asia 2001–2013. *Remote Sensing of Environment*, *170*, 48–61. doi:10.1016/j.rse.2015.08.018

de Beurs, K. M. [Kirsten M], & Henebry, G. M. [Geoffrey M]. (2004). Land surface phenology, climatic variation, and institutional change: Analyzing agricultural land cover change in Kazakhstan. *Remote Sensing of Environment*, *89*(4), 497–509. doi:10.1016/j.rse.2003.11.006

de Jong, R. [R.], & de Bruin, S. (2012). Linear trends in seasonal vegetation time series and the modifiable temporal unit problem. *Biogeosciences*, *9*(1), 71–77. doi:10.5194/bg-9-71-2012

de Jong, R. [Rogier], de Bruin, S., de Wit, A., Schaepman, M. E., & Dent, D. L. (2011). Analysis of monotonic greening and browning trends from global NDVI time-series. *Remote Sensing of Environment*, *115*(2), 692–702. doi:10.1016/j.rse.2010.10.011

de Jong, R. [Rogier], Schaepman, M. E., Furrer, R., de Bruin, S., & Verburg, P. H. (2013). Spatial relationship between climatologies and changes in global vegetation activity. *Global Change Biology*, *19*(6), 1953–1964. doi:10.1111/gcb.12193

de Jong, R. [Rogier], Verbesselt, J., Schaepman, M. E., & de Bruin, S. (2012). Trend changes in global greening and browning: Contribution of short-term trends to longer-term change. *Global Change Biology*, *18*(2), 642–655. doi:10.1111/j.1365-2486.2011.02578.x

de Jong, R. [Rogier], Verbesselt, J., Zeileis, A., & Schaepman, M. E. (2013). Shifts in Global Vegetation Activity Trends. *Remote Sensing*, *5*(3), 1117–1133. doi:10.3390/rs5031117

de Beurs, K. M., & Henebry, G. M. [Geoffrey M.]. (2010). Spatio-Temporal Statistical Methods for Modelling Land Surface Phenology. In I. L. Hudson & M. R. Keatley (Eds.), *Phenological Research* (pp. 177–208). Springer Netherlands.

Dorigo, W., de Jeu, R., Chung, D., Parinussa, R., Liu, Y., Wagner, W., & Fernández-Prieto, D. (2012). Evaluating global trends (1988–2010) in harmonized multi-satellite surface soil moisture. *Geophysical Research Letters*, *39*(18), L18405. doi:10.1029/2012GL052988

Dubovyk, O., Landmann, T., Dietz, A., & Menz, G. (2016). Quantifying the Impacts of Environmental Factors on Vegetation Dynamics over Climatic and Management Gradients of Central Asia. *Remote Sensing*, *8*(7), 600. doi:10.3390/rs8070600

Dubovyk, O., Landmann, T., Erasmus, B. F. N., Tewes, A., & Schellberg, J. (2015). Monitoring vegetation dynamics with medium resolution MODIS-EVI time series at sub-regional scale in southern Africa. *International Journal of Applied Earth Observation and Geoinformation*, *38*, 175–183. doi:10.1016/j.jag.2015.01.002

Dubovyk, O., Menz, G., Conrad, C., Kan, E., Machwitz, M., & Khamzina, A. (2013). Spatio-temporal analyses of cropland degradation in the irrigated lowlands of Uzbekistan using remote-sensing and logistic regression modeling. *Environmental Monitoring and Assessment*, *185*(6), 4775–4790. doi:10.1007/s10661-012-2904-6

E. Vermote. (2015). Mod09a1 modis/terra surface reflectance 8-day l3 global 500m sin grid v006. doi:10.5067/MODIS/MOD09A1.006

Eastman, J. R., Sangermano, F., Machado, E. A., Rogan, J., & Anyamba, A. (2013). Global Trends in Seasonality of Normalized Difference Vegetation Index (NDVI), 1982–2011. *Remote Sensing*, *5*(10), 4799–4818. doi:10.3390/rs5104799

Eklundh, L., & Jönsson, P. (2015). TIMESAT: A Software Package for Time-Series Processing and Assessment of Vegetation Dynamics. In C. Kuenzer, S. Dech, & W. Wagner (Eds.), *Remote Sensing Time Series* (22, pp. 141–158). Remote Sensing and Digital Image Processing. Springer International Publishing.

Eklundh, L., & Jönsson, P. (2016). TIMESAT for Processing Time-Series Data from Satellite Sensors for Land Surface Monitoring. In *Multitemporal Remote Sensing* (pp. 177–194). Remote Sensing and Digital Image Processing. doi:10.1007/978-3-319-47037-5_9

Elste, S., Glässer, C., Walther, I., & Götze, C. (2015). Multi-temporal Analysis of RapidEye Data to Detect Natural Vegetation Phenology During Two Growing Seasons in the Northern Negev, Israel. *Photogrammetrie - Fernerkundung - Geoinformation*, *2015*(2), 117–127. doi:10.1127/pfg/2015/0258

Enenkel, M., Steiner, C., Mistelbauer, T., Dorigo, W., Wagner, W., See, L., ... Rogenhofer, E. (2016). A Combined Satellite-Derived Drought Indicator to Support Humanitarian Aid Organizations. *Remote Sensing*, *8*(4), 340. doi:10.3390/rs8040340

ESA CCI Soil Moisture. (n.d.). https://www.esa-soilmoisture-cci.org/.

Estel, S., Kuemmerle, T., Alcántara, C., Levers, C., Prishchepov, A., & Hostert, P. (2015). Mapping farmland abandonment and recultivation across Europe using MODIS NDVI time series. *Remote Sensing of Environment*, *163*, 312–325. doi:10.1016/j.rse.2015.03.028

Evans, J. P., Pitman, A. J., & Cruz, F. T. (2011). Coupled atmospheric and land surface dynamics over southeast Australia: A review, analysis and identification of future research priorities. *International Journal of Climatology*, *31*(12), 1758–1772. doi:10.1002/joc.2206

FAO. (2008). Country Report on the State of Plant Genetic Resources for Food and Agriculture.

FAO. (2018). Food and Agriculture Organization Statistical Pocketbook 2018.

Fensholt, R., Horion, S., Tagesson, T., Ehammer, A., Grogan, K., Tian, F., ... Rasmussen, K. (2015). Assessment of Vegetation Trends in Drylands from Time Series of Earth Observation Data. In C. Kuenzer, S. Dech, & W. Wagner (Eds.), *Remote Sensing Time Series* (22, pp. 159–182). Remote Sensing and Digital Image Processing. Springer International Publishing.

Fensholt, R., Rasmussen, K., Nielsen, T. T., & Mbow, C. (2009). Evaluation of earth observation based long term vegetation trends — Intercomparing NDVI time series trend analysis consistency of Sahel from AVHRR GIMMS, Terra MODIS and SPOT VGT data. *Remote Sensing of Environment*, *113*(9), 1886–1898. doi:10.1016/j.rse.2009.04.004

Fisher, J. I., & Mustard, J. F. (2007). Cross-scalar satellite phenology from ground, Landsat, and MODIS data. *Remote Sensing of Environment*, *109*(3), 261–273. doi:10.1016/j.rse.2007.01.004

Foga, S., Scaramuzza, P. L., Guo, S., Zhu, Z., Dilley, R. D., Beckmann, T., ... Laue, B. (2017). Cloud detection algorithm comparison and validation for operational Landsat data products. *Remote Sensing of Environment*, *194*, 379–390. doi:10.1016/j.rse.2017.03.026

Fontanelli, G., Crema, A., Azar, R., Stroppiana, D., Villa, P., & Boschetti, M. (2014). Agricultural crop mapping using optical and SAR multi-temporal seasonal data: A case study in Lombardy region, Italy. In *2014 IEEE Geoscience and Remote Sensing Symposium* (pp. 1489–1492). doi:10.1109/IGARSS.2014.6946719

Foody, G. M. [G. M.], & Mathur, A. [A.]. (2004). A relative evaluation of multiclass image classification by support vector machines. *IEEE Transactions on Geoscience and Remote Sensing*, *42*(6), 1335–1343. doi:10.1109/TGRS.2004.827257

Foody, G. M. [Giles M.]. (2004). Thematic map comparison. *Photogrammetric Engineering & Remote Sensing*, *70*(5), 627–633. doi:10.14358/pers.70.5.627

Forkel, M., Carvalhais, N., Verbesselt, J., Mahecha, M. D., Neigh, C. S. R., & Reichstein, M. (2013). Trend Change Detection in NDVI Time Series: Effects of Inter-Annual Variability and Methodology. *Remote Sensing*, *5*(5), 2113–2144. doi:10.3390/rs5052113

Forkel, M., Migliavacca, M., Thonicke, K., Reichstein, M., Schaphoff, S., Weber, U., & Carvalhais, N. (2015). Codominant water control on global interannual variability and trends in land surface phenology and greenness. *Global Change Biology*, n/a–n/a. doi:10.1111/gcb.12950

Forkuor, G., Conrad, C., Thiel, M., Ullmann, T., & Zoungrana, E. (2014). Integration of Optical and Synthetic Aperture Radar Imagery for Improving Crop Mapping in Northwestern Benin, West Africa. *Remote Sensing*, *6*(7), 6472–6499. doi:10.3390/rs6076472

Gao, F. [F.], Hilker, T., Zhu, X., Anderson, M., Masek, J., Wang, P., & Yang, Y. (2015). Fusing Landsat and MODIS Data for Vegetation Monitoring. *IEEE Geoscience and Remote Sensing Magazine*, *3*(3), 47–60. doi:10.1109/MGRS.2015.2434351

Gao, F. [Feng], Wang, P., & Masek, J. (2013). Integrating remote sensing data from multiple optical sensors for ecological and crop condition monitoring. (Vol. 8869, pp. 886903-886903–8). doi:10.1117/12.2023417

Ghaleb, F., Mario, M., & Sandra, A. N. (2015). Regional Landsat-Based Drought Monitoring from 1982 to 2014. *Climate*, *3*(3), 563–577. doi:10.3390/cli3030563

Ghazaryan, G., Dubovyk, O., Löw, F., Lavreniuk, M., Kolotii, A., Schellberg, J., & Kussul, N. (2018). A rule-based approach for crop identification using multi-temporal and multi-sensor phenological metrics. *European Journal of Remote Sensing*, *51*(1), 511–524. doi:10.1080/22797254.2018.1455540

Giuliani, G., Chatenoux, B., Honeck, E. C., & Richard, J.-P. (2018). Towards Sentinel-2 Analysis Ready Data: A Swiss Data Cube Perspective, 8668–8671.

Godfray, H. C. J., Beddington, J. R., Crute, I. R., Haddad, L., Lawrence, D., Muir, J. F., ... Toulmin, C. (2010). Food Security: The Challenge of Feeding 9 Billion People. *Science*, *327*(5967), 812–818. doi:10.1126/science.1185383

Google Inc. (2016). Earth Engine Documentation. https://sites.google.com/site/earthengineapidocs/.

Gorelick, N., Hancher, M., Dixon, M., Ilyushchenko, S., Thau, D., & Moore, R. (2017). Google Earth Engine: Planetary-scale geospatial analysis for everyone. *Remote Sensing of Environment*. doi:10.1016/j.rse.2017.06.031

Graw, V., Ghazaryan, G., Dall, K., Delgado Gómez, A., Abdel-Hamid, A., Jordaan, A., ... Dubovyk, O. (2017). Drought Dynamics and Vegetation Productivity in Different Land Management Systems of Eastern Cape, South Africa—A Remote Sensing Perspective. *Sustainability*, *9*(10), 1728. doi:10.3390/su9101728

Griffiths, P., van der Linden, S., Kuemmerle, T., & Hostert, P. (2013). A pixel-based landsat compositing algorithm for large area land cover mapping. *IEEE Journal of Selected Topics in Applied Earth Observations and Remote Sensing*, *6*(5), 2088–2101. doi:10.1109/jstars.2012.2228167

Gu, Y., Brown, J. F., Verdin, J. P., & Wardlow, B. (2007). A five-year analysis of MODIS NDVI and NDWI for grassland drought assessment over the central Great Plains of the United States. *Geophysical Research Letters*, *34*(6). doi:10.1029/2006GL029127

Gu, Y., Hunt, E., Wardlow, B., Basara, J. B., Brown, J. F., & Verdin, J. P. (2008). Evaluation of MODIS NDVI and NDWI for vegetation drought monitoring using Oklahoma Mesonet soil moisture data. *Geophysical Research Letters*, *35*(22), L22401. doi:10.1029/2008GL035772

Guttman, N. B. (1998). Comparing the Palmer Drought Index and the Standardized Precipitation Index1. *JAWRA Journal of the American Water Resources Association*, *34*(1), 113–121. doi:10.1111/j.1752-1688.1998.tb05964.x

Hao, P., Wang, L., Zhan, Y., & Niu, Z. (2016). Using Moderate-Resolution Temporal NDVI Profiles for High-Resolution Crop Mapping in Years of Absent Ground Reference Data: A Case Study of Bole and Manas Counties in Xinjiang, China. *ISPRS International Journal of Geo-Information*, *5*(5), 67. doi:10.3390/ijgi5050067

Hao, P., Zhan, Y., Wang, L., Niu, Z., & Shakir, M. (2015). Feature Selection of Time Series MODIS Data for Early Crop Classification Using Random Forest: A Case Study in Kansas, USA. *Remote Sensing*, *7*(5), 5347–5369. doi:10.3390/rs70505347

Harris, I., Jones, P., Osborn, T., & Lister, D. (2014). Updated high-resolution grids of monthly climatic observations – the CRU TS3.10 Dataset. *International Journal of Climatology*, *34*(3), 623–642. doi:10.1002/joc.3711

Hazaymeh, K., & Hassan, Q. K. (2016). Remote sensing of agricultural drought monitoring: A state of art review. *environmental 2016, Vol. 3, Pages 604-630*. doi:10.3934/environsci.2016.4.604

He, B., Chen, A., Wang, H., & Wang, Q. (2015). Dynamic Response of Satellite-Derived Vegetation Growth to Climate Change in the Three North Shelter Forest Region in China. *Remote Sensing*, *7*(8), 9998–10016. doi:10.3390/rs70809998

He, M., Kimball, J., Maneta, M., Maxwell, B., Moreno, A., Beguería, S., ... Wu, X. (2018). Regional Crop Gross Primary Productivity and Yield Estimation Using Fused Landsat-MODIS Data. *Remote Sensing*, *10*(3), 372. doi:10.3390/rs10030372

Hentze, K., Thonfeld, F., & Menz, G. (2016). Evaluating Crop Area Mapping from MODIS Time-Series as an Assessment Tool for Zimbabwe's "Fast Track Land Reform Programme". *PLOS ONE*, *11*(6), e0156630. doi:10.1371/journal.pone.0156630

Holloway, J., & Mengersen, K. (2018). Statistical Machine Learning Methods and Remote Sensing for Sustainable Development Goals: A Review. *Remote Sensing*, *10*(9), 1365. doi:10.3390/rs10091365

Horion, S., Prishchepov, A. V., Verbesselt, J., de Beurs, K., Tagesson, T., & Fensholt, R. (2016). Revealing turning points in ecosystem functioning over the Northern Eurasian agricultural frontier. *Global Change Biology*, *22*(8), 2801–2817. doi:10.1111/gcb.13267

Hostert, P., Griffiths, P., van der Linden, S., & Pflugmacher, D. (2015). Time Series Analyses in a New Era of Optical Satellite Data. In C. Kuenzer, S. Dech, & W. Wagner (Eds.), *Remote Sensing Time Series: Revealing Land Surface Dynamics* (pp. 25–41). Remote Sensing and Digital Image Processing. doi:10.1007/978-3-319-15967-6_2

Hostert, P., Kuemmerle, T., Prishchepov, A., Sieber, A., Lambin, E. F., & Radeloff, V. C. (2011). Rapid land use change after socio-economic disturbances: The collapse of the Soviet Union versus Chernobyl. *Environmental Research Letters*, *6*(4), 045201. doi:10.1088/1748-9326/6/4/045201

Houborg, R., & McCabe, M. F. (2018). A Cubesat enabled Spatio-Temporal Enhancement Method (CESTEM) utilizing Planet, Landsat and MODIS data. *Remote Sensing of Environment*, *209*, 211–226. doi:10.1016/j.rse.2018.02.067

Housman, I., Chastain, R., Finco, M., Housman, I. W., Chastain, R. A., & Finco, M. V. (2018). An Evaluation of Forest Health Insect and Disease Survey Data and Satellite-Based Remote Sens-

ing Forest Change Detection Methods: Case Studies in the United States. *Remote Sensing*, *10*(8), 1184. doi:10.3390/rs10081184

Hütt, C., Koppe, W., Miao, Y., & Bareth, G. (2016). Best Accuracy Land Use/Land Cover (LULC) Classification to Derive Crop Types Using Multitemporal, Multisensor, and Multi-Polarization SAR Satellite Images. *Remote Sensing*, *8*(8), 684. doi:10.3390/rs8080684

Ibrahim, Y., Balzter, H., Kaduk, J., & Tucker, C. (2015). Land Degradation Assessment Using Residual Trend Analysis of GIMMS NDVI3g, Soil Moisture and Rainfall in Sub-Saharan West Africa from 1982 to 2012. *Remote Sensing*, *7*(5), 5471–5494. doi:10.3390/rs70505471

Imperatore, P., Azar, R., Calò, F., Stroppiana, D., Brivio, P. A., Lanari, R., & Pepe, A. (2017). Effect of the Vegetation Fire on Backscattering: An Investigation Based on Sentinel-1 Observations. *IEEE Journal of Selected Topics in Applied Earth Observations and Remote Sensing*, *10*(10), 4478–4492. doi:10.1109/JSTARS.2017.2717039

Inglada, J., Vincent, A., Arias, M., & Marais-Sicre, C. (2016). Improved Early Crop Type Identification By Joint Use of High Temporal Resolution SAR And Optical Image Time Series. *Remote Sensing*, *8*(5), 362. doi:10.3390/rs8050362

Ivits, E., Horion, S., Fensholt, R., & Cherlet, M. (2014). Drought footprint on European ecosystems between 1999 and 2010 assessed by remotely sensed vegetation phenology and productivity. *Global Change Biology*, *20*(2), 581–593. doi:10.1111/gcb.12393

Jakubauskas, M. E., Legates, D. R., & Kastens, J. H. (2002). Crop identification using harmonic analysis of time-series AVHRR NDVI data. *Computers and Electronics in Agriculture*, *37*(1–3), 127–139. doi:10.1016/S0168-1699(02)00116-3

Jamali, S., Jönsson, P., Eklundh, L., Ardö, J., & Seaquist, J. (2015). Detecting changes in vegetation trends using time series segmentation. *Remote Sensing of Environment*, *156*, 182–195. doi:10.1016/j.rse.2014.09.010

Jimenez-Munoz, J. C., & Sobrino, J. A. (2010). A Single-Channel Algorithm for Land-Surface Temperature Retrieval From ASTER Data. *IEEE Geoscience and Remote Sensing Letters*, *7*(1), 176–179. doi:10.1109/LGRS.2009.2029534

Johnson, D. M. (2014). An assessment of pre- and within-season remotely sensed variables for forecasting corn and soybean yields in the United States. *Remote Sensing of Environment*, *141*, 116–128. doi:10.1016/j.rse.2013.10.027

Jönsson, P., & Eklundh, L. (2004). TIMESAT—a program for analyzing time-series of satellite sensor data. *Computers & Geosciences*, *30*(8), 833–845. doi:10.1016/j.cageo.2004.05.006

Joshi, N., Baumann, M., Ehammer, A., Fensholt, R., Grogan, K., Hostert, P., ... Waske, B. (2016). A Review of the Application of Optical and Radar Remote Sensing Data Fusion to Land Use Mapping and Monitoring. *Remote Sensing*, *8*(1), 70. doi:10.3390/rs8010070

Karnieli, A., Agam, N., Pinker, R. T., Anderson, M., Imhoff, M. L., Gutman, G. G., ... Goldberg, A. (2010). Use of NDVI and Land Surface Temperature for Drought Assessment: Merits and Limitations. *Journal of Climate*, *23*(3), 618–633. doi:10.1175/2009JCLI2900.1

Kittler, J., Hatef, M., Duin, R. P. W., & Matas, J. (1998). On combining classifiers. *IEEE Transactions on Pattern Analysis and Machine Intelligence*, *20*(3), 226–239. doi:10.1109/34.667881

Klisch, A., & Atzberger, C. (2016). Operational Drought Monitoring in Kenya Using MODIS NDVI Time Series. *Remote Sensing*, *8*(4), 267. doi:10.3390/rs8040267

Kogan, F. (2018). *Remote Sensing for Food Security*. Springer International Publishing.

Kogan, F. (2019). Monitoring Drought from Space and Food Security. In F. Kogan (Ed.), *Remote Sensing for Food Security* (pp. 75–113). Sustainable Development Goals Series. doi:10.1007/978-3-319-96256-6_5

Kogan, F., Adamenko, T., & Guo, W. (2013). Global and regional drought dynamics in the climate warming era. *Remote Sensing Letters*, *4*(4), 364–372. doi:10.1080/2150704X.2012.736033

Kovalskyy, V., & Henebry, G. M. [G. M.]. (2009). Change and persistence in land surface phenologies of the Don and Dnieper river basins. *Environmental Research Letters*, *4*(4), 045018. doi:10.1088/1748-9326/4/4/045018

Kuemmerle, T., Chaskovskyy, O., Knorn, J., Radeloff, V. C., Kruhlov, I., Keeton, W. S., & Hostert, P. (2009). Forest cover change and illegal logging in the Ukrainian Carpathians in the transition period from 1988 to 2007. *Remote Sensing of Environment*, *113*(6), 1194–1207. doi:10.1016/j.rse.2009.02.006

Kuemmerle, T., Olofsson, P., Chaskovskyy, O., Baumann, M., Ostapowicz, K., Woodcock, C. E., ... Radeloff, V. C. (2011). Post-Soviet farmland abandonment, forest recovery, and carbon sequestration in western Ukraine. *Global Change Biology*, *17*(3), 1335–1349. doi:10.1111/j.1365-2486.2010.02333.x

Kuenzer, C., Dech, S., & Wagner, W. (2015). *Remote Sensing Time Series: Revealing Land Surface Dynamics*. Springer.

Kussul, N. [N.], Skakun, S., Shelestov, A., Lavreniuk, M., Yailymov, B., & Kussul, O. (2015). Regional scale crop mapping using multi-temporal satellite imagery. *ISPRS - International Archives of the Photogrammetry, Remote Sensing and Spatial Information Sciences*, *XL-7/W3*, 45–52. doi:10.5194/isprsarchives-XL-7-W3-45-2015

Kussul, N. [Nataliia], Lemoine, G., Gallego, J., Skakun, S., & Lavreniuk, M. (2015). Parcel based classification for agricultural mapping and monitoring using multi-temporal satellite image sequences. (pp. 165–168). doi:10.1109/IGARSS.2015.7325725

Kussul, N. [Nataliia], Mykola, L., Shelestov, A., & Skakun, S. (2018). Crop inventory at regional scale in Ukraine: Developing in season and end of season crop maps with multi-temporal optical and SAR satellite imagery. *European Journal of Remote Sensing*, *51*(1), 627–636. doi:10.1080/22797254.2018.1454265

Landmann, T., & Dubovyk, O. (2014). Spatial analysis of human-induced vegetation productivity decline over eastern Africa using a decade (2001–2011) of medium resolution MODIS time-series data. *International Journal of Applied Earth Observation and Geoinformation*, *33*, 76–82. doi:10.1016/j.jag.2014.04.020

Lavreniuk, M., Kussul, N., Skakun, S., Shelestov, A., & Yailymov, B. (2015). Regional retrospective high resolution land cover for Ukraine: Methodology and results. (pp. 3965–3968). doi:10.1109/IGARSS.2015.7326693

Lerman, Z. (2004). Policies and institutions for commercialization of subsistence farms in transition countries. *Journal of Asian Economics*, *15*(3), 461–479.

Lerman, Z., Sedik, D., Pugachov, N., & Goncharuk, A. (2007). *Rethinking agricultural reform in Ukraine*. Studies on the Agricultural and Food Sector in Central and Eastern Europe.

Lessel, J., & Ceccato, P. (2016). Creating a basic customizable framework for crop detection using Landsat imagery. *International Journal of Remote Sensing*, *37*(24), 6097–6107. doi:10.1080/2150704X.2016.1252471

Liu, J. [J.], & Zhan, P. (2016). The impacts of smoothing methods for time-series remote sensing data on crop phenology extraction. In *2016 IEEE International Geoscience and Remote Sensing Symposium (IGARSS)* (pp. 2296–2299). doi:10.1109/IGARSS.2016.7729593

Liu, J. [Jinxiu], Heiskanen, J., Aynekulu, E., Maeda, E. E., & Pellikka, P. K. E. (2016). Land Cover Characterization in West Sudanian Savannas Using Seasonal Features from Annual Landsat Time Series. *Remote Sensing*, *8*(5), 365. doi:10.3390/rs8050365

Liu, Y. Y., Parinussa, R. M., Dorigo, W. A., De Jeu, R. A. M., Wagner, W., van Dijk, A. I. J. M., ... Evans, J. P. (2011). Developing an improved soil moisture dataset by blending passive and active microwave satellite-based retrievals. *Hydrol. Earth Syst. Sci. 15*(2), 425–436. doi:10.5194/hess-15-425-2011

Liu, Y., Li, Y., Li, S., & Motesharrei, S. (2015). Spatial and Temporal Patterns of Global NDVI Trends: Correlations with Climate and Human Factors. *Remote Sensing*, *7*(10), 13233–13250. doi:10.3390/rs71013233

Loosvelt, L., Peters, J., Skriver, H., Baets, B. D., & Verhoest, N. E. C. (2012). Impact of Reducing Polarimetric SAR Input on the Uncertainty of Crop Classifications Based on the Random Forests Algorithm. *IEEE Transactions on Geoscience and Remote Sensing*, *50*(10), 4185–4200. doi:10.1109/TGRS.2012.2189012

Lopes, A., Nezry, E., Touzi, R., & Laur, H. (1990). Maximum A Posteriori Speckle Filtering And First Order Texture Models In Sar Images. In *10th Annual International Symposium on Geoscience and Remote Sensing* (pp. 2409–2412). doi:10.1109/IGARSS.1990.689026

Löw, F. [F.], Michel, U., Dech, S., & Conrad, C. (2013). Impact of feature selection on the accuracy and spatial uncertainty of per-field crop classification using Support Vector Machines. *ISPRS Journal of Photogrammetry and Remote Sensing*, *85*, 102–119. doi:10.1016/j.isprsjprs.2013.08.007

Löw, F. [Fabian], Biradar, C., Dubovyk, O., Fliemann, E., Akramkhanov, A., Vallejo, A. N., & Waldner, F. (2017). Regional-scale monitoring of cropland intensity and productivity with multi-source satellite image time series. *GIScience & Remote Sensing*, *0*(0), 1–29. doi:10.1080/15481603.2017.1414010

Löw, F. [Fabian], Conrad, C., & Michel, U. (2015). Decision fusion and non-parametric classifiers for land use mapping using multi-temporal RapidEye data. *ISPRS Journal of Photogrammetry and Remote Sensing*, *108*(Supplement C), 191–204. doi:10.1016/j.isprsjprs.2015.07.001

Löw, F. [Fabian], & Duveiller, G. (2014). Defining the spatial resolution requirements for crop identification using optical remote sensing. *Remote Sensing*, *6*(9), 9034–9063.

Marais Sicre, C., Inglada, J., Fieuzal, R., Baup, F., Valero, S., Cros, J., ... Demarez, V. (2016). Early Detection of Summer Crops Using High Spatial Resolution Optical Image Time Series. *Remote Sensing*, *8*(7), 591. doi:10.3390/rs8070591

Mathur, A. [Ajay], & Foody, G. M. [Giles M.]. (2008). Crop classification by support vector machine with intelligently selected training data for an operational application. *International Journal of Remote Sensing*, *29*(8), 2227–2240. doi:10.1080/01431160701395203

Maus, V., Câmara, G., Cartaxo, R., Sanchez, A., Ramos, F. M., & de Queiroz, G. R. (2016). A Time-Weighted Dynamic Time Warping Method for Land-Use and Land-Cover Mapping. *IEEE Journal of Selected Topics in Applied Earth Observations and Remote Sensing*, *9*(8), 3729–3739. doi:10.1109/JSTARS.2016.2517118

Meroni, M., Verstraete, M. M., Rembold, F., Urbano, F., & Kayitakire, F. (2014). A phenology-based method to derive biomass production anomalies for food security monitoring in the horn of africa. *International Journal of Remote Sensing*, *35*(7), 2472–2492. doi:10.1080/01431161.2014.883090

Meyfroidt, P., Schierhorn, F., Prishchepov, A. V., Müller, D., & Kuemmerle, T. (2016). Drivers, constraints and trade-offs associated with recultivating abandoned cropland in Russia, Ukraine and Kazakhstan. *Global Environmental Change*, *37*, 1–15. doi:10.1016/j.gloenvcha.2016.01.003

Miao, L., Ye, P., He, B., Chen, L., & Cui, X. (2015). Future Climate Impact on the Desertification in the Dry Land Asia Using AVHRR GIMMS NDVI3g Data. *Remote Sensing*, *7*(4), 3863–3877. doi:10.3390/rs70403863

Mishra, A. K., Ines, A. V. M., Das, N. N., Prakash Khedun, C., Singh, V. P., Sivakumar, B., & Hansen, J. W. (2015). Anatomy of a local-scale drought: Application of assimilated remote sensing products, crop model, and statistical methods to an agricultural drought study. *Journal of Hydrology*. Drought Processes, Modeling, and Mitigation, *526*, 15–29. doi:10.1016/j.jhydrol.2014.10.038

Moran, M. S., Alonso, L., Moreno, J. F., Mateo, M. P. C., de la Cruz, D. F., & Montoro, A. (2012). A RADARSAT-2 Quad-Polarized Time Series for Monitoring Crop and Soil Conditions in Barrax, Spain. *IEEE Transactions on Geoscience and Remote Sensing*, *50*(4), 1057–1070. doi:10.1109/TGRS.2011.2166080

Nazarov, N., Cook, H. F., & Woodgate, G. (2001). Environmental issues in the post-communist Ukraine. *Journal of Environmental Management*, *63*(1), 71–86. doi:10.1006/jema.2001.0460

Nemani, R. R., Keeling, C. D., Hashimoto, H., Jolly, W. M., Piper, S. C., Tucker, C. J., ... Running, S. W. (2003). Climate-Driven Increases in Global Terrestrial Net Primary Production from 1982 to 1999. *Science*, *300*(5625), 1560–1563. doi:10.1126/science.1082750

Nguyen, D. B., Clauss, K., Cao, S., Naeimi, V., Kuenzer, C., & Wagner, W. (2015). Mapping Rice Seasonality in the Mekong Delta with Multi-Year Envisat ASAR WSM Data. *Remote Sensing*, *7*(12), 15868–15893. doi:10.3390/rs71215808

Ozdarici Ok, A. (2012). Evaluation of random forest method for agricultural crop classification. *European Journal of Remote Sensing*, 421–432. doi:10.5721/EuJRS20124535

Paganini, M., Petiteville, I., Ward, S., Dyke, G., Steventon, M., Harry, J., & Kerblat, F. (2018). *Satellite Earth Observation in Support of the Sustainable Development Goals*. European Space Agency: Paris, France.

Palmer, W. (1965). Meteorological drought. *US. Weather Bureau Res. Paper*, (45), 1–58.

Pan, Y., Li, L., Zhang, J., Liang, S., Zhu, X., & Sulla-Menashe, D. (2012). Winter wheat area estimation from MODIS-EVI time series data using the Crop Proportion Phenology Index. *Remote Sensing of Environment*, *119*, 232–242. doi:10.1016/j.rse.2011.10.011

Parplies, A., Dubovyk, O., Tewes, A., Mund, J.-P., & Schellberg, J. (2016). Phenomapping of rangelands in South Africa using time series of RapidEye data. *International Journal of Applied Earth Observation and Geoinformation*, *53*, 90–102. doi:10.1016/j.jag.2016.08.001

Pathe, C., Wagner, W., Sabel, D., Doubkova, M., & Basara, J. B. (2009). Using ENVISAT ASAR Global Mode Data for Surface Soil Moisture Retrieval Over Oklahoma, USA. *IEEE Transactions on Geoscience and Remote Sensing*, *47*(2), 468–480. doi:10.1109/TGRS.2008.2004711

Peng, J., Li, Y., Tian, L., Liu, Y., & Wang, Y. (2015). Vegetation Dynamics and Associated Driving Forces in Eastern China during 1999–2008. *Remote Sensing*, *7*(10), 13641–13663. doi:10.3390/rs71013641

Pinzon, J. E., & Tucker, C. J. (2014). A Non-Stationary 1981–2012 AVHRR NDVI3g Time Series. *Remote Sensing*, *6*(8), 6929–6960. doi:10.3390/rs6086929

R Core Team. (2016). R: A Language and Environment for Statistical Computing; R Foundation for Statistical Computing.

Reiche, J., Verhoeven, R., Verbesselt, J., Hamunyela, E., Wielaard, N., & Herold, M. (2018). Characterizing Tropical Forest Cover Loss Using Dense Sentinel-1 Data and Active Fire Alerts. *Remote Sensing*, *10*(5), 777. doi:10.3390/rs10050777

Robinson, N. P., Allred, B. W., Jones, M. O., Moreno, A., Kimball, J. S., Naugle, D. E., ... Richardson, A. D. (2017). A Dynamic Landsat Derived Normalized Difference Vegetation Index (NDVI) Product for the Conterminous United States. *Remote Sensing*, *9*(8), 863. doi:10.3390/rs9080863

Roy, D. P., Wulder, M. A., Loveland, T. R., C.e., W., Allen, R. G., Anderson, M. C., ... Zhu, Z. (2014). Landsat-8: Science and product vision for terrestrial global change research. *Remote Sensing of Environment*, *145*, 154–172. doi:10.1016/j.rse.2014.02.001

Rozelle, S., & Swinnen, J. F. M. (2004). Success and Failure of Reform: Insights from the Transition of Agriculture. *Journal of Economic Literature*, *42*(2), 404–456. doi:10.1257/0022051041409048

Sadegh, M., Love, C., Farahmand, A., Mehran, A., Tourian, M. J., & AghaKouchak, A. (2017). Multi-Sensor Remote Sensing of Drought from Space. In V. Lakshmi (Ed.), *Remote Sensing of Hydrological Extremes* (pp. 219–247). Springer Remote Sensing/Photogrammetry. doi:10.1007/978-3-319-43744-6_11

Schierhorn, F., Müller, D., Beringer, T., Prishchepov, A. V., Kuemmerle, T., & Balmann, A. (2013). Post-Soviet cropland abandonment and carbon sequestration in European Russia, Ukraine, and Belarus. *Global Biogeochemical Cycles*, *27*(4), 1175–1185. doi:10.1002/2013GB004654

Schlaffer, S., Chini, M., Dettmering, D., & Wagner, W. (2016). Mapping Wetlands in Zambia Using Seasonal Backscatter Signatures Derived from ENVISAT ASAR Time Series. *Remote Sensing*, *8*(5), 402. doi:10.3390/rs8050402

Schmullius, C., Thiel, C., Pathe, C., & Santoro, M. (2015). Radar Time Series for Land Cover and Forest Mapping. In *Remote Sensing Time Series* (pp. 323–356). Remote Sensing and Digital Image Processing. doi:10.1007/978-3-319-15967-6_16

Schroeder, R., McDonald, K. C., Azarderakhsh, M., & Zimmermann, R. (2016). ASCAT MetOp-A diurnal backscatter observations of recent vegetation drought patterns over the contiguous U.S.: An assessment of spatial extent and relationship with precipitation and crop yield. *Remote Sensing of Environment*, *177*, 153–159. doi:10.1016/j.rse.2016.01.008

Seddon, A. W. R., Macias-Fauria, M., Long, P. R., Benz, D., & Willis, K. J. (2016). Sensitivity of global terrestrial ecosystems to climate variability. *Nature*, *531*(7593), 229–232. doi:10.1038/nature16986

Shishenko, P., & Munich, N. (2008). *Physical Geography of Ukraine*. Zodiak-EKO.

Siachalou, S., Mallinis, G., & Tsakiri-Strati, M. (2015). A Hidden Markov Models Approach for Crop Classification: Linking Crop Phenology to Time Series of Multi-Sensor Remote Sensing Data. *Remote Sensing*, *7*(4), 3633–3650. doi:10.3390/rs70403633

Sidhu, N., Pebesma, E., & Câmara, G. (2018). Using Google Earth Engine to detect land cover change: Singapore as a use case. *European Journal of Remote Sensing*, *51*(1), 486–500. doi:10.1080/22797254.2018.1451782

Simonetti, D., Simonetti, E., Szantoi, Z., Lupi, A., & Eva, H. D. (2015). First Results From the Phenology-Based Synthesis Classifier Using Landsat 8 Imagery. *IEEE Geoscience and Remote Sensing Letters*, *12*(7), 1496–1500. doi:10.1109/LGRS.2015.2409982

Skakun, S., Franch, B., Vermote, E., Roger, J.-C., Becker-Reshef, I., Justice, C., & Kussul, N. (2017). Early season large-area winter crop mapping using MODIS NDVI data, growing degree days information and a Gaussian mixture model. *Remote Sensing of Environment*, *195*, 244–258. doi:10.1016/j.rse.2017.04.026

Skakun, S., Kussul, N., Shelestov, A., & Kussul, O. (2015). The use of satellite data for agriculture drought risk quantification in Ukraine. *Geomatics, Natural Hazards and Risk*, *0*(0), 1–18. doi:10.1080/19475705.2015.1016555

Smaliychuk, A., Müller, D., Prishchepov, A. V., Levers, C., Kruhlov, I., & Kuemmerle, T. (2016). Recultivation of abandoned agricultural lands in Ukraine: Patterns and drivers. *Global Environmental Change*, *38*, 70–81. doi:10.1016/j.gloenvcha.2016.02.009

Sohoulande Djebou, D. C., & Singh, V. P. (2015). Retrieving vegetation growth patterns from soil moisture, precipitation and temperature using maximum entropy. *Ecological Modelling*, *309–310*, 10–21. doi:10.1016/j.ecolmodel.2015.03.022

Sonnenschein, R., Kuemmerle, T., Udelhoven, T., Stellmes, M., & Hostert, P. (2011). Differences in Landsat-based trend analyses in drylands due to the choice of vegetation estimate. *Remote Sensing of Environment*, *115*(6), 1408–1420. doi:10.1016/j.rse.2011.01.021

State Statistical Department of Kiev region. (2015). Statistical bulletin: The area under cultivation of crops for the harvest 2015 in farms of Kyiv region. itemType: dataset.

State Statistical Department of Kiev region. (2016). Statistical bulletin: The area under cultivation of crops for the harvest 2016 in farms of Kyiv region. itemType: dataset.

Stefanski, J., Kuemmerle, T., Chaskovskyy, O., Griffiths, P., Havryluk, V., Knorn, J., ... Waske, B. (2014). Mapping Land Management Regimes in Western Ukraine Using Optical and SAR Data. *Remote Sensing*, *6*(6), 5279–5305. doi:10.3390/rs6065279

Sutton, W. R., Whitford, P., Montanari Stephens, E., Pedroso Galinato, S., Nevel, B., Plonka, B., & Karamete, E. (2008). *Integrating environment into agriculture and forestry: Progress and prospects in Eastern Europe and Central Asia*. The World Bank.

Teferi, E., Uhlenbrook, S., & Bewket, W. (2015). Inter-annual and seasonal trends of vegetation condition in the Upper Blue Nile (Abbay) basin: Dual scale time series analysis. *Earth Syst. Dynam. Discuss.* *6*(1), 169–216. doi:10.5194/esdd-6-169-2015

Tian, F., Fensholt, R., Verbesselt, J., Grogan, K., Horion, S., & Wang, Y. (2015). Evaluating temporal consistency of long-term global NDVI datasets for trend analysis. *Remote Sensing of Environment*, *163*, 326–340. doi:10.1016/j.rse.2015.03.031

Tüshaus, J., Dubovyk, O., Khamzina, A., & Menz, G. (2014). Comparison of Medium Spatial Resolution ENVISAT-MERIS and Terra-MODIS Time Series for Vegetation Decline Analysis: A Case Study in Central Asia. *Remote Sensing*, *6*(6), 5238–5256. doi:10.3390/rs6065238

U.S. Landsat Analysis Ready Data (ARD) | Landsat Missions. (n.d.). https://landsat.usgs.gov/ard.

Urban, M., Berger, C., Mudau, T., Heckel, K., Truckenbrodt, J., Onyango Odipo, V., ... Schmullius, C. (2018). Surface Moisture and Vegetation Cover Analysis for Drought Monitoring in the Southern Kruger National Park Using Sentinel-1, Sentinel-2, and Landsat-8. *Remote Sensing*, *10*(9), 1482. doi:10.3390/rs10091482

van Hoek, M., Jia, L., Zhou, J., Zheng, C., & Menenti, M. (2016). Early Drought Detection by Spectral Analysis of Satellite Time Series of Precipitation and Normalized Difference Vegetation Index (NDVI). *Remote Sensing*, *8*(5), 422. doi:10.3390/rs8050422

Veloso, A., Mermoz, S., Bouvet, A., Le Toan, T., Planells, M., Dejoux, J.-F., & Ceschia, E. (2017). Understanding the temporal behavior of crops using Sentinel-1 and Sentinel-2-like data for agricultural applications. *Remote Sensing of Environment*, *199*, 415–426. doi:10.1016/j.rse.2017.07.015

Venteris, E. R., Tagestad, J. D., Downs, J. L., & Murray, C. J. (2015). Detection of anomalous crop condition and soil variability mapping using a 26 year Landsat record and the Palmer crop moisture index. *International Journal of Applied Earth Observation and Geoinformation*, *39*, 160–170. doi:10.1016/j.jag.2015.03.008

Verbesselt, J., Hyndman, R., Newnham, G., & Culvenor, D. (2010). Detecting trend and seasonal changes in satellite image time series. *Remote Sensing of Environment*, *114*(1), 106–115. doi:10.1016/j.rse.2009.08.014

Verbesselt, J., Hyndman, R., Zeileis, A., & Culvenor, D. (2010). Phenological change detection while accounting for abrupt and gradual trends in satellite image time series. *Remote Sensing of Environment*, *114*(12), 2970–2980. doi:10.1016/j.rse.2010.08.003

Verbesselt, J., Zeileis, A., & Herold, M. (2012). Near real-time disturbance detection using satellite image time series. *Remote Sensing of Environment*, *123*, 98–108. doi:10.1016/j.rse.2012.02.022

Vicente-Serrano, S. M., Beguería, S., & López-Moreno, J. I. (2009). A Multiscalar Drought Index Sensitive to Global Warming: The Standardized Precipitation Evapotranspiration Index. *Journal of Climate*, *23*(7), 1696–1718. doi:10.1175/2009JCLI2909.1

Vogelmann, J. E., Xian, G., Homer, C., & Tolk, B. (2012). Monitoring gradual ecosystem change using Landsat time series analyses: Case studies in selected forest and rangeland ecosystems. *Remote Sensing of Environment*. Landsat Legacy Special Issue, *122*, 92–105. doi:10.1016/j.rse.2011.06.027

Vreugdenhil, M., Wagner, W., Bauer-Marschallinger, B., Pfeil, I., Teubner, I., Rüdiger, C., & Strauss, P. (2018). Sensitivity of Sentinel-1 Backscatter to Vegetation Dynamics: An Austrian Case Study. *Remote Sensing*, *10*(9), 1396. doi:10.3390/rs10091396

Wagner, W., Lemoine, G., & Rott, H. (1999). A Method for Estimating Soil Moisture from ERS Scatterometer and Soil Data. *Remote Sensing of Environment*, *70*(2), 191–207. doi:10.1016/S0034-4257(99)00036-X

Waldner, F., Canto, G. S., & Defourny, P. (2015). Automated annual cropland mapping using knowledge-based temporal features. *ISPRS Journal of Photogrammetry and Remote Sensing*, *110*, 1–13. doi:10.1016/j.isprsjprs.2015.09.013

Wang, R., Cherkauer, K., Bowling, L., Wang, R., Cherkauer, K., & Bowling, L. (2016). Corn Response to Climate Stress Detected with Satellite-Based NDVI Time Series. *Remote Sensing*, *8*(4), 269. doi:10.3390/rs8040269

Wang, S., Azzari, G., & Lobell, D. B. (2019). Crop type mapping without field-level labels: Random forest transfer and unsupervised clustering techniques. *Remote Sensing of Environment*, *222*, 303–317. doi:10.1016/j.rse.2018.12.026

Wardlow, B. D., Anderson, M. C., & Verdin, J. P. (2012). *Remote Sensing of Drought: Innovative Monitoring Approaches*. CRC Press.

Wardlow, B. D., & Egbert, S. L. (2008). Large-area crop mapping using time-series MODIS 250 m NDVI data: An assessment for the U.S. Central Great Plains. *Remote Sensing of Environment*, *112*(3), 1096–1116. doi:10.1016/j.rse.2007.07.019

Waske, B., & Benediktsson, J. A. (2007). Fusion of Support Vector Machines for Classification of Multisensor Data. *IEEE Transactions on Geoscience and Remote Sensing*, *45*(12), 3858–3866. doi:10.1109/TGRS.2007.898446

Waske, B., van der Linden, S., Benediktsson, J. A., Rabe, A., & Hostert, P. (2010). Sensitivity of Support Vector Machines to Random Feature Selection in Classification of Hyperspectral Data. *IEEE Transactions on Geoscience and Remote Sensing*, *48*(7), 2880–2889. doi:10.1109/TGRS.2010.2041784

Waylen, P., Southworth, J., Gibbes, C., & Tsai, H. (2014). Time Series Analysis of Land Cover Change: Developing Statistical Tools to Determine Significance of Land Cover Changes in Persistence Analyses. *Remote Sensing*, *6*(5), 4473–4497. doi:10.3390/rs6054473

Wegmann, M., Leutner, B., & Dech, S. (Eds.). (2016). *Remote Sensing and GIS for Ecologists: Using Open Source Software*. Exeter: Pelagic Publishing.

Weng, Q. (2011). *Advances in Environmental Remote Sensing: Sensors, Algorithms, and Applications* (New.). Boca Raton: Remote Sensing Applications.

Whitcraft, A. K., Becker-Reshef, I., & Justice, C. O. (2015). Agricultural growing season calendars derived from MODIS surface reflectance. *International Journal of Digital Earth*, *8*(3), 173–197. doi:10.1080/17538947.2014.894147

Wu, D., Qu, J. J., & Hao, X. (2015). Agricultural drought monitoring using MODIS-based drought indices over the USA Corn Belt. *International Journal of Remote Sensing*, *36*(21), 5403–5425. doi:10.1080/01431161.2015.1093190

Yagci, A. L., Di, L., & Deng, M. (2015). The effect of corn–soybean rotation on the NDVI-based drought indicators: A case study in Iowa, USA, using Vegetation Condition Index. *GIScience & Remote Sensing*, *52*(3), 290–314. doi:10.1080/15481603.2015.1038427

Yan, E., Wang, G., Lin, H., Xia, C., & Sun, H. (2015). Phenology-based classification of vegetation cover types in Northeast China using MODIS NDVI and EVI time series. *International Journal of Remote Sensing*, *36*(2), 489–512. doi:10.1080/01431161.2014.999167

Zastavnyi, F. (1994). *Geography of Ukraine*. Lviv: Svit.

Zhang, L., Jiao, W., Zhang, H., Huang, C., & Tong, Q. (2017). Studying drought phenomena in the Continental United States in 2011 and 2012 using various drought indices. *Remote Sensing of Environment*, *190*, 96–106. doi:10.1016/j.rse.2016.12.010

Zhang, X. [Xiang], Chen, N., Li, J., Chen, Z., & Niyogi, D. (2017). Multi-sensor integrated framework and index for agricultural drought monitoring. *Remote Sensing of Environment*, *188*, 141–163. doi:10.1016/j.rse.2016.10.045

Zhang, X. [Xiaoyang], Friedl, M. A., Schaaf, C. B., Strahler, A. H., Hodges, J. C., Gao, F., ... Huete, A. (2003). Monitoring vegetation phenology using MODIS. *Remote Sensing of Environment*, *84*(3), 471–475. doi:10.1016/s0034-4257(02)00135-9

Zhong, L., Hu, L., Yu, L., Gong, P., & Biging, G. S. (2016). Automated mapping of soybean and corn using phenology. *ISPRS Journal of Photogrammetry and Remote Sensing*, *119*, 151–164. doi:10.1016/j.isprsjprs.2016.05.014

Zhou, Y. [Yu], Zhang, L., Fensholt, R., Wang, K., Vitkovskaya, I., & Tian, F. (2015). Climate Contributions to Vegetation Variations in Central Asian Drylands: Pre- and Post-USSR Collapse. *Remote Sensing*, *7*(3), 2449–2470. doi:10.3390/rs70302449

Zhou, Y. [Yuting], Xiao, X., Zhang, G., Wagle, P., Bajgain, R., Dong, J., ... Otkin, J. A. (2017). Quantifying agricultural drought in tallgrass prairie region in the U.S. Southern Great Plains through analysis of a water-related vegetation index from MODIS images. *Agricultural and Forest Meteorology*, *246*, 111–122. doi:10.1016/j.agrformet.2017.06.007

Zhu, X. X., Tuia, D., Mou, L., Xia, G., Zhang, L., Xu, F., & Fraundorfer, F. (2017). Deep Learning in Remote Sensing: A Comprehensive Review and List of Resources. *IEEE Geoscience and Remote Sensing Magazine*, *5*(4), 8–36. doi:10.1109/MGRS.2017.2762307

Zhu, X., Cai, F., Tian, J., Williams, T., Zhu, X., Cai, F., ... Williams, T. K.-A. (2018). Spatiotemporal Fusion of Multisource Remote Sensing Data: Literature Survey, Taxonomy, Principles, Applications, and Future Directions. *Remote Sensing*, *10*(4), 527. doi:10.3390/rs10040527

Zhu, Z., Wang, S., & Woodcock, C. E. (2015). Improvement and expansion of the Fmask algorithm: Cloud, cloud shadow, and snow detection for Landsats 4–7, 8, and Sentinel 2 images. *Remote Sensing of Environment*, *159*, 269–277. doi:10.1016/j.rse.2014.12.014